Advanced physical and chemical characterization of oil spill residues

by

Yuling Han

A dissertation submitted to the Graduate Faculty of
Auburn University
in partial fulfillment of the
requirements for the Degree of
Environmental Engineering, Doctor of Philosophy

Auburn, Alabama
May 4, 2019

Keywords: Deepwater Horizon oil spill, Chennai oil spill, in-situ burning, petroleum biomarkers, oil fingerprinting, tar balls

Approved by

T. Prabhakar Clement (Chair), Professor of Civil Engineering
Dongye Zhao (Co-Chair), Professor of Civil Engineering
Clifford Lange, Associate Professor of Civil Engineering
Muralikrishnan Dhanasekaran, Professor of Drug Discovery and Development

Abstract

Oil spill contamination is a worldwide problem. On April 20th, 2010, the Deepwater Horizon (DWH) oil platform located off the coast of Louisiana exploded and sank after 2 days. The wellhead could not be sealed until July 15th, 2010, and this resulted releasing about 4.9 million barrels (650,000 metric tons) of crude oil into the Gulf of Mexico (GOM). It was reported that the DWH oil spill contaminated over 1,700 kilometers of GOM shoreline and impacted several amenity beaches, marshes and other ecologically sensitive coastal ecosystems along Texas, Louisiana, Mississippi, Alabama and Florida. More recently, on January 28th, 2017, another relatively smaller oil spill occurred when two cargo ships collided about two miles away from the Ennore Kamarajar shipping terminal near Chennai City, India, resulting in a major oil spill known as the Chennai oil spill. This accident released about 75 metric tons of the heavy bunker oil into the Bay of Bengal and contaminated 25 miles of the coastline extending from Chennai's northern suburban town Ennore all the way to the southern suburban town Thiruvanmiyur. In this study, source identification and advanced characterization methods were completed to investigate the residues from these two oil spills.

In the first part of the study, a simple 2-tier field testing protocol, which is based on unique physical characteristics of the oil spill residues, is developed for identifying DWH oil spill residues. A variety of oil samples originated from different oil spill events were tested using the protocol and the samples were classified into "DWH samples" and "non-DWH samples". The results were verified by analyzing the samples with advanced chemical fingerprinting methods. The verification results matched the results derived from the field testing protocol. The proposed protocol is a reliable and cost-effective field testing approach for differentiating DWH oil spill residues from other types of petroleum residues.

The second part of the study is to understand the impacts of burning and excessive heating on hopane biomarkers which are typically used for fingerprinting oil spill residues. In the study, laboratory-scale in situ burning (ISB) experiments were conducted using two types of oils: a model oil prepared using C_{30}-αβ hopane standard, and a DWH reference crude collected from the MC252 well. Our experimental data show that C_{30}-αβ hopane will decrease following an ISB event, although the diagnostic ratios of hopanes will remain stable. Therefore, while relative concentration of different types of hopanes can be used for fingerprinting, C_{30}-αβ hopane cannot be used as a conservative biomarker.

In the third part, thermal degradation patterns of hopane biomarkers at high temperatures were investigated by heating the oil samples in an oven. Our data show that C_{30}-αβ hopane in crude oil starts to degrade at about 160 °C, which is lower than the temperature an oil slick will encounter during a typical ISB event. We also found the degradation level of C_{30}-αβ hopane increases with the increase of heating temperature and heating time. The diagnostic ratios of hopanes also changed when the oil was heated at higher temperatures for longer times. Overall, heating is an important process that can degrade hopane biomarkers and it can also change their relative ratios and hence the fingerprint.

In the fourth part, we completed a case study of 2017 Chennai oil spill based on both field-scale observational data and chemical characterization data. Our field survey shows that after the spill large amounts of oil was trapped within a relatively stagnant zones near the seawall-groin intersection regions, and this trapping pattern was unique to the Chennai oil spill. The initial cleanup efforts that used manual methods to skim the floating oil and scrub the oil contaminated rocks were relatively effective. The chemical characterization data studied the unique hopanes and steranes fingerprints for the source oil, which can be used for identification

and tracking of the oil spill residues. Our experimental studies also show that evaporation is a significant weathering process. During initial hours, the volatile compounds depleted rather rapidly, resulting in the accumulation of heavy polycyclic aromatic hydrocarbons (PAHs) in the crude. Most of these highly toxic heavy PAHs are recalcitrant, and their long-term environmental impacts are largely unknown.

In the final section, we summarize the key findings of this study and also point out some recommendations for future research.

Acknowledgments

I would like to express my sincere acknowledgments to my advisor, Dr. T. Prabhakar Clement, for his patient guidance, mentorship and support during my study at Auburn University. Without his guidance and persistent help this dissertation would not have been possible. I would also like to thank my committee members, Dr. Dongye Zhao, Dr. Clifford Lange and Dr. Muralikrishnan Dhanasekaran, and my dissertation reader Dr. Ramesh B. Jeganathan for their valuable comments and suggestions regarding my dissertation.

Special thanks to my group colleagues, Dr. Fang Yin and Dr. Gerald John for their help in project design, experimental preparation and instrumental exploration. My other colleagues Sarah Gustitus, Sama S. Memari and Qing Chang helped with sample collection. I value their friendship and support.

Finally, my great gratitude goes to my husband, Nan Shi, for his enduring love and selfless dedication. I want to express my profound appreciation to my parents and older sister. Their unfailing love and constant encouragement always guide and inspire me. Thanks to the City of Orange Beach, Alabama, USA, the National Science Foundation (NSF) and Samuel Ginn College of Engineering, Auburn University, and the Center for Water Quality Research at the University of Alabama for funding this research. Thanks to China Scholarship Council (CSC) for the financial support.

Table of contents

List of Tables

List of Figures

List of Abbreviations

DWH	Deepwater Horizon
BP	British Petroleum
GOM	Gulf of Mexico
MC252	Macondo Prospect 252
GB	Galveston Bay
ISB	In-situ burning
PAHs	Polycyclic aromatic hydrocarbons
TPH	Total petroleum hydrocarbons
TSH	Total saturated hydrocarbons
TAH	Total aromatic hydrocarbons
UCM	Unresolved complex mixture
GC/MS	Gas Chromatograph/Single Quadrupole Mass Spectrometer
GC/MS/MS	Gas Chromatograph/Triple Quadrupole Mass Spectrometer
GC/FID	Gas Chromatograph/Flame ionization detector
SIM	Selected ion monitoring
MRM	Multiple reaction monitoring
QqQ	Triple quadrupole
CE	Collision energy
CID	Collision induced dissociation
TS	Time segment
SOMs	Sediment-oil mats
SRBs	Surface residual oil balls

SOAs	Sediment-oil agglomerates
OSAT	Operational science advisory team
NRC	National research council
NIST	National Institutes of Standards and Technology
USEPA	United States Environmental Protection Agency
IS	Internal standard
SS	Surrogate standards
EI	Electron ionization
DRs	Diagnostic ratios
RRF	Relative response factor
LOD	Limit of detection
LOQ	Limit of quantitation
DL	Below detection limit

Chapter 1

Introduction

1.1 Background

On April 20th, 2010, a semi-submersible drilling rig located 50 miles off Louisiana shoreline experienced well blow-out and exploded. Until July 15th, 2010 when the wellhead was sealed, approximately 4.9 million barrels of crude oil was released from the Macondo well (MC252) at a depth of 1500 m, resulting in one of the largest marine oil spill disasters in the US history (McNutt et al., 2012). Alabama is around 120 miles distance from the spill location. After about one month of DWH oil spill, in early June 2010, the oil started washing onto Alabama shoreline (J. S. Hayworth, Clement, & Valentine, 2011; Nixon et al., 2016). It was reported that about 31 miles of Alabama beaches were heavily contaminated by the spilled oil (Joel S Hayworth, Clement, John, & Yin, 2015). The oil arrived on Alabama shoreline underwent long distance ocean scale weathering and it was predominantly in the form of mousse with high viscosity and brownish color. The oil mousse continued to weather and interact with the suspended sediment in the nearshore environment, forming highly weathered oil tar balls (F. Yin, John, Hayworth, & Clement, 2015). The oil tar balls have been deposited on the shoreline beaches for several years and their long-term environmental impacts are largely unknown.

Apart from offshore drilling accidents like DWH oil spill, oil tanker accidents have also caused several world-wide oil spills. Hebei Spirit oil spill occurred on December 7th, 2007 due to collision with a crane barge released 10,900 tons of crude oil and contaminated about 375 km of western Korea shoreline (Un Hyuk Yim et al., 2011). Exxon Valdez oil spill occurred on March 24th, 1989 due to the grounding of the oil tanker released approximately 258,000 barrels of crude oil and impacted about 1,300 miles of the coastline (Short et al., 2004). More recently,

on January 28th, 2017, two cargo ships collided about 10 miles away from Chennai city in south India. This Chennai oil spill accident resulted in a release of about 75 metric tons of the heavy bunker oil into the Bay of Bengal. After a few days, around 25 miles of coastline along Chennai was heavily contaminated by the thick layers of emulsified oil. The initial cleanup efforts employed workers to manually scoop the floating oil and these efforts indeed recovered a large amount of oil. However, the fate of the remaining oil and the long-term environmental impacts on the coastal system are unclear.

1.2 Fate of spilled oil

After the crude oil is released into the marine environment, it undergoes various physiochemical processes. While a portion of the floating oil can be recovered by mechanical methods, some of the oil can dissolve and disperse into the water column. In the meantime, oil can deplete through weathering processes such as evaporation, photo-degradation and biodegradation (M. Board, Board, & Council, 2003). The fate and behavior of oil is governed by a variety of factors including oil properties, environmental conditions, natural processes and human interventions (Lubchenco et al., 2010; Ramseur, 2010).

1.2.1 Factors that affect the initial fate of spilled oil

1.2.1.1 Oil evaporative properties

Crude oil is a complex mixture of hundreds of different types of petroleum hydrocarbons and non-hydrocarbons (Z. Wang et al., 2003). The complex physical and chemical properties of crude oil determine how it reacts in the environment. For example, the light crude oil evaporates more readily than heavy crude when released on the water surface. It was reported that during the initial days, up to 70% of volume can be removed by evaporation for light crudes, while only

40% and 10% can be removed for medium and heavy crudes, respectively (M. Board et al., 2003).

1.2.1.2 Impacts of environmental conditions on oil spills

Environmental conditions are important factors that impact the fate of the spilled oil. Temperature is one of the key parameters that control the oil evaporation (Merv F Fingas, 2013). Higher temperature and warmer water can facilitate the evaporation and dissolution processes. The transport of the spilled oil including advection and turbulent diffusion is governed by wind, waves and current around the ocean environment (S. D. Wang, Shen, & Zheng, 2005). Other environmental factors such as nutrients and oxygen concentration in the water system can significantly influence the biodegradation of the spilled oil (M. Board et al., 2003). Following the 2010 DWH oil spill, it is believed that biodegradation of petroleum hydrocarbons took place rather rapidly. This is because the microorganisms in the Gulf of Mexico (GOM) waters are well adapted to hydrocarbon exposure where natural seeps and tanker spills occur frequently (Atlas & Hazen, 2011). Also the oxygen level and nutrient in the warm water of GOM enhanced the oil biodegradation (Lubchenco et al., 2010).

1.2.1.3 Natural weathering processes

When crude oil is released into the marine environment, it can be impacted by various natural processes, which consist of spreading, advection, evaporation, dissolution, photo-degradation, emulsification, sedimentation and biodegradation (M. Board et al., 2003; Robert M Garrett, Pickering, Haith, & Prince, 1998; Guo & Wang, 2009; G. F. John, Han, & Clement, 2016; Roger C. Prince et al., 2003; S. D. Wang et al., 2005). Spreading occurs immediately after the oil is released on the water surface and it contributes to the formation of oil slick and greatly increases the surface area (Robert M Garrett et al., 1998). Evaporation plays a critical role in

reducing the spilled volume especially during the initial spilling days (Merv F Fingas, 2013). Only a small fraction of chemicals in crude oil including polar compounds and small aromatic hydrocarbons can dissolve into the water column. But the dissolved chemicals significantly impact the coastal ecosystem due to their high toxicity to aquatic species (M. Board et al., 2003). Photo-degradation can transform petroleum hydrocarbons into oxidized products with high polarity and water solubility (Christoph Aeppli et al., 2012; Robert M Garrett et al., 1998).

1.2.1.4 Human interventions

During a marine oil spill event, various response techniques are employed to reduce the environmental impact such as skimming, in-situ burning and chemical dispersion (Dave & Ghaly, 2011; Atle B Nordvik, 1995). The applications of the human responses affect the fate of the spilled oil. Skimming is a mechanical removal method to recover the floating oil. In-situ burning (ISB) also removes the floating oil from the environment, but ISB may transfer a portion of burnt residues into air and water column (Mullin & Champ, 2003; S. A. Stout & Payne, 2016). Another commonly used method is the use of chemical dispersants, which can break the oil slick into small oil droplets and disperse the oil into the water column (Kujawinski et al., 2011). The use of dispersant can reduce the oil contamination of sensitive shoreline and beaches (Lessard & DeMarco, 2000).

1.2.2 Understanding the overall oil spill budget (case for the DWH oil spill)

According to the DWH oil budget estimates released by the federal government, the fate of the released oil was divided into seven categories (Ramseur, 2010). 17% of released oil was recovered directly from the wellhead and transported to surface level. 3% of the oil was skimmed from the water surface. 5% of spilled oil was removed by 410 different in-situ burns during DWH oil spill. The burn efficiency was estimated to be 85% and the burns have

generated about 38,800 to 54,700 barrels of residues (S. A. Stout & Payne, 2016). The fate of the chemicals during ISB and the long-term ecological impacts of the burnt residues are not fully understood. 16% of the oil was chemically dispersed by two types of dispersants Corexit 9527 and Corexit 9500A. During DWH oil spill, approximately 1.8 million gallons of chemical dispersant were applied to both surface and sub-surface water (Kujawinski et al., 2011). The application of dispersant can efficiently disperse oil slick into small oil droplets that are more available for biodegradation (O. S. Board & Council, 2005). 13% of oil was naturally dispersed by ocean turbulence. 24% of oil either evaporated or dissolved. Evaporation accounted for a large portion of oil loss because the spilled oil was light in composition (API 35) (Atlas & Hazen, 2011). Dissolution was also significant since the oil was released and transported from deep sea at a depth of 1500 m to the water surface (Liu, Liu, Zhu, & Wu, 2012). 22% of the total estimated oil release was designated as "other", which mainly included the oil remaining on the water surface and the weathered oil residues that deposited or buried along shoreline. It was estimated that over 1,700 kilometers of GOM shoreline was contaminated by DWH oil spill residues (Michel et al., 2013). Field studies have shown that the oil level on Alabama beaches was significantly increased by at least thousand-fold (Clement, John, & Yin, 2017). And these oil residues are likely to persist in the beach system for a long time (F. Yin et al., 2015).

1.3 Petroleum biomarkers and their role in oil spill investigations

In general, the chemical compounds in crude oil are classified into four groups, saturates, aromatics, resin and asphaltenes (SARA) (Z. D. Wang, Stout, & Fingas, 2006). Among them, petroleum biomarkers are one of the most important classes of hydrocarbons. Biological markers or biomarkers are a complex group of saturated cyclic hydrocarbons that are naturally present in the oil. Petroleum biomarkers contain useful information for oil source identification

and are widely used to trace the biological origins of petroleum products. Therefore, petroleum biomarkers are generally referred to as indicators used for characterizing the chemical fingerprints of oil spill samples (Z. D. Wang, Fingas, & Page, 1999).

Petroleum biomarkers originated from formerly living organisms and accumulated while the organic materials are preserved over geologic times (Peters, Walters, & Moldowan, 2005). Therefore, biomarkers are called molecular fossils as their structure is stable with time and recalcitrant to weathering (Peters et al., 2005). For example, pentacyclic hopanes are believed to be "molecular fossils" derived from the cellular and membrane lipids of prokaryotes (Brocks, Logan, Buick, & Summons, 1999; Prahl, Dymond, & Sparrow, 2000). The distribution and relative abundance of biomarkers differ considerably for different types of oil, since crude oil formed under different geological conditions and ages reveals a unique chemical fingerprint (Hostettler, Lorenson, & Bekins, 2013; Z. D. Wang, Stout, et al., 2006). Biomarkers levels in crude oils are largely determined by the geological source concentration, and feedstocks also effect for refined products (Z. Wang, Fingas, Yang, & Christensen, 1964; Z. D. Wang et al., 1999).

Petroleum biomarkers mainly contain bicyclic sesquiterpanes, diamondoids, polycyclic terpanes, and polycyclic steranes, and they are the most important hydrocarbons for oil fingerprinting and source identification (Merv Fingas, 2014a).

1.3.1 Bicyclic sesquiterpanes

Bicyclic sesquiterpanes are small biomarker hydrocarbons with drimane skeletons $C_{15}H_{28}$ formed from biodegradation of larger terpanes or from bicyclic compounds (Yang, Wang, Hollebone, Brown, & Landriault, 2009). They are ubiquitous in crude oils and especially in light petroleum products. When the petroleum refining processes removed most of the high

molecular weight biomarkers (hopanes and steranes), sesquiterpanes are concentrated in the refined light products. In addition, sesquiterpanes are resistant to weathering and particularly biodegradation, which enable them to be ideally used in oil-source correlation analysis (S. A. Stout, Uhler, & McCarthy, 2005; Z. D. Wang et al., 2005). It was reported that the characteristic fragment ions for a series of sesquiterpanes are m/z 123 ($C9H15^+$), 179, 193 and 207 (Yang et al., 2009).

1.3.2 Diamondoids

Similar to bicyclic sesquiterpanes, diamondoids are also a group of small biomarker hydrocarbons and are ideally used for oil origin identification in refined light petroleum products. Diamondoids are saturated hydrocarbons with three-dimensionally fused cyclohexane rings and their general molecular formula is $C_{4n+6}H_{4n+12}$ started from adamantane ($C_{10}H_{16}$) to hexamantane ($C_{30}H_{36}$) (Mervin Fingas, 2016). Diamondoids are stable during thermal cracking, therefore they have been widely developed and used in oil forensic fingerprinting analysis (S. A. Stout & Douglas, 2004; Z. D. Wang, Yang, Hollebone, & Fingas, 2006).

1.3.3 Biomarker terpanes (hopanes)

Biomarker hopanes are the most widely used compounds in oil identification, as hopanes are stable and abundant in highly weathered oil samples (C. Aeppli et al., 2014; Douglas, Bence, Prince, McMillen, & Butler, 1996). Hopanes are branched cycloalkanes with a five-ring skeleton formed by 21 carbons as shown in Figure 1.1. Additional carbons can substitute on the ring, resulting in a wide distribution of hopane homologs from C_{27} to C_{35}. According to the orientation of hydrogen atom in the structural space, α and β hydrogens are defined for these biomarker stereoisomers. The α hydrocarbons are located below the plane of the molecule and the β hydrogens are located above the plane of the molecule, such as 17α(H), 21β(H)-hopane (Z.

D. Wang, Stout, et al., 2006). In addition, R and S are present the two stereoisomers of C31-C35 hopanes that have an additional side chain with asymmetric center at C_{22}, referred to as two homologs 22R- and 22S- hopanes. Therefore, biomarker hopane has a series of isomers and epimers theoretically. For example, C_{30} hopane has four isomers: 17α,21α-, 17α,21β-, 17β,21α- and 17β,21β-hopane. However, the thermodynamic stability of these isomers is different, resulting in different abundance levels in petroleum. Specifically, 17α,21β-hopane is the most stable isomer and shows high abundance in crude oils, whereas, 17β,21β-hopane is the most unstable isomer and it has depleted during early catagenesis (Peters et al., 2005). The absence of 17β,21β-hopane in crude oil makes it a desirable internal standard for biomarker compounds quantification (Mervin Fingas, 2016). The characteristic fragment ion for hopanes is m/z 191 ($C_{14}H_{23}^{+}$).

1.3.4 Steranes

Steranes are another important group of biomarker compounds. Steranes contain a four-ring skeleton with 17 carbons. Additional carbons substitute on the ring skeleton to form a series of sterane homologs from C_{24} to C_{30} steranes as shown in Figure 1.1. Different from hopanes, steranes are considered to be derived from cell membranes of eukaryotes (Volkman et al., 1998). Since commercial standards are unavailable, the distribution and relative abundance of steranes are typically used for comparison with potential source oil. The characteristic fragment ions for

steranes are m/z 217 ($C_{16}H_{25}^{+}$) and m/z 218 ($C_{16}H_{26}^{+}$).

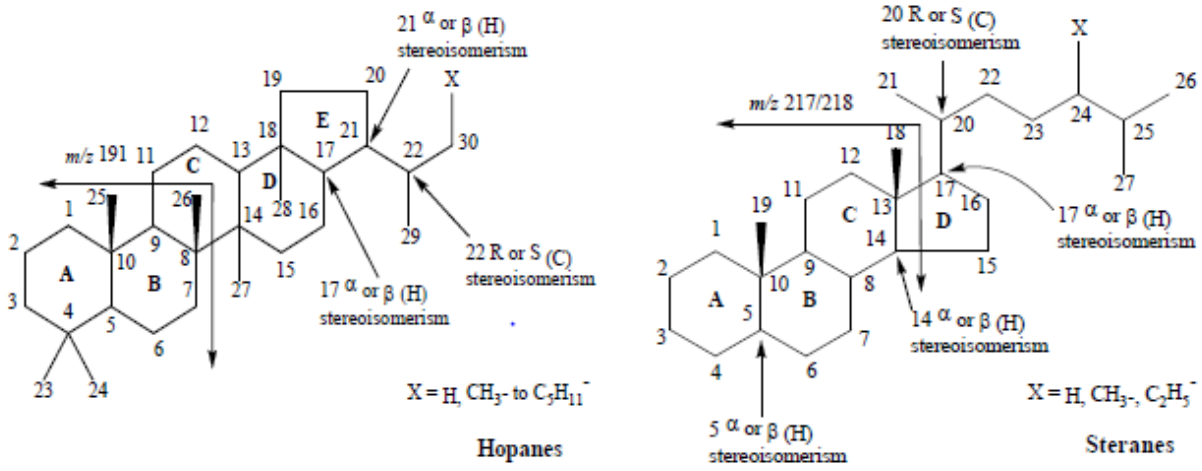

Figure 1.1 Molecular structures of hopanes and steranes (Mervin Fingas, 2016).

1.4 Application of petroleum biomarkers

Petroleum biomarkers, due to their stability and resistance to weathering, have been widely applied in various oil spill investigations. In 1994, a method for fractionation of light crude oil was developed to better identify and quantitate the petroleum hydrocarbon compounds (Z. D. Wang, Fingas, & Li, 1994a, 1994b). After that, biomarkers, together with alkanes, PAHs and other types of hydrocarbons present in crude oil were extensively used for forensic investigation.

1.4.1 Source identification and differentiation

Boehm et al. (1997) overviewed the development of chemical fingerprinting techniques that utilize petroleum biomarkers to characterize and differentiate Exxon Valdez oil spill samples from other petroleum sources in the Prince William Sound region. After 12 years of Exxon Valdez oil spill, the oil remaining in Prince William Sound was estimated and hopanes were applied to track and confirm the source of the oil residues by comparing the hopane distribution patterns with the source oil fingerprint (Short et al., 2004). The Hebei Spirit oil spill occurred in 2007 resulted in a mixture of three different types of the Middle East crude oil. Therefore, tiered

fingerprinting approaches dependent on biomarkers were implemented for defensible source identification and allocation (U. H. Yim et al., 2011). Mulabagal et al. (2013) confirmed the Deepwater Horizon (DWH) origin of the stranded oil residues on Alabama shoreline by comparing the chromatographic signatures and diagnostic ratios of hopane petroleum biomarkers.

1.4.2 Oil type differentiation

Petroleum biomarkers can also be used for differentiation of different types of petroleum products. For example, Wang et al. (1999) differentiated six types of petroleum products based on the distribution profile of saturated hydrocarbons. Five crude oils from the Gulf of Suez, Egypt were grouped into three different source-related types of oil by analyzing the biomarker distribution (Barakat, Mostafa, ElGayar, & Rullkotter, 1997). Wang et al. (2006) presented the different distribution and abundance of biomarkers in crude oil, refined petroleum fuels and lubricating oils respectively for oil correlation and differentiation.

1.4.3 Quantifying toxic chemicals and their weathering levels

C_{30}-αβ hopane was used as a conservative biomarker for tracking the fate of toxic contaminants in oil residues (R. M. Garrett, Guenette, Haith, & Prince, 2000; F. Yin et al., 2015) and for evaluating weathering degree of the spilled oil samples (C. Aeppli et al., 2014; Z. D. Wang & M. Fingas, 2003). The following two equations are typically used to calculate the weathering level and actual PAH depletion levels in the oil spill samples (G. F. John et al., 2016; F. Yin et al., 2015).

$$\%weathering = \left(1 - \frac{H_{oil}}{H_{weathered}}\right) X\ 100$$

$$Actual\ \%depletion\ of\ PAH = \left(1 - \frac{PAH\ in\ weathered\ sample}{PAH\ in\ reference\ oil} \times \frac{H_{oil}}{H_{weathered}}\right) X\ 100$$

In this equation, H_{oil} is the ratio of the peak area of C_{30}-αβ hopane in crude oil to the peak area of C_{30}-ββ hopane (internal standard) and $H_{weathered}$ is the ratio of the peak area of C_{30}-αβ hopane in a weathered oil spill sample to the peak area of C_{30}-ββ hopane.

1.5 The utilization of biomarkers in DWH oil spill studies

Characterization of biomarkers related to the DWH oil spill event has been widely studied. To track the oil source of the stranded oil spill residues present along GOM shoreline, Mulabagal et al. (2013) analyzed the petroleum biomarkers and confirmed the DWH oil spill origin by comparing the distribution profile of hopanes and steranes. Kirman et al. (2016) analyzed biomarker patterns and the related diagnostic ratios in Barataria Bay marsh sediments and the information provided strong support that the hydrocarbon input in the sediments originated from DWH oil spill. Romero et al. (2015) measured the concentration of hopanes, steranes and diasteranes in sediments recovered from northeast of the DWH wellhead after DWH oil spill, and the concentration levels were used for estimation of the contribution of hydrocarbons input from different petroleum products. When crude or fuel oil is spilled into the coastal environment it can be impacted by various weathering processes which include spreading, advection, evaporation, dissolution, photo-degradation, emulsification, sedimentation and biodegradation (M. Board et al., 2003; S. D. Wang et al., 2005). In order to track the fate of toxic contaminants in oil spill residues after a long period of weathering, C_{30}-αβ hopane is routinely used as a conservative marker (Z. D. Wang, Fingas, & Sergy, 1994). Fang et al. (2015) determined the actual PAHs depletion levels in the weathered DWH oil residues samples by normalizing the data to C_{30}-αβ hopane concentrations. Researchers have also shown that the photo-degradation level of PAHs in oil residue samples is also dependent on C_{30}-αβ hopane normalized values (G. F. John et al., 2016). During DWH oil spill, in-situ burn was employed as a remediation method,

and 411 burns removed 5% of total released oil (Perring et al., 2011; Schaum et al., 2010). Stout and Payne (2016) characterized the chemical composition of floating and sunken ISB residues from the DWH oil spill and used C_{30}-αβ hopane as a conservative biomarker to quantify the apparent enrichment of PAHs.

1.6 Objectives of this study

Oil spill residues depositing onto shoreline beaches is a worldwide environmental problem. The focus of this study is to identify and characterize different types of oil spill residues. This dissertation is divided into the six chapters with each focusing on a specific objective.

The introduction chapter (current chapter) provides a general overview of oil spill contamination problems and reviews the fate and transport mechanisms and the types of biomarkers present in different types of crude oil.

The objective of the second chapter is to develop a simple field testing protocol for identifying the DWH oil spill residues deposited along the Alabama shoreline and differentiate them from other petroleum contaminants.

The objective of the third chapter is to understand the fate of hopane biomarkers during in-situ burning of crude oil.

The objective of the fourth chapter is to study the thermal degradation patterns of hopane biomarkers present in crude oil under high temperature heating conditions.

The objective of the fifth chapter is to apply oil spill characterization techniques to characterize the residues collected from the Chennai oil spill site.

The objective of the last chapter is to summarize the key finding of the dissertation and point out some possible recommendations for future research.

Chapter 2

Development of a field testing protocol for identifying Deepwater Horizon oil spill residues trapped near Gulf of Mexico beaches

2.1 Introduction

DWH oil spill has contaminated about 50 kilometers of Alabama sandy beaches located in between Orange Beach to Fort Morgan. Field studies have shown that the DWH spill has substantially increased the background oil levels of several GOM beaches (Clement et al., 2017; Joel S Hayworth et al., 2015; F. Yin et al., 2015). For example, Clement et al. (2017) estimated that the background oil levels in Alabama's beaches have increased by at least thousand fold. The average historic background level for Alabama's beaches prior to the DWH oil spill event was estimated to be 2 g/km/year (about 2 to 4 tar balls/km/year; they are highly weathered tar balls with each weighing about 0.5 to 1 g). The levels estimated for Alabama beaches based on a field survey completed on January, 2016 ranged from 2,400 to 31,000 g/km/year. Some of the beaches were heavily contaminated; for example, from a kilometer long beach in Fort Morgan they recovered 233 fragments of oil residues, weighting about 1,310 grams, within an hour (Clement et al., 2017). The size of each residue ranged from 0.5 cm to 7 cm and the weight ranged from 0.5 to 50 g. Previous studies have also shown that the DWH oil spill residues found along GOM beaches have partially weathered crude oil that contain various types of toxic polycyclic aromatic hydrocarbons (C. Aeppli et al., 2014; Liu et al., 2012; Urbano, Elango, & Pardue, 2013; F. Yin et al., 2015).

Historically, most GOM beaches are often contaminated by different types of petroleum residues (residues that are not of DWH origin) that could have originated from natural oil seeps, accidental releases from oil rigs and ship oil, or anthropogenic waste oil dumping activities

(Kennicutt, 2017; MacDonald et al., 2015). Therefore, in order to assess the impacts of the DWH oil spill, one needs to identify and differentiate DWH residues from other petroleum residues. The DWH oil spill residues are often referred to as "tar balls," a term that normally refers to rubbery, black, highly-weathered masses of oil, which could be found along some GOM beaches. However, DWH oil residues have several physical and chemical characteristics that are different from these traditional black tar balls (Mulabagal et al., 2013).

When crude oil is discharged into the ocean, various weathering processes that are driven by winds and waves break the floating oil into smaller patches, which are then transported by ocean currents. During this process, almost all the lighter components in the crude oil rapidly evaporate (M. Board et al., 2003). The unevaporated portion of the oil eventually mixes with water to form a thick brownish emulsion, known as mousse (Merv Fingas & Fieldhouse, 2004). When the mousse is stranded in deep ocean for a long period (several months to years), it will be stretched and torn apart by winds and waves to eventually form highly weathered black tar balls (Goodman, 2003).

The DWH oil spill residues found along Alabama's beaches were formed by different types of nearshore processes. The sweet crude oil released from the DWH well rapidly emulsified forming brownish mousse, and within weeks the mousse was transported by ocean currents towards the Alabama shoreline. When the floating weathered mousse approached the shoreline, it interacted with suspended sediments and sank in the nearshore environment. Gustitus and Clement (2017) recently presented a detailed conceptual model for describing the coastal transport mechanisms that facilitated the formation of sunken DWH oil spill residues. After sinking, the submerged oil accumulated more sediments to form large deposits of oily mats, known as submerged oil mats or sediment-oil mats (SOMs). Waves and other shoreline

transport processes eventually broke SOMs into smaller fragments, known as surface residual oil balls (SRBs) or sediment-oil agglomerates (SOAs) (Gustitus & Clement, 2017). Typical size of SRB/SOAs found along the Alabama shoreline can range from about 0.5 cm to 8 cm (Clement et al., 2017; Joel S Hayworth et al., 2015). Over time, these residues are physically disintegrated by nearshore erosion processes and become too small to be recoverable. Our field observations have indicated that SOAs less than about 0.5 cm are difficult to identify and hence are unlikely to be recovered.

Identifying the source of oil in various types of petroleum residues is an important task in any oil spill investigation (Scott A Stout, 2016; Suneel et al., 2014; Z. D. Wang et al., 1999; Zakaria et al., 2000). Several published analytical procedures are available that can be used to objectively track and identify the source of oil spill residues. These procedures analyze recalcitrant biomarkers or other petroleum chemicals, which are naturally present in the crude oil, using advanced GC/FID or GC/MS methods (Hostettler et al., 2013; Scott A Stout, 2016; Z. D. Wang, Stout, et al., 2006). After obtaining the analytical data, various methods are used to compute different types of ratios and fingerprints to differentiate the oils (Z. Wang & Stout, 2010; Z. D. Wang et al., 1999). While these advanced source identification methods are highly efficient, it is rather impractical to routinely use them to analyze hundreds (and even thousands) of field samples collected after a large spill event, such as the DWH oil spill (Clement et al., 2017; Joel S Hayworth et al., 2015). Also, conducting advanced laboratory studies can be cost-prohibitive and almost infeasible for most local municipalities, regulatory agencies and community groups that use their own employees, temporary workers and/or volunteers to conduct the monitoring surveys. These field workers might not have sufficient training and/or have access to a laboratory to conduct detailed chemical characterization studies. Therefore, in

order to develop cost effective long-term monitoring strategies, one would need simpler field methods that can be rapidly deployed and can used by minimally-trained field workers to identify oil spill residues. The focus of this study is to develop a practical field method for monitoring DWH oil spill residues that continue to be deposited along sandy GOM beaches in the form of SOM/SOAs.

As discussed before, DWH SOAs were formed by the rapid burial of emulsified mousse after it interacted with suspended sediments and sank in the nearshore environment. Our past laboratory studies and field observations have indicated that these conditions have resulted in forming oil residues that have distinctive physical characteristics (Joel S Hayworth et al., 2015; Mulabagal et al., 2013; F. Yin et al., 2015). The objective of this study is to develop a practical field method that can help assess some of these unique physical characteristics and use them to differentiate the DWH residues from other petroleum residues found along sandy GOM beaches. The robustness of the method was tested by analyzing several DWH residues along with other oil spill residues and comparing the results of the physical characterization method with the results obtained from detailed chemical characterization methods. This work is novel because, as per our knowledge, so far no one has developed a well-tested field protocol for identifying DWH oil spill residues based on a series of physical characterization tests.

2.2 Materials and methods

2.2.1 Details of the field samples

A total of 11 oil spill samples were used in this study. Sample-1 is a well-known DWH reference sample, which was collected by our team during a field survey completed on September 24, 2011, at a site located about 500 meters west of Lagoon Pass in Gulf Shores, Alabama. This survey was a joint SOM excavation survey completed by the U.S. Coast Guard,

Alabama, Department of Environmental Management and Auburn University. Sample 1 is considered as a DWH reference sample since it has been extensively analyzed in other published work (G. F. John et al., 2016).

Samples 2 through 6 were collected during a detailed beach survey which was completed by our team along the Alabama shoreline on November 11, 2015. During this survey, we collected 693 pieces of oil residues, with a total weight of 2,376 g, from five beaches located in between Fort Morgan and Orange Beach. Figure 2.1a (left) shows all the samples collected during this survey, and Figure 2.1b (right) shows a close-up view of samples collected from Fort Morgan beach (beach length ~1 km) facing the Mobile Bay. Table 2.1 provides a summary of the size distribution of the residues collected during this survey. Sizes of the samples were determined by measuring the length (largest dimension) using a ruler. Samples 2 through 6 were random samples selected from the residues collected at Lagoon Pass (30°14'24.0"N 87°44'24.0"W), Fort Morgan (30°13'52.1"N 88°01'15.2"W), Morgan Town (30°13'50.38"N 87°54'33.69"W), Bon Secour (30°13′44.90″N 87°49′41.26″W) and Orange Beach (30°16'18.6"N 87°34'18.0"W), respectively.

Figure 2.1 Oil spill residues collected from five different Alabama beaches on November 11th 2015 in the left side picture and residues collected from Fort Morgan (218 samples of total weight 836 grams; sampling distance ~1 km, and sampling time ~1 hour) in the right side picture.

Table 2.1 Details of DWH oil spill residues collected during a field survey completed on Nov. 11, 2015.

Location	Weight (g)	Total numbers	Size Distribution (cm)				
			~1	~2	2-3	3-4	4-7
Lagoon Pass	685	108	84	47	25	19	5
Fort Morgan	836	218	102	61	17	29	9
Morgan Town	373	107	35	46	13	12	1
Bon Secour	330	80	70	23	12	3	-
Orange Beach	152	180	32	34	6	8	-

Sample 7 was collected by our team from a beach in Goa, India (15°34'33.8"N 73°44'24.2"E), on September 15, 2014; tar balls are routinely deposited by southwest monsoon currents on several of Goa's beaches (Suneel, Vethamony, Zakaria, Naik, & Prasad, 2013). Sample 8 was retrieved by our team from Gulfport, Mississippi (30°21'32.3"N 89°06'30.6"W) during a field survey completed in January 2013. Sample 9 was collected by our team in Grand Isle, Louisiana (29°14'11.8"N 89°59'14.3"W) during our field survey completed in January 2013. Sample 10, which looked like a traditional tar ball, was collected from Orange Beach, Alabama (30°16'18.6"N 87°34'18.0"W), during our November 2015 survey. Sample 11 was provided by the Texas General Land Office and was collected at a beach near Houston area (GPS coordinates are not available).

2.2.2 Details of the proposed protocol

Figure 2.2 summarizes the details of the proposed field testing protocol, which is a two-tier procedure that uses multiple physical characterization methods. As shown in the Figure, the protocol includes a set of simple screening tests that can be conducted at any field site (identified as Tier-1 tests), and a set of confirmation tests that can be conducted in a temporary field

laboratory (identified as Tier-2 tests). The Tier-1 tests can be conducted by any non-technical personal by following a simple set of directions that can be summarized in a two-page pamphlet. The Tier-2 tests require basic chemistry training and a temporary field laboratory. Since Tier-2 tests are confirmatory tests they can be done later, on a limited number of sub samples. In addition to Tier-1 and Tier-2 tests, we have also completed a series of advanced fingerprinting tests (identified as Tier-3 tests). The Tier-3 tests are not a part of the proposed field protocol; they were completed in this study to verify the results of the protocol. In routine field projects, the Tier-3 tests should only be occasionally performed to verify the findings.

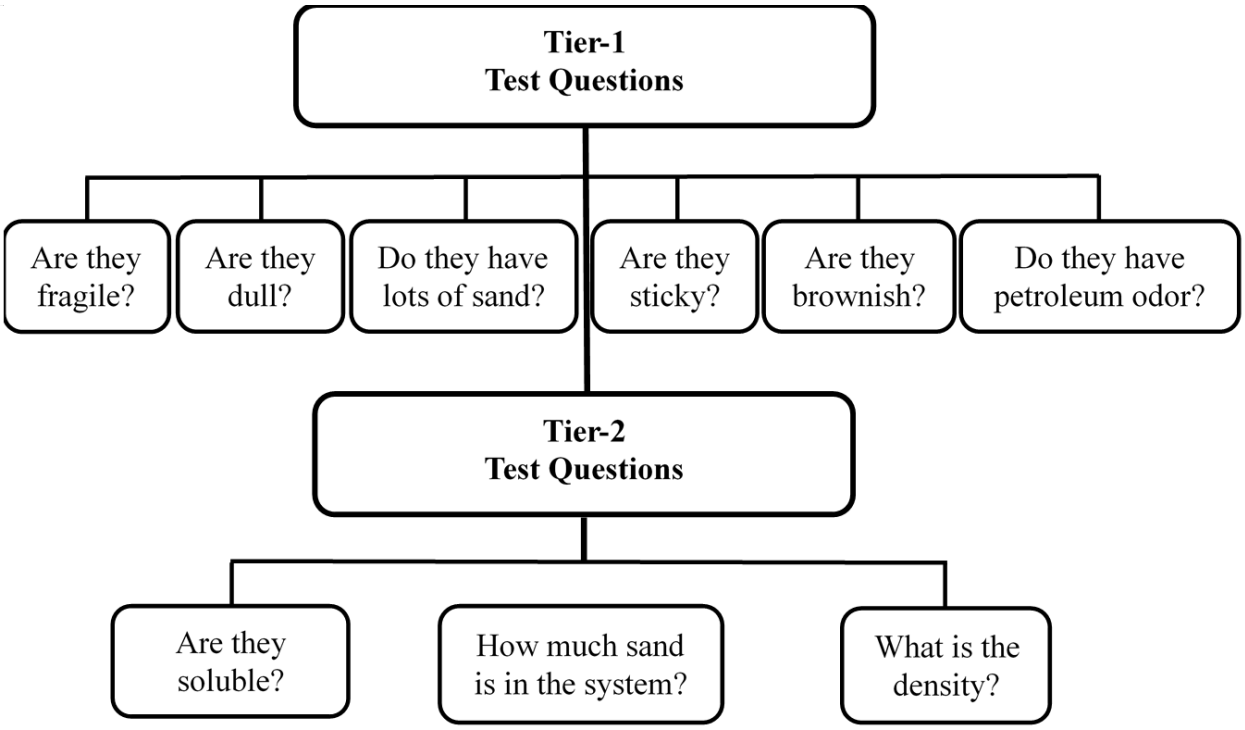

Figure 2.2 Details of proposed field testing protocol for identifying DWH oil spill residues.

2.2.2.1 Tier-1 field testing methods

During field surveys, the oil spill residues can either be directly picked up by hand from dry beaches, or can be collected using a crab net from the swash zone (Joel S Hayworth et al., 2015). The Tier-1 screening tests were designed based on the results from previously published

studies which have demonstrated that the DWH oil spill residues found along sandy GOM beaches are fragile, dull, sticky, brownish and petroleum-smelling agglomerates that contain considerable amount of sand content (Clement et al., 2017; Joel S Hayworth et al., 2015; F. Yin et al., 2015). As part of this screening procedure, six screening tests should be completed to answer the following set of yes or no question:

1) Strength test: Are the samples fragile (as opposed to being hard and rubbery)? The objective is to test whether the samples can be easily broken apart into sand-grain sized particles.
2) Shine test: Are they dull? (typical DWH residues will be dull, whereas the non-DWH tar balls will be shiny, especially when they are broken apart)
3) Sand test: Do they have considerable amount of sand (as opposed to little or no sand)?
4) Stickiness test: Are they sticky when squeezed between fingers? When DWH oil spill residues are squeezed they will leave sticky residues.
5) Color test: Do they look brownish when broken apart? Typical DWH residues break into brownish aggregates (as opposed to dark black solids).
6) Odor test: Do the residue have a strong petroleum odor (as opposed to little or no petroleum odor)?

If the answers to all of the above questions are yes, it is likely that the residues have originated from the DWH oil spill.

2.2.2.2 Tier-2 field testing methods

The Tier-2 tests are confirmatory tests that simply add further evidence to support Tier-1 findings. These tests require a makeshift laboratory that can be setup in a local public facility or

in a temporary field facility. As part of Tier-2 screening, we propose to conduct the following two confirmatory tests:

1) Solvent test: Under field conditions, at times, it is difficult to distinguish certain petroleum residues from other marine debris. However, it has been well established that all types of petroleum residues are soluble in an organic solvent. The objective of this solvent test is to examine whether the sample will dissolve in an organic solvent (such as hexane, dichloromethane or gasoline). Commercial gasoline can be used if the test needs to be done in a field laboratory. Preliminary experiments completed in our laboratory have shown that DWH oil spill residues are fully soluble in commercial gasoline. If the solvent test was completed in a chemical laboratory, it is preferable to use dichloromethane since it can easily dissolve DWH residues as well as other highly weathered tar balls. It is important to note that the primary objective of the solubility test is to differentiate petroleum residues from other dark looking marine debris. A positive solvent test provides a conclusive evidence that the sample is indeed a petroleum residue. Furthermore, the DWH oil spill samples typically would dissolve in an organic solvent to yield a characteristic brownish solution, and also leave considerable amount of inorganic debris, such as sand and crushed shell fragments, at the bottom. These observations add further evidence that the sample could be of DWH origin.

2) Sand-content/ density test: The objective of this test is to evaluate sand and oil contents of the sample and use them to compute the relative density of the residue. The OSAT-2 (2011) study has shown that DWH oil spill residues (both SOM and SRB/SOA samples) will have very high sand content ranging from 83.2% to 95.8% of sand by mass. Other previously published studies have also shown that the sand content in DWH residues collected from the Alabama beaches can range from 75% to 90% (Mulabagal et al., 2013; F. Yin et al., 2015).

In order to estimate the amount of sand and shell fragments, the sample should be first homogenized by squeezing between fingers, and the aggregates should be gently dried using a paper towel. About 2 to 3 grams of the homogenized sample should be weighed using an analytical balance and transferred into a glass vial. The sample should then be sequentially washed using about 5 mL of organic solvent for at least four times. The dissolved oil should be decanted and discarded after each wash. The solids remaining at the bottom (DWH residues will have considerable amount of sand or shell fragments) should be first dried using a paper towel and then air-dried for a few minutes (to let all the residual solvents evaporate). The dried sample should be weighed to compute the sand fraction (f_{sand}) and oil fraction (f_{oil}) using the following formulae: foil = (wt. of original sample – wt. of sand)/wt. of original sample; and $f_{sand} = 1 - f_{oil}$.

Density is an important physical parameter that can be used to differentiate DWH residues from traditional tar balls. Since DWH residues are a mixture of oil and sand (formed after the floating mousse sank mixing with sediments or after the beached mouse was buried under sand (Gustitus & Clement, 2017)), their relative density should always be higher than 1. According to a USGS study, the average relative density of DWH residues should be around 2 (Plant, Long, Dalyander, Thompson, & Raabe, 2013). Traditional tar balls, in contrast, are mostly of pelagic origin (formed when the oil was floating over the ocean), and hence their relative density will be less than 1. In some cases, even traditional tar balls can sink after collecting little bit of sand on its surface. However, since most of these tar balls are made of hard and rubbery material, the sand particles cannot penetrate deep into the core and hence sand accumulation will be mostly limited to the surface, and therefore the net relative density can only be slightly higher than 1. Balkas et al. (1982) reported that the relative density of the traditional floating and/or sunken tar balls could range from 0.80 to 1.25.

The relative density of an oil spill residue can be computed from the oil and sand values using the formula (Plant et al., 2013): $\rho = (foil/0.9 + fsand/2.65)-1$. This formula assumes that these residues are two-phase systems (oil/sand), and neither water nor air will be trapped within the sample. This is a reasonable approximation for most traditional tar balls. However, our observations have indicated that large DWH SRB/SOAs found along dry beaches can trap some air and hence their effective density can be slightly lower than the value estimated using the above formula.

2.2.2.3 Tier-3 laboratory verification methods

Tier-3 uses several advanced laboratory testing methods that are primarily used here to validate the findings of the field protocol. All organic solvents used in this study were of analytical or higher grade. The organic solvents, silica gel (60-200 μm) and anhydrous sodium sulfate were purchased from VWR International (Suwanee, GA). A standard PAH mixture with 27 PAHs (naphthalene, 1-methylnaphthalene, 2-methylnaphthalene, 2,6-dimethylnaphthalene, 2,3,5-trimethylnaphthalene, biphenyl, acenaphthylene, acenaphthene, fluorene, phenanthrene, 1-methylphenanthrene, anthracene, dibenzothiophene, fluoranthene, pyrene, benzo(a)anthracene, chrysene, benzo(b)fluoranthene, benzo(j)fluoranthene, benzo(k)fluoranthene, benzo(e)pyrene, benzo(a)pyrene, perylene, dibenz(a,c)anthracene, dibenz(a,h)anthracene, indeno(1,2,3,-cd)pyrene and benzo(ghi)perylene) was purchased from Agilent Technologies (Wilmington, DE). The PAH surrogate standards (SS) consisting of naphthalene-d8, acenaphthene-d10, phenanthrene-d10 and benzo(a) pyrene-d12 were purchased from Ultra Scientific Analytical Solutions (North Kingstown, RI). Internal standard (IS) p-terphenyl-d14 (purity 98.5%) was purchased from AccuStandard (New Haven, CT).

The silica gel was activated according to a well-established protocol (Z. D. Wang, Fingas, et al., 1994b). Column chromatographic fractionation step was conducted following published methods (Z. D. Wang, Fingas, et al., 1994a; F. Yin et al., 2015). Briefly, a glass column (250 mm × 10 mm) with a Teflon stopcock was plugged with deactivated glass wool at the bottom and packed with 3 g of activated silica gel, and topped with 1 g of anhydrous sodium sulfate. The column was conditioned using 20 mL of hexane and the eluent was discarded. Sample containing about 25 mg of residual oil was weighed in a 12 mL vial and was dissolved using 1 mL of hexane. The solution was then spiked with 20 µL of 50 µg/mL four surrogate standards. The mixture was transferred to the column, and the vial was sequentially washed with 1 mL of hexane for twice; contents from sequential washes were transferred to the column. About 12 mL of hexane was added to the column to elute aliphatic hydrocarbon fractions, and this hexane fraction was labeled as F1. Then 15 mL of hexane: dichloromethane (50%, v/v) solvent mixture was used to elute the aromatic hydrocarbon fraction, and this fraction was labeled as F2. The F1 and F2 fractions were concentrated under a gentle stream of nitrogen and required amount of solvent was added to adjust the final volume to 10 mL. Exactly 1 mL of the adjusted F2 sample was spiked with internal standard of p-terphenyl-d14, prior to chemical analysis. All the samples were prepared in duplicate and analyzed in triplicate.

Agilent Gas Chromatograph coupled to an Agilent Mass Spectrometer was used to identify all the chemical compounds. Agilent's Mass Hunter software was used to analyze the data. Chromatographic separation of various PAH compounds was achieved using a J&W DB-EUPAH (Agilent Technologies) column (20 m × 180 µm × 0.14 µm).

F1 fraction analysis was accomplished using a GC/MS selected ion monitoring (SIM) mode. The hopanes and steranes fingerprints were observed at the target ion m/z values of 191

and 217, respectively. The electron ionization (EI) source temperature was set at 280°C with the carrier gas of Helium. The initial GC oven temperature of 50 °C (0.5 min hold) was ramped to 310 °C for 15 min at 6 °C/min, resulting in total run time of 58.8 min. Diagnostic ratios (DRs) were estimated by computing various peak areas.

The F2 fraction was used to analyze the five groups of parent PAHs (naphthalene, phenanthrene, dibenzothiophene, fluorine and chrysene) and their alkylated homologs using a SIM method. The EI source temperature was set at 350°C. The inlet temperature was set at 300 °C. The initial GC oven temperature of 50 °C (1 min hold) was ramped to 300 °C for 12 min at 5 °C/min, resulting in total run time of 63 min. Commercially available PAH standards for naphthalene, 2-methylnaphthalene, 2,6-dimethylnaphthalene, 2,3,5-trimethylnaphthalene, phenanthrene, 1-methylphenanthrene, dibenzothiophene, fluorine and chrysene were used for identifying and quantifying the above five groups of compounds.

The calibration curves of PAHs used seven concentration levels: 5, 10, 20, 50, 100, 200, 500 ng/mL. All the calibration curves were found to be linear within the target concentration range. Since several alkylated PAHs standards are not commercially available, a semi-quantitative method was employed by using a relative response factor (RRF) to estimate alkylated PAH concentrations (G. F. John et al., 2016; Kirman et al., 2016). Specifically, C0-naphthalene was quantified by using naphthalene response; C1-naphthalenes by 2-methylnaphthalene; C2-naphthalenes by 2,6-dimethylnaphthalene; and C3- and C4-naphthalenes by 2,3,5-trimethylnaphthalene; C0-phenanthrene was quantified by phenanthrene; and C1- to C4-phenanthrenes by 1-methylphenanthrene. C0- to C3-dibenzothiophenes were quantified by dibenzothiophene; C0- to C3-fluorenes were quantified by fluorine, and C0- to C4-chrysenes were quantified by chrysene.

The F2 fraction of each sample was spiked with the internal standard p-terphenyl-d14 to compensate for any instrument variations. Four surrogate standards (naphthalene-d8, acenaphthene-d10, phenanthrene-d10 and benzo(a)pyrene-d12) were used to quantify recovery levels. The recovery levels of the four surrogates ranged from 72-91%, 69-95%, 70-97% and 85-131%, respectively. The limit of detection (LOD) and limit of quantitation (LOQ) for the PAH characterization method has been previously established as 0.20 to 3.65 ng/mL and 0.24 to 4.32 ng/mL, respectively (F. Yin et al., 2015).

2.3 Results and discussion

2.3.1 Tier-1 test results

Figure 2.3 shows digital photographs taken while conducting the Tier-1 tests for all the samples, except for Sample 1, a known DWH reference sample (G. F. John et al., 2016). As shown in Figure 2.3, Samples 2 to 6 were all brownish samples with little or no shine. Samples 1 to 6 matched all the physical characteristics of DWH residues: they were all fragile, can be easily broken apart into fine fragments, contained large amounts of sand, and they left a sticky brownish stain on the finger. Samples 7 to 11 did not match one or more of the DWH residue physical characteristics. Specifically, Samples 7 to 11 were all dark (blackish), hard solid masses and hence were deemed as likely non-DWH residues. Some of these samples did have one or two DWH residue characteristics. For example, Sample 7 was sticky and soft and had a strong petroleum odor; Sample 8 was dull looking and had some petroleum odor; Sample 9 was dull looking; and Sample 10 had plenty of sand. Sample 11 was the only sample that failed to yield positive results to all six screening tests.

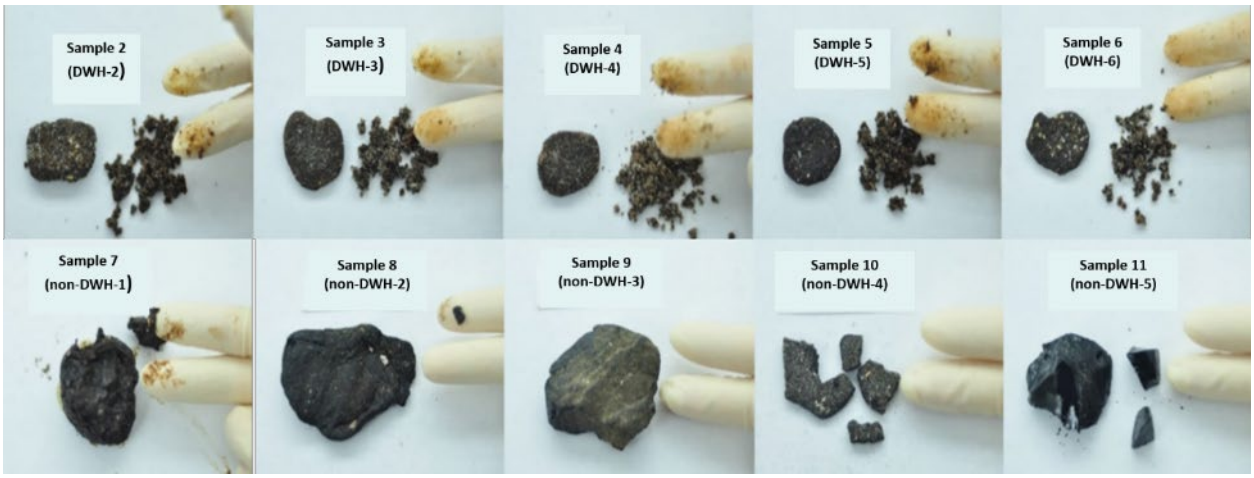

Figure 2.3 Tier-1 test results for the field samples.

The results of all six Tier-1 screening tests completed for all 11 test samples are summarized in Table 2.2. The last column in this table indicates the preliminary conclusion that identifies the sample either as a DWH sample or as a non-DWH sample. In this protocol, a sample will be identified as a DWH sample if and only if all six screening test results are positive. If a sample yielded negative result even for one of the Tier-1 tests then it will be designated as a non-DWH sample. As shown in the table, Samples 1 to 6 yielded positive results for all six screening tests and hence were identified as DWH samples. Samples 7 to 11 did not yield positive result to one or more of the screening tests and hence were identified as non-DWH samples. Although, some of samples were already known to be non-DWH samples (for example, the Goa sample that came from India). In this study, we identified a sample as a non-DWH sample if and only if it failed to yield a positive answer to one or more of the Tier-1 screening questions. In addition to above tests, we also conducted Tier-1 screening tests to rapidly screen all 693 residues collected from Alabama's beaches during our November 2015 survey (samples shown in Figure 2.1). Except for one sample (which was used as our test sample 10), all other 692 samples tested positive and had all six DWH oil spill residue characteristics.

Table 2.2 Summary of Tier-1 screening test results for all the field samples.

Sample name	Field screening of physical properties						Partial conclusion
	Fragile	Dull	Contain lot of sand	Sticky	Brownish	Petroleum odor	
Sample 1	Yes	Yes	Yes	Yes	Yes	Yes	DWH-1
Sample 2	Yes	Yes	Yes	Yes	Yes	Yes	DWH-2
Sample 3	Yes	Yes	Yes	Yes	Yes	Yes	DWH-3
Sample 4	Yes	Yes	Yes	Yes	Yes	Yes	DWH-4
Sample 5	Yes	Yes	Yes	Yes	Yes	Yes	DWH-5
Sample 6	Yes	Yes	Yes	Yes	Yes	Yes	DWH-6
Sample 7	No	No	No	Yes	No	Yes	Non-DWH-1
Sample 8	No	Yes	No	No	No	Yes	Non-DWH-2
Sample 9	No	Yes	No	No	No	No	Non-DWH-3
Sample 10	No	No	Yes	No	No	No	Non-DWH-4
Sample 11	No	No	No	No	No	No	Non-DWH-5

2.3.2 Tier-2 tests results

2.3.2.1 Solvent-test results

All eleven samples fully dissolved in the organic solvent (dichloromethane was used in this study). The solvent test indicated that all the samples are petroleum residues, and are not other marine debris. Samples 1 through 6 (DWH samples) dissolved to yield a brownish solution with considerable amount of white sand settling at the bottom of the vial. The non-DWH samples dissolved to yield a black solution with very little or no sediments at the bottom.

2.3.2.2 Sand-content and density test results

Table 2.3 provides a summary of sand-content data collected for all 11 samples. The sand content of the DWH samples ranged from 77% to 87%, which is consistent with other published data (Mulabagal et al., 2013; OSAT-2, 2011; F. Yin et al., 2015). The sand content values for most of the non-DWH samples (Sample 8, 9 and 11) were extremely low and ranged from 1% to 4%. However, two non-DWH sample did have relatively high amount of sand; Sample 7 (non-DWH-1) had 22% sand and Sample 10 (non-DWH-4) had 75% sand. The table also provides a

summary of density values estimated for all 11 samples. The data show that the relative density values for DWH samples range from 1.83 to 2.12, which is within the expected range (Plant et al., 2013). The relative density values for all the non-DWH samples, except for Sample 10 (non-DWH-4), were around 1, which is also consistent with literature data (Balkas et al., 1982). The Sample 10 was a clear outlier and had very high sand content and density values; however as shown in Table 2.2, this sample failed all other screening tests and hence it cannot be a DWH residue.

Table 2.3 Summary of the results of Tier-2 tests.

Sample name		Solubility in DCM	Sand content	Density
Sample 1	DWH-1	Soluble	0.87	2.12
Sample 2	DWH-2	Soluble	0.83	2.00
Sample 3	DWH-3	Soluble	0.85	2.04
Sample 4	DWH-4	Soluble	0.80	1.91
Sample 5	DWH-5	Soluble	0.82	1.95
Sample 6	DWH-6	Soluble	0.77	1.83
Sample 7	Non-DWH-1	Soluble	0.22	1.05
Sample 8	Non-DWH-2	Soluble	0.04	0.92
Sample 9	Non-DWH-3	Soluble	0.01	0.90
Sample 10	Non-DWH-4	Soluble	0.75	1.78
Sample 11	Non-DWH-5	Soluble	0.01	0.90

2.3.3 Verification of the proposed field test results using Tier-3 chemical characterization datasets

2.3.3.1 Results of hopane and sterane fingerprints

Source specific biomarkers such as hopane and sterane are widely used for forensic fingerprinting of oil spill residues. Biomarker compounds can provide important data for identifying the origin of the oil, monitoring the degree of weathering, and for quantifying biodegradation processes occurring under different environmental conditions (Mervin Fingas, 2016; Z. D. Wang & M. Fingas, 2003). Crude oils can be differentiated based on the relative

distribution of different types of hopanes and steranes, and also the concentration levels of various other chemicals (Hostettler et al., 2013; Z. D. Wang et al., 1999; Z. D. Wang, Stout, et al., 2006). In this study we used hopanes and steranes to verify the findings of the proposed protocol that only Samples 1 to 6 should have originated from the DWH oil spill.

The diagnostic ratios (DRs) of various hopanes levels in all 11 test samples are listed in Table 2.4. These data show that seven different hopane DRs for Samples 2 to 6 are similar to the values estimated for Sample 1, a reference sample which has already been tested to match the fingerprint of DWH source crude (G. F. John et al., 2016). These data show that the Samples 2 to 6 must have originated from the DWH oil. On the other hand, several of the DRs of non-DWH samples, especially the values of Ts/Tm and C29/C30, are significantly different from DWH samples indicating that these residues must have originated from sources other than the DWH crude. The ratios Ts/Tm and C29/C30, are some of the most reliable DRs that have been widely used for identifying petroleum sources (C. Aeppli et al., 2014; Peters et al., 2005; Z. D. Wang, Fingas, & Sergy, 1994). When compared to Tm, Ts is more stable and less susceptible to degradation during sedimentation and diagenesis and therefore the ratio of Ts/Tm is an indicator of oil maturity (Shen, 1984). Larger Ts/Tm indicates the higher maturity level of the crude oil. Similarly, C29 and C30 are another important set of thermodynamically stable hopanes that are resistant to weathering even under extreme conditions, and hence they are widely used for source identification (Peters et al., 2005). Also, C29 and C30 are typically the most abundant hopanes in crude oils and therefore the ratio of C29/C30 can be estimated with a higher level of certainty (Z. D. Wang, Fingas, & Sergy, 1994). The other five ratios are similar for all the 11 samples (see Table 2.4), indicating that these ratios are not good indicators for differentiating these oils. All seven different DRs of the five non-DWH samples are summarized in the form of radar plots

and are then compared against the Sample 1 radar plot in Figure 2.4. These figures futher show that all the non-DWH samples must have originated from different types of sources.

Table 2.4 The diagnostic ratios (DRs) of hopanes for all the field samples.

Sample name	Ts/Tm	C29/C30	C31S/C31 (S+R)	C32S/C32 (S+R)	C33S/C33 (S+R)	C34S/C34 (S+R)	C35S/C35 (S+R)
DWH oil	0.91	0.38	0.61	0.65	0.60	0.67	0.61
Sample 1	0.92	0.36	0.59	0.59	0.58	0.59	0.59
Sample 2	0.94	0.37	0.59	0.59	0.59	0.61	0.60
Sample 3	0.93	0.37	0.59	0.60	0.59	0.60	0.58
Sample 4	0.93	0.38	0.59	0.59	0.60	0.60	0.59
Sample 5	0.93	0.36	0.59	0.60	0.59	0.59	0.58
Sample 6	0.93	0.36	0.60	0.60	0.59	0.60	0.59
Sample 7	0.53	0.56	0.57	0.60	0.63	0.69	0.51
Sample 8	0.61	0.99	0.57	0.54	0.64	0.67	0.64
Sample 9	1.44	0.35	0.57	0.58	0.63	0.65	0.62
Sample 10	0.35	0.64	0.59	0.57	0.62	0.63	0.59
Sample 11	0.19	0.73	0.59	0.62	0.62	0.66	0.62

Figure 2.4 Radar plots of hopane diagnostic ratios of the field samples.

Similar to hopane, the relative distribution of various sterane compounds in a crude oil can be used to identify the oil source. Figure 2.5 shows the sterane chromatograms of all 11 samples presented in the form of mountain plots, which was developed by connecting various major peaks in sterane chromatograms. The figure shows that all DWH sample have similar looking mountain-peak pattern, whereas the non-DWH oils have mountain-peak patterns that are

different from the DWH oil pattern. These data once again confirm that Samples 1 to 6 are the only samples that must have originated from the DWH crude.

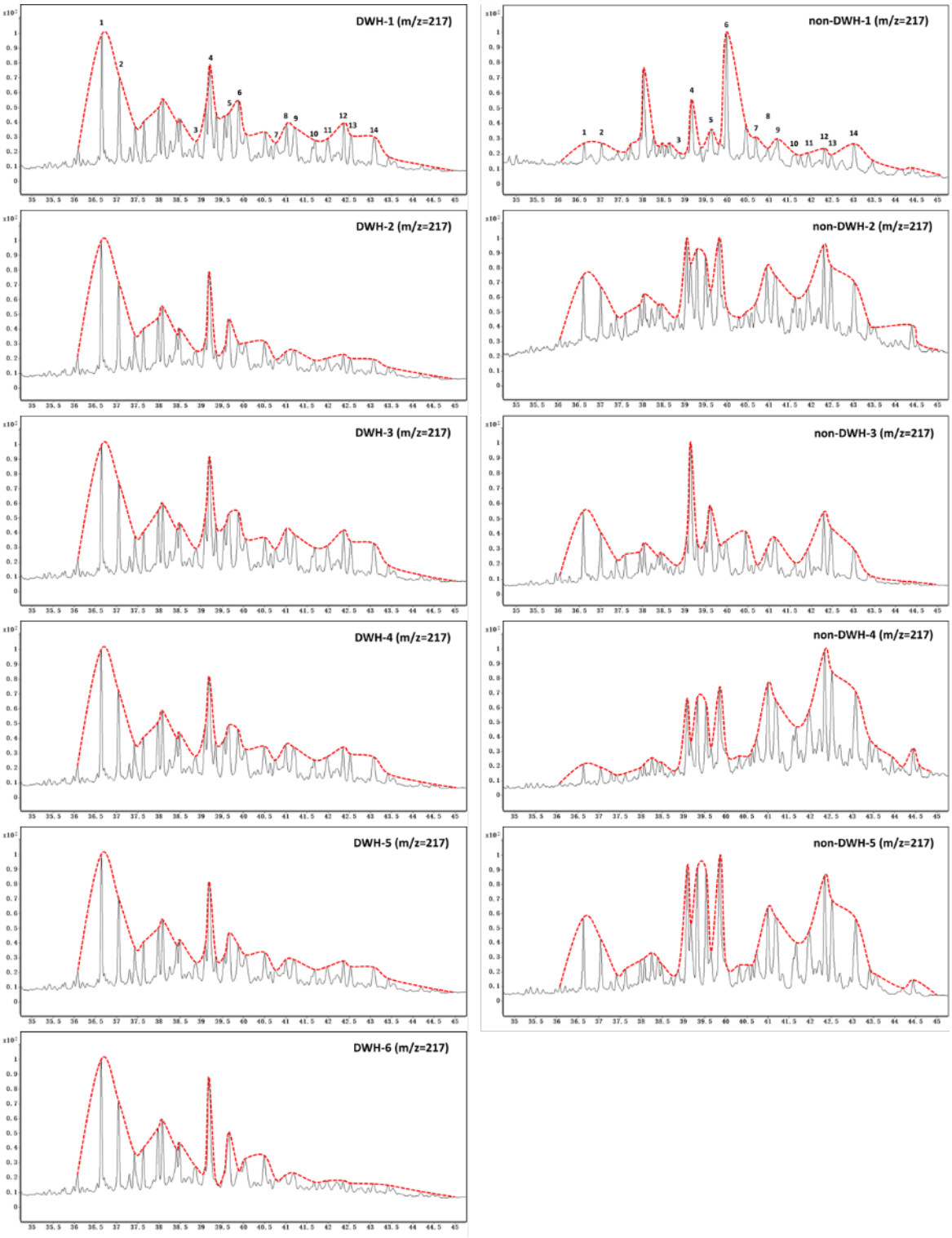

Figure 2.5 Mountain plots of sterane chromatograms (m/z = 217) for all eleven samples. Data for DWH residues are on the right and non-DWH samples are in the left. [Peak 1: DiaC27βα(S), 2: DiaC27βα(R), 3: C27ααα(S), 4: αββ(R), 5: C27αββ(S), 6: C27ααα(R), 7: C28ααα(S), 8: C28αββ(R), 9: C28αββ(S), 10: C28ααα(R), 11: C29ααα(S), 12: C29αββ(R), 13: C29αββ(S), 14: C29ααα(R)].

2.3.3.2 Analysis of PAH data

PAHs are an important group of toxic compounds present in oil spill residues, and several of them are listed in USEPA's priority pollutant list (USEPA, 1993). Investigators have used the relative distribution of different types of PAHs to distinguish the oil spill source (Z. Wang, Fingas, & Sergy, 1995; Z. D. Wang et al., 1999; Fang Yin, Hayworth, & Clement, 2015). The concentration distribution of 5 major types of most abundant PAHs (naphthalenes, fluorenes, phenanthrenes, dibenzothiophenes and chrysenes) and their alkylated PAH homologs in all eleven oil spill samples were estimated, and results are summarized in Table 2.5. Figure 2.6 shows the relative distribution of these five major groups of PAHs in all eleven samples. These data show that the six DWH samples have similar distribution patterns, whereas the non-DWH samples have different patterns. The concentration data summarized in the table indicate that among the 5 groups of major PAHs, phenanthrene and its alkylated homologs are the most dominant compounds in all DWH samples, ranging between 44% to 63% of total PAHs. The percentage of phenanthrenes in Samples 7 through 11 (non-DWH samples) are: 40%, 24%, 39%, 20% and 10%, respectively; overall, these values are relatively lower when compared to DWH sample values.

Table 2.5 Concentrations of PAHs measured in all the field samples.

Compound	Sample 1	Sample 2	Sample 3	Sample 4	Sample 5	Sample 6	Sample 7	Sample 8	Sample 9	Sample 10	Sample 11
C_0-naphthalene	DL	DL	DL	DL	DL	DL	DL	DL	DL	DL	77.8
C_1-naphthalenes	DL	DL	DL	DL	DL	DL	6.4	DL	DL	DL	149.2
C_2-naphthalenes	11.3	7.1	5.9	7.5	6.9	7.7	235.7	15.8	9.6	12.5	575.4
C_3-naphthalenes	72.6	19.0	11.4	14.0	19.9	16.9	706.0	29.1	16.0	24.2	291.4
C_4-naphthalenes	169.0	51.4	14.6	17.4	40.9	33.6	1056.6	35.0	23.6	31.4	336.4
C_0-phenanthrene	65.3	4.1	4.3	6.9	3.7	3.5	92.8	4.7	4.5	3.5	23.6
C_1-phenanthrenes	506.0	19.7	56.9	12.3	28.6	5.6	508.5	10.9	15.0	3.6	60.2
C_2-phenanthrene	728.2	239.9	179.2	130.9	289.5	154.6	738.2	21.2	48.8	11.7	64.0
C_3-phenanthrene	435.3	275.8	144.1	162.3	316.5	208.6	504.1	23.1	85.7	16.2	61.2
C_4-phenanthrene	222.5	181.0	95.6	115.8	176.3	126.4	287.8	21.3	80.0	20.8	64.4
C_0-dibenzothiophene	7.9	2.8	2.6	2.9	2.5	2.7	34.4	3.4	2.9	2.8	176.4
C_1-dibenzothiophenes	34.0	4.8	5.2	4.1	4.7	4.1	66.6	6.0	4.5	4.1	171
C_2-dibenzothiophenes	76.4	20.0	17.2	12.0	24.4	15.1	79.5	9.9	8.7	5.1	188.6
C_3-dibenzothiophenes	58.6	30.4	20.0	20.1	35.3	23.7	52.0	11.4	11.2	6.7	142.8
C_0-fluorene	5.0	2.9	2.8	3.0	2.7	2.9	9.5	3.5	3.2	3.2	16.4
C_1-fluorenes	59.9	15.6	10.4	12.2	15.6	12.7	123.9	15.3	14.2	19.3	52.0
C_2-fluorenes	134.3	26.2	15.1	14.6	27.0	18.5	218.9	14.8	13.3	16.6	48.0
C_3-fluorenes	171.5	69.9	36.7	34.0	78.8	56.9	280.1	35.1	32.2	41.8	114.2
C_0-chrysenen	62.6	54.7	45.2	46.2	59.8	45.6	36.8	1.5	17.3	0.1	1.2
C_1-chrysenens	95.9	89.1	65.7	68.9	92.5	68.5	45.8	4.4	33.5	1.7	2.6
C_2-chrysenens	73.4	61.7	41.7	43.6	65.4	47.1	55.9	6.8	58.5	4.1	6.8
C_3-chrysenens	30.6	22.2	14.1	14.9	23.6	17.2	35.9	5.8	44.5	5.2	6.6
C_4-chrysenens	12.0	8.7	6.5	7.6	10.1	7.2	13.7	3.3	15.8	3.0	2.6

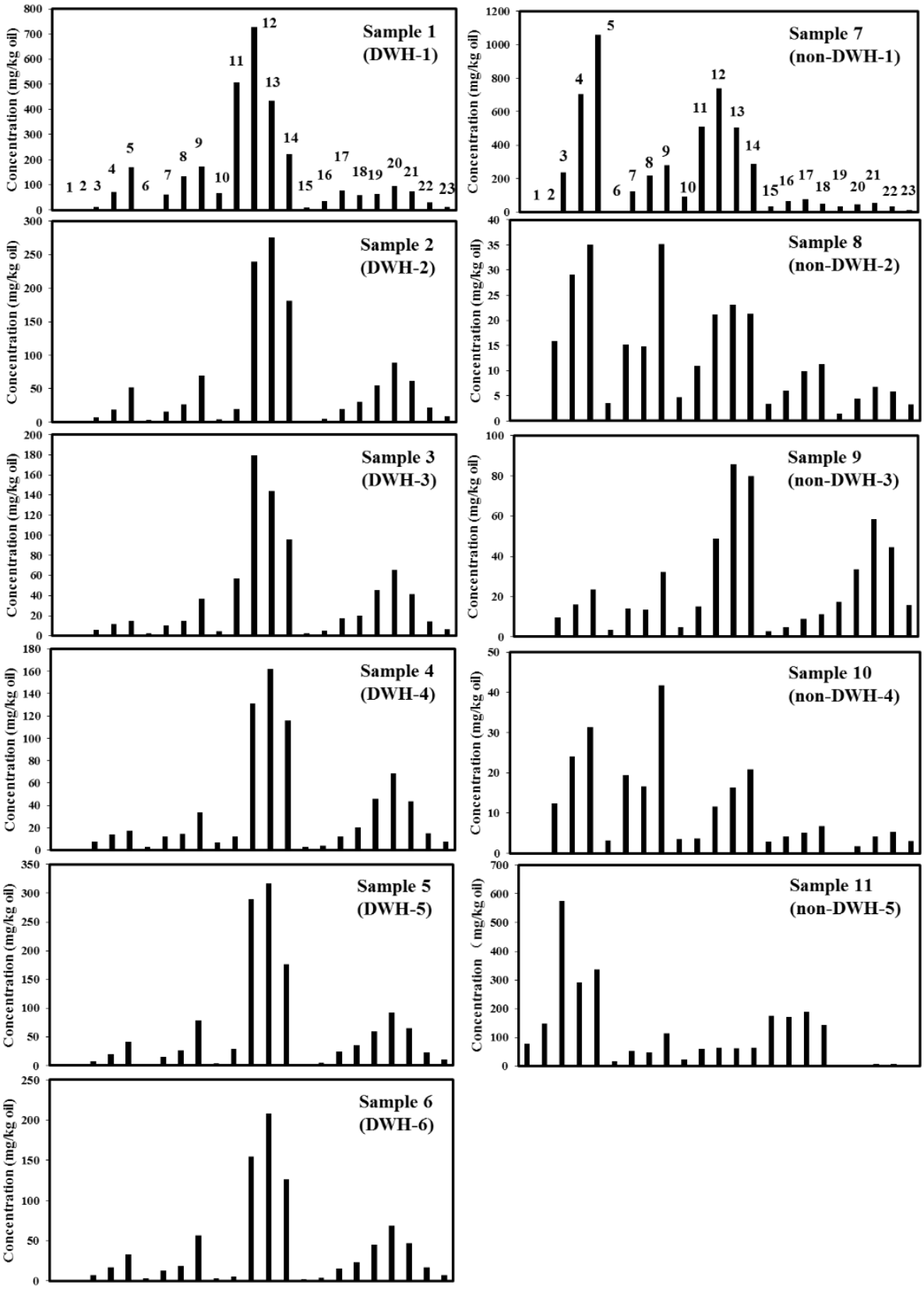
Sample 1
(DWH-1)
Sample 2
(DWH-2)
Sample 3
(DWH-3)
Sample 4
(DWH-4)
Sample 5
(DWH-5)
Sample 6
(DWH-6)
Sample 7
(non-DWH-1)
Sample 8
(non-DWH-2)
Sample 9
(non-DWH-3)
Sample 10
(non-DWH-4)
Sample 11
(non-DWH-5)
Concentration (mg/kg oil)

Figure 2.6 Comparison of PAH concentration levels of five important groups of PAHs and their alkylated homologs in the field samples. [1: C_0-naphthalene, 2: C_1-naphthalenes, 3: C_2-naphthalenes, 4: C_3-naphthalenes, 5: C_4-naphthalenes, 6: C_0-fluorene, 7: C_1-fluorenes, 8: C_2-fluorenes, 9: C_3-fluorenes, 10: C_0-phenanthrene, 11: C_1-phenanthrenes, 12: C_2-phenanthrenes, 13: C_3-phenanthrenes, 14: C_4-phenanthrenes, 15: C_0-dibenzothiophene, 16: C_1-dibenzothiophenes, 17: C_2-dibenzothiophenes, 18: C_3-dibenzothiophenes, 19: C_0-chrysene, 20: C_1-chrysenes, 21: C_2-chrysenes, 22: C_3-chrysenes, 23: C_4-chrysenes].

2.4 Summary and conclusions

In this study, we propose a two-tier field testing protocol for monitoring DWH oil spill residues found along sandy GOM beaches. The proposed method uses six physical characterization tests to differentiate DWH residues from other types of petroleum residues. The field protocol was tested using eleven field samples collected from different sites. The goal was to use the protocol to test a working hypothesis that these eleven field samples could have originated from the DWH oil. The Tier-1 analysis for Samples 1 to 6 yielded positive results for all the physical characterization tests, and hence supported the hypothesis that these samples must have originated from the DWH oil. The Tier-2 results indicated that Samples 1 to 6 will dissolve in an organic solvent, and their relative density values are close to 2. These results provided further confirmative evidence for supporting the hypothesis. The Samples 7 to 11, on the other hand, yielded negative results for one or more of the Tier-1 tests. Therefore, we reject the working hypothesis and conclude that Samples 7 to 11 did not originate from the DWH oil spill. These conclusions were independently verified by completing a detailed set of advanced chemical characterization tests on all eleven samples. The chemical characterization results verified the conclusions derived using the proposed field testing protocol.

As pointed out in previous studies (Clement et al., 2017; Joel S Hayworth et al., 2015), the sandy beaches located along the GOM shoreline, which were severely impacted by the DWH spill, have been slowly recovering for the past eight years. However, some of these beaches are continuing to be impacted by the residues trapped in the nearshore environment. For example,

the DWH mousse submerged near the Alabama shoreline still continue to deposit large amount of oil spill residues along Alabama's amenity beaches; this has increased the background oil level in this region by about four orders of magnitude (Clement et al., 2017). Furthermore, these DWH residues contain considerable amounts of recalcitrant toxic PAHs that are weathering rather slowly (G. F. John et al., 2016; Mulabagal et al., 2013; F. Yin et al., 2015). Therefore, it is important that we continue to monitor the fate of DWH oil spill residues and fully understand their long-term environmental impacts. Unfortunately, the local city/municipal offices or environmental management agencies have very little resource to employ highly trained laboratory staff to conduct these long-term beach monitoring surveys. If and when possible, they instead use field workers and/or volunteers to conduct these surveys. Also, the amount of oil deposited along these beaches can have large variations, and the rates can increase substantially after a major storm event (Joel S Hayworth et al., 2015). For example, a few days after the landfall of Tropical Storm Isaac (which crossed the GOM shoreline on August 29, 2012) our team collected about 11 kg of residues from the Alabama shoreline (Dave & Ghaly, 2011). In situations like these, it is cost-prohibitive to conduct detailed laboratory characterization studies on all these samples. Therefore, there is a need for a simple field method that can be cost-effectively used by field workers to rapidly identify DWH oil spill residues. Our study addresses this need and provides a reliable, cost-effective, practical field approach for differentiating DWH residues from other types of petroleum residues.

Chapter 3

Fate of hopane biomarkers during in-situ burning of crude oil – A laboratory-scale study

3.1 Introduction

During a marine oil spill event, numerous remediation methods are employed to reduce various environmental impacts. One of the commonly used oil spill remediation methods is in-situ burning (ISB), also known as controlled burning (Atle B Nordvik, 1995; Ventikos, Vergetis, Psaraftis, & Triantafyllou, 2004). ISB has gained widespread acceptance since it is a relatively easy method (Z. Wang et al., 1999) and it has the potential to rapidly remove large volumes of oil from the surface of the water (Buist, 2003; Mullin & Champ, 2003). The removal efficiency of ISB depends on oil type, oil thickness, water content, and weathering level (Lin et al., 2005). One of the disadvantages of ISB is smoke generation, which can adversely impact the health of cleanup crews and the members of the public who are exposed to the smoke (Merv Fingas, 2014b; Mervin F Fingas et al., 1999; Janne Fritt-Rasmussen, Ascanius, Brandvik, Villumsen, & Stenby, 2013). However, the overall advantages of this technology far outweigh some of these disadvantages (Allen & Ferek, 1993).

ISB was one of the major remediation methods that was employed during the 2010 Deepwater Horizon (DWH) oil spill (Perring et al., 2011). It has been estimated that a total of 411 burns were used to remove about 222,000 to 313,000 barrels of oil, which is about 5% of total oil released during the DWH spill (Schaum et al., 2010). The removal efficiency of ISB events was estimated to be about 85%, and burning yielded about 38,800 to 54,700 barrels of residues that most likely sank to the ocean bottom (S. A. Stout & Payne, 2016). The long term

ecological impacts of these residues are largely unknown (J. Fritt-Rasmussen, Wegeberg, & Gustavson, 2015).

The physical characteristics of ISB residues are similar to those of highly weathered oil; they are viscous and dark tar-like residues, and have a higher density than the parent oil. They contain enriched amounts of asphaltenes, resins, metals, combustion-derived products, and toxic compounds such as polycyclic aromatic hydrocarbons (PAHs) (Gullett et al., 2017; Ramesh et al., 2018; S. A. Stout & Payne, 2016). Efforts to quantify the percent degradation of hazardous chemicals, such as PAHs, trapped in ISB residues require an internal recalcitrant biomarker compound. One of the most common oil spill biomarkers used for this purpose is C30-αβ hopane (17α(H), 21β(H)-hopane) (R. M. Garrett et al., 2000; Jézéquel, Simon, & Pirot, 2014). Additionally, diagnostic ratios of different hopane compounds are also routinely employed to develop chemical fingerprints, which are used for source identification (C. Aeppli et al., 2014; Clement et al., 2017; Han & Clement, 2018).

While hopanes, such as C30-αβ hopane, are known to be stable compounds since they are highly resistant to biochemical degradation (Roger C Prince et al., 1994), they can potentially undergo thermal degradation at higher temperatures. Prince et al. (1994) analyzed various distillation fractions of Alaska North Slope crude oil and found that the fraction collected in the range of 196 to 344 °C did not have any hopanes; this study noted that hopanes would volatilize at temperatures in excess of 344 °C (Roger C Prince et al., 1994). During ISB operations, the internal temperature of the slick can rise up to 350 to 500 °C and the flame temperature can reach up to 900 to 1200 °C (Buist, 2003; Mullin & Champ, 2003), and therefore these high temperature conditions could potentially impact hopane concentrations in the crude oil residues. However,

the thermal degradation patterns of other hopane compounds present in crude oil at these higher ISB temperatures are largely unknown.

Despite these uncertainties, C30-αβ hopane has been routinely employed as a conservative internal biomarker for characterizing ISB residues. Lin et al. (2005) measured the concentration of C30-αβ hopane in pre-burn and post-burn oil spill samples while evaluating the effects of ISB on oil spill cleanup at a coastal marsh. Their data showed that several high boiling fraction compounds, including C30-αβ hopane, became concentrated in the burnt residues. Stout and Payne (2016) characterized the chemical composition of floating and sunken ISB residues from the DWH oil spill and used C30-αβ hopane as a conservative biomarker to quantify the apparent enrichment of PAHs. Garrett et al. (2000) used C30-αβ hopane as a conservative biomarker to quantify the degradation of PAHs in a lab-scale ISB study. Jézéquel et al. (2014) used C30-αβ hopane as a conservative biomarker to assess the fate of various hydrocarbons in a bench-scale ISB study. All of these investigations assume that hopanes are stable compounds and are resistant to degradation during the burning conditions.

The objective of this study is to test the following two hypotheses: a) the internal biomarker C30-αβ hopane will remain as a conservative compound during the ISB process, and b) the characteristic hopane diagnostic ratios will remain stable and hence it can be used for fingerprinting ISB residues. We conducted two sets of controlled burning experiments using a model oil containing pure C30-αβ hopane and a reference crude oil collected during the DWH oil spill event to test the validity of these two hypotheses. In order to enhance the burning efficiency of oil in all our laboratory-scale ISB experiments, hexane was used as a burning aid.

3.2 Experimental methods

3.2.1 Materials

MC252 crude oil (released during DWH accident) was supplied by British Petroleum (BP). Since only a limited amount of MC252 crude oil was available in our laboratory, all the oil on water burning experiments, which required relatively large amount of oil, were conducted using MC252 surrogate oil supplied by AECOM (Fort Collins, CO, USA). This oil had similar physio-chemical characteristics as the MC252 oil and hence was identified as a surrogate to the original MC252 source crude oil (Pelz et al., 2014); in this study we referred to it as Surrogate Oil. The organic solvents dichloromethane and hexane used in this study were of analytical grade or higher. The solvents, silica gel (60–200 μm), and anhydrous sodium sulfate (ACS grade) were purchased from VWR International (Suwanee, GA). All hopane standards were purchased from Chiron (Trondheim, Norway). Chromatographic separation of various hydrocarbons was achieved using a J&W DBEUPAH (Agilent Technologies) column (20m×180 μm×0.14 μm).

3.2.2 Experimental design

The burning experiments were designed to be conducted within a laboratory hood which offered a controlled environment. For safety reasons, when burning the oil, the experiments were designed to have a smaller flame and generated minimum fumes and smoke that can be contained within the laboratory hood. In order to achieve higher degradation of oil in these laboratory setups, similar to that of a real world ISB event in the open ocean, the oil was relit several times. In order to enhance oil burning efficiency, we used hexane whenever the combustion ceased.

3.2.2.1 Model oil experiment

The model oil containing 200 ng/mL of C30-αβ hopane was prepared using hexane as the solvent. 1 mL of the model oil, which contained 200 ng of C30-αβ hopane, was added into an aluminum dish. The sample was lit in a fume hood using a kitchen lighter and the residue remaining after combustion was designated as the 1-burn sample. Typical combustion time for a burn ranged from 25 to 35 s. For preparing 2, 4, 8 and 16-burn samples, an additional 1 mL of hexane was added to the aluminum dish and mixed thoroughly with the residues of the previous burn, and then the sample was reignited. After the appropriate number of burns had been completed, the ISB residues in the aluminum dish were extracted using hexane, concentrated under a gentle stream of nitrogen and reconstituted to a total volume of 1 mL using hexane. The pre-burn (control) and post-burn solutions were spiked with C30-ββ hopane (IS) prior to GC/MS analysis. The 2, 8 and 16-burn experiments were completed in triplicates, and all GC/MS analyses were completed in duplicates.

3.2.2.2 Crude oil experiment

Literature data show that the concentration of C30-αβ hopane in fresh MC252 oil is about 50 mg/kg-oil (Mulabagal et al., 2013; Schantz & Kucklick, 2011). We took about 200 mg of MC252 oil and dissolved it in 5 mL of dichloromethane to prepare a solution containing crude oil concentration of 40 mg/mL. 100 μL of this solution was transferred into an aluminum dish, which resulted in an estimated C30-αβ hopane mass of about 200 ng in the dish, which is similar to that of the hopane content used in our model oil. Similar to the model-oil experiment, 1 mL of hexane was added to the aluminum dish and the contents were mixed and then lit sequentially to prepare 1, 2, 4, 8 and 16 burn samples. Small scale crude oil burning experiments are expected to have lower efficiency (van Gelderen, Malmquist, & Jomaas, 2017), however addition of

hexane helped to maintain sustained combustion and increased the overall burning efficiency. The post-burn residues in the aluminum dish were extracted using dichloromethane and the contents were transferred to a vial. 100 μL of pre-burn crude oil solution was also taken in a separate vial and was used as the control sample. The residual amount of dichloromethane solvent present in all the ISB samples was removed by evaporation under gentle stream of nitrogen prior to the sample cleanup step.

3.2.2.3 Burning oil on water surface

Under field conditions, spilled oil is typically collected using a boom and burnt over the ocean water. In order to test the efficiency of hopanes degradation processes under more realistic field conditions, we designed a laboratory experiment where the crude oil was burnt over water. Due to limited availability of the MC252 source crude oil, this burning experiment was conducted using the Surrogate Oil. About 10 g of Surrogate Oil was dissolved in a solvent mixture of hexane and dichloromethane (4:1) and diluted to 25 mL, yielding oil concentration of 0.4 g/mL. About 200 mL de-ionized water was taken in a 150 mL Erlenmeyer flask (water filled up to the flask neck), and 5 mL of the diluted oil solution was carefully introduced onto the water surface. The water was gently stirred at the bottom to ensure uniform temperature distribution; the stirring rate was extremely low to avoid mixing of oil and water. The oil was lit using a kitchen lighter. Since this is also a small scale burning, hexane was used to increase the overall burning efficiency. Whenever the combustion ceased, 4 mL of hexane was added and contents were lit again. This process was repeated until a total of 16 burns were completed. The water and oil residues were extracted with dichloromethane and made up to a volume of 300 mL. Control sample was prepared by adding 5 mL of oil solution onto the water surface, the contents were then extracted with dichloromethane and made up to a volume of 300 mL. And 3 mL of

this extract was taken and the dichloromethane was solvent-exchanged with hexane and fractionated using the cleanup method described in the previous section. The F1 fraction was adjusted to 5 mL using hexane, and 1 mL of the fraction was spiked with C30-ββ hopane prior to GC/MS analysis. All GC/MS analysis were conducted in duplicates. The control and burnt samples were analyzed in duplicates.

3.2.3 Column fractionation and GC/MS analysis

Column chromatographic fractionation for the crude oil was performed using an approach outlined in previous studies (G. F. John et al., 2016; Z. D. Wang, Fingas, et al., 1994a). A glass column (250mm×10 mm) was plugged with glass wool at the bottom, and then packed with 3 g of activated silica gel and topped with 1 g of anhydrous sodium sulfate. The chromatographic column was charged with 20 mL of hexane and the eluent was discarded. The control or ISB residue samples in the vials were sequentially extracted three times, using 1 mL hexane at each time, and the contents were transferred to the column. About 12 mL of hexane was added to the column to elute all aliphatic hydrocarbons. The eluent was then concentrated under gentle stream of nitrogen, adjusted to 1 mL using hexane, and was then spiked with C30-ββ hopane (IS) prior to GC/MS analysis. All GC/MS analyses were completed in duplicates.

Hopane content was analyzed using a GC/MS procedure described in the published literature (G. F. John et al., 2016; F. Yin et al., 2015). An Agilent 7890 gas chromatograph coupled with an Agilent 7000B triple quadrupole (QqQ) mass spectrometer was used. The GC oven temperature program is as follows: 35 °C (0.8 min hold); 7 °C/min to 120 °C (0 min hold); 5 °C/min to 240 °C (0 min hold); 3 °C/min to 320 °C (0 min hold) and a post run of 4 min at 330 °C with a total run time of 67.61 min. The temperatures of the electron ionization (EI) source and quadrupoles (Q1 and Q2) were set at 280 °C and 180 °C, respectively.

3.2.4 Quantification of hopane degradation

In this study, we employed a unique experimental design where the entire post-burn residue was always analyzed for quantifying the changes in hopane levels. This helped to minimize various experimental errors associated with other efforts that have analyzed subsamples taken from a larger burn (Jezaquel, 2014). To quantify the hopane loss in the model oil, the level of the C30-αβ hopane response for the control sample was first quantified by computing a ratio Hcontrol, which is the ratio of the peak area of C30-αβ hopane in control oil to the peak area of the IS. Similarly, Hburn level was estimated by computing the ratio of C30-αβ hopane in various burnt residues to the peak area of the IS. The percent remaining C30-αβ in burnt residues were estimated using the formula:

$$\%remaining = \left(\frac{H_{burn}}{H_{control}}\right) \times 100$$

The percent remaining for other types of hopane present in crude oil were also estimated using this method.

3.3 Results and discussion

Figure 3.1 shows the amount of C30-αβ hopane remaining in post-burn samples of the model oil and MC252 crude after 1, 2, 4, 8 and 16 burns and compares the results with control data (zero-burn samples). The extracted ion chromatograms of C30-αβ hopane and various terpanes (m/z of 191) of the two oil samples are presented in Figure 3.2. The hopane responses were normalized to internal standard C30-ββ hopane. These data show that the C30-αβ hopane abundance have decreased in both oils with increasing number of burns. After 16 consecutive burns, C30-αβ hopane level decreased by about 77% in the model oil, and by 39% in the crude oil. These results demonstrate that our first hypothesis that C30-αβ hopane will remain as a conservative biomarker during ISB events is false. Figure 3.2 also shows that the degree of

hopane degradation is much higher in the model oil containing pure hopane standard than in the crude oil. This is because hopane in the crude oil is mixed with other hydrocarbons and hence it could have been trapped within the oil matrix and was shielded by other compounds. On the other hand, hopane in the model oil would have been directly exposed to all thermal degradation processes. Therefore, it is reasonable to expect that the crude oil would require more number of burns to obtain a similar level of oil degradation observed for the model oil.

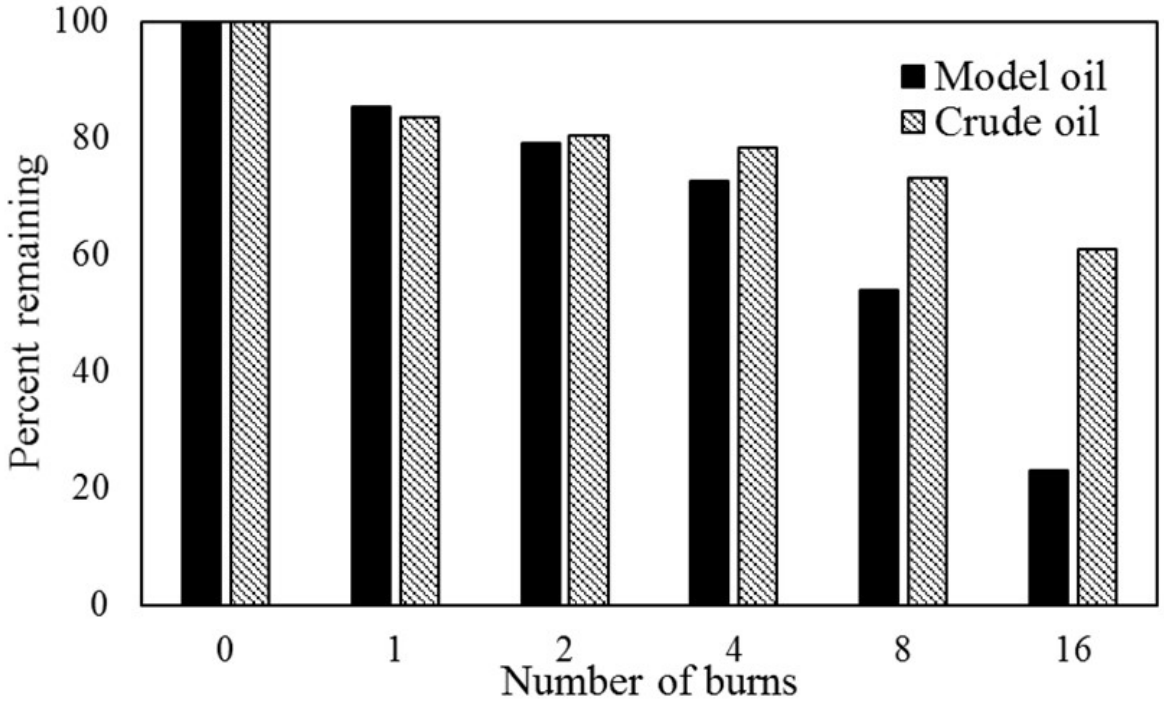

Figure 3.1 Comparison of C30-αβ hopane remaining in pre-burn and post-burn solutions of model and crude oils after 1,2,4,8 and 16 burns.

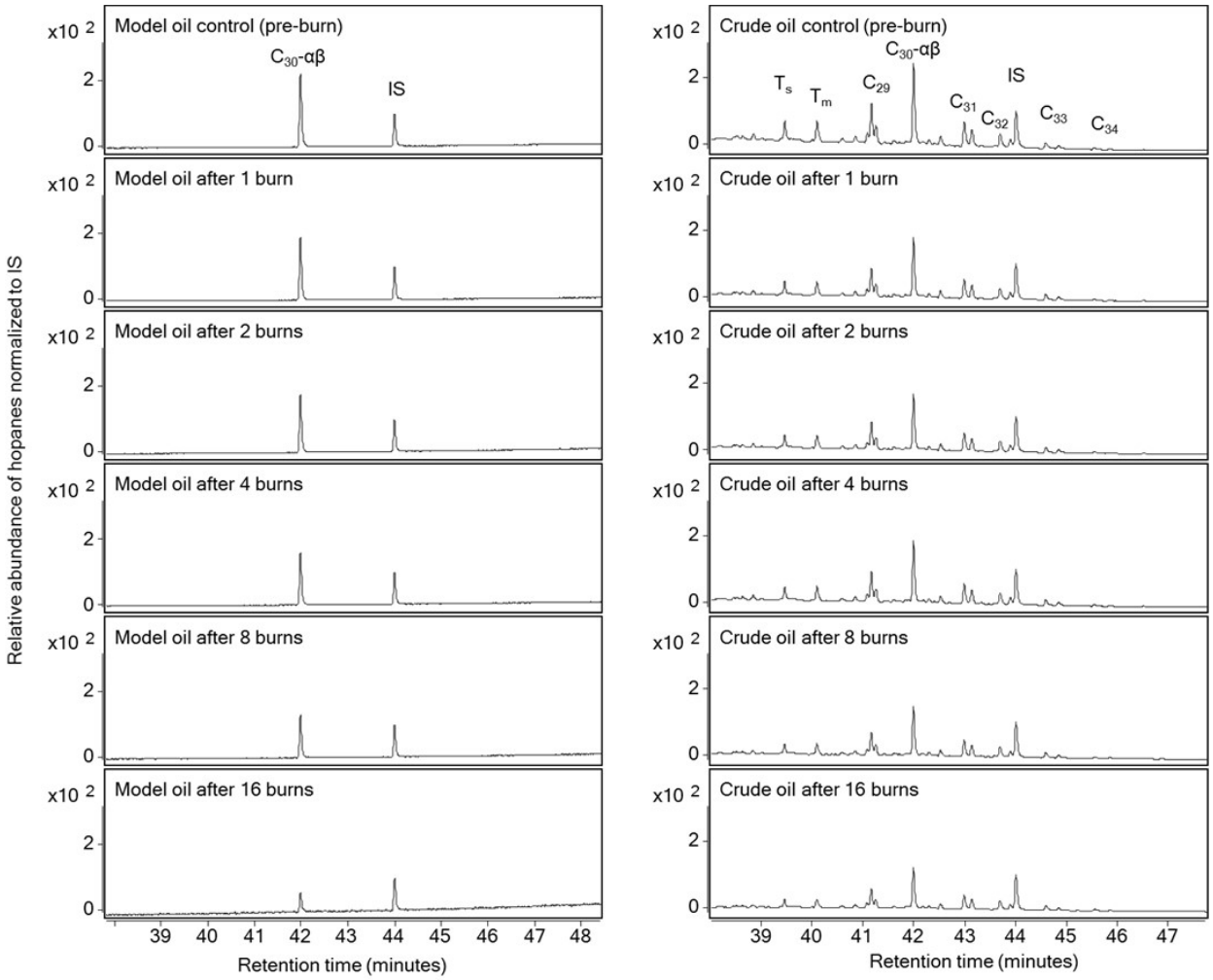

Figure 3.2 Extracted ion chromatogram of terpanes (m/z of 191) in pre-burn solutions of model and crude oils.

As shown in Figure 3.2, apart from C30-αβ hopane, the other hopanes also degraded with increase in the number of burns. Figure 3.3 shows the changes in different types of hopanes in the control and post-burn solutions of MC252 crude oil. These hopanes are typically used for developing diagnostic ratios to fingerprint crude oils which are used for source identification purposes (Z. Wang & M. F. Fingas, 2003). The degradation data for different hopanes shown in the figure indicate that the percent mass removed is inversely proportional to the carbon number (increase in molecular weight) of the biomarker compound. For example, after 16 repetitive

burns, heavier C34-hopane weathered only by about 10%, whereas the lighter Ts and Tm (C27) degraded by about 50%. Our results are consistent with a previous study that analyzed field collected ISB residues after the DWH oil spill and they reported a similar trend (S. A. Stout & Payne, 2016). In all the ISB residues analyzed in this study there was some loss of tricyclic terpanes and some increase in C31 to C35 homohopanes relative to C30-αβ hopane, indicating that in-situ burning process removed some amount of hopane and also other less volatile terpanes. However, Stout and Payne (2016) study did not quantify the degradation levels of different types of hopanes using controlled experiments, and more importantly they did not investigate the stability of hopane diagnostic ratios.

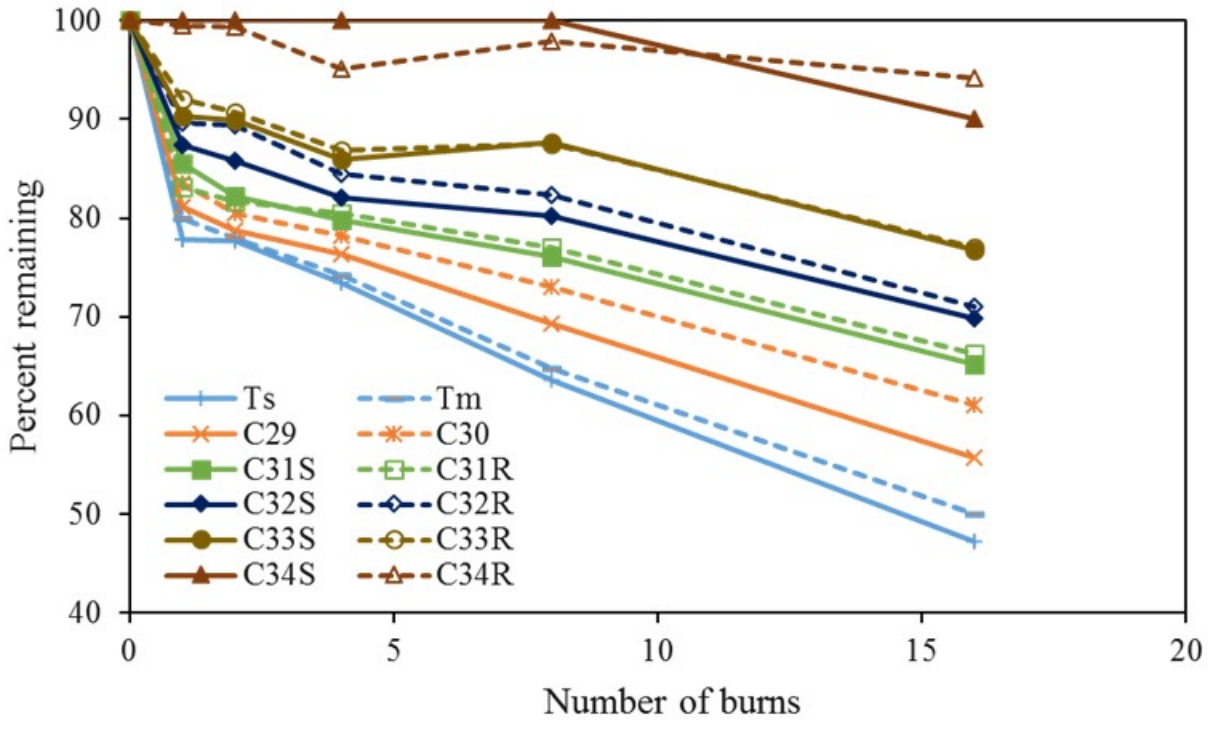

Figure 3.3 Different types of hopanes (that are typically used for developing diagnostic ratios) remaining in post-burn residues of MC252 crude oil after 1,2,4,8 and 16 burns.

In published literature, the following set of hopane diagnostic ratios are typically used for fingerprinting source crude oils and weathered oil spill residues: Ts/Tm, Ts/(Ts+Tm), C29/C30-αβ, C31S/C31(S+R), C32S/C32(S+R), C33S/C33(S+R) and C34S/C34(S+R) (Mulabagal et al.,

2013; Z. Wang & M. F. Fingas, 2003; Fang Yin et al., 2015). As discussed before, during ISB the quantity of hopanes present in crude oil will decrease at various levels; however, the isomers experienced similar levels of weathering (see Figure 3.3). Since all the diagnostic ratios, except C29/C30-αβ, are estimated using its respective isomers, one would expect that their ratios would be conserved. Our data also show that while C29 did weather slightly more than C30-αβ, because their carbon numbers are close, their overall weathering levels are quite similar. Therefore, one should expect the hopane diagnostic ratios of ISB residues to reasonably match the fingerprint of the original source oil. Figure 3.4 shows the radar plot of characteristic hopane diagnostic ratios for the control and all five post-burn residues of MC252 oil. The figure shows that the radar plots of all the samples have similar shape and they all have similar biomarker diagnostic ratios. These data validate our second hypothesis that diagnostic ratios of hopanes can be used for fingerprinting ISB residues. Our data is consistent with other field studies that have used hopane diagnostic ratios to successfully trace ISB residues generated after the DWH oil spill to the MC252 source oil (Shigenaka, Overton, Meyer, Gao, & Miles, 2015). Also, the Stout and Payne (2016) study noted that the distributions of various biomarker compounds in field collected ISB residues appear qualitatively comparable to MC252 source oil patterns (S. A. Stout & Payne, 2016).

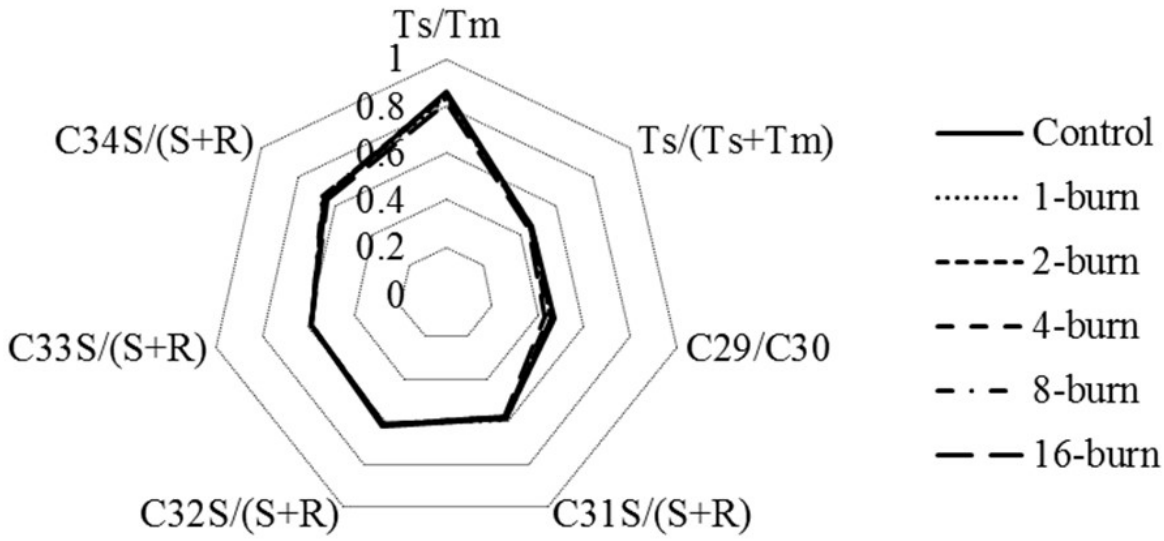

Figure 3.4 Comparison of characteristic hopane diagnostic ratios in post-burn residues of MC252 crude oil after 1,2,4,8 and 16 burns with that of pre-burn MC252 oil (control).

It is evident from the above discussions that the quantities of hopanes are vulnerable for degradation when crude oil is subjected to ISB. However, in real world field conditions, the crude oil will be collected and burnt over water where the heat can be dissipated rather rapidly by the infinite amount of water present underneath the oil. During our oil on-water burning experiment, we observed that the water below the oil slick was not boiling, indicating that the temperature at the oil-water interface was certainly below the boiling point of water. Figure 3.5a shows the changes in different types of hopanes in the oil-on-water burnt residues to that of the unburnt control sample. The amount of hopanes remaining in the burnt residue ranged about 74-87%, compared to that of the unburnt control sample. These data clearly shows that the hopanes present in the crude oil are vulnerable to degradation even when the oil was burnt on water. Figure 3.5b shows the radar plot of characteristic diagnostic ratios for the control and oil-on-water burnt residues. Similar to that of our earlier finding, the hopane diagnostic ratios of

control and burnt residue match, further supporting our second hypothesis that the hopane diagnostic ratios will be conserved.

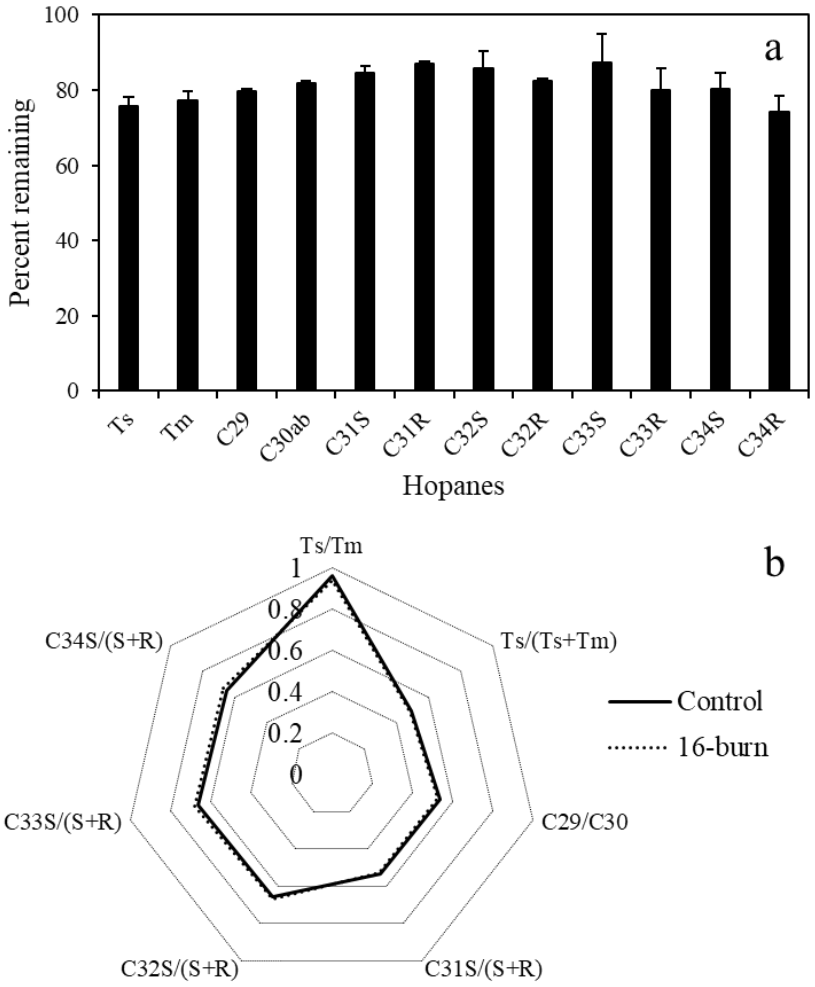

Figure 3.5 (a) Comparison of hopanes remaining in the oil-on-water burning experiment. The floating oil was consecutively burnt 16 times over water and hopane levels were normalized to the levels in the unburnt control sample. (b) Comparison of hopane diagnostic ratios of unburnt control and burnt residues.

3.4 Conclusion

Understanding the degradation patterns of hopanes during ISB process has implications for quantifying the effective degradation rates of various types of hazardous hydrocarbon chemicals trapped in burnt oil residues. Degradation rates of toxic compounds, such as PAHs, are often quantified by using C30-αβ hopa ne as an internal marker (R. M. Garrett et al., 2000; S. A. Stout

& Payne, 2016), therefore the results of this study have major implication on understanding the relative enrichment and/or depletion levels of toxic compounds trapped in ISB residues. Our data show that C30-αβ hopane might not be an ideal conservative biomarker for characterizing these residues. However, in this effort we used a simple laboratory-scale ISB experimental setup. Additionally, in our experiments we used hexane to enhance the burning efficiency. Furthermore, the temperature distribution within the flame was also not measured. Under non-ideal field conditions, the degree of burning will be impacted by changes in water-surface temperature, slick-surface temperature, flame temperature, wind speed, and other environmental conditions. Therefore, it is likely that the degradation levels of hopanes in the burnt residues could have considerable variability. Therefore, more studies are needed to further test these findings using different types of field recovered ISB residues. The data presented in this study, however, provides sufficient evidence to demonstrate that ISB has the potential to degrade C30-αβ and other hopanes. Therefore, one should exercise caution when using C30-αβ hopane as an internal biomarker for characterizing ISB residues. The data also demonstrates that the use of characteristic hopane diagnostic ratios to fingerprint these residues could still be a reasonable approach.

Chapter 4

Understanding the thermal degradation patterns of hopane biomarker compounds present in crude oil

4.1 Introduction

In situ burning (ISB) or controlled burning, is one of the emergency response techniques commonly used for managing marine oil spill (Dave & Ghaly, 2011; A. B. Nordvik, 1995). ISB is considered as an effective oil spill remediation method as it can rapidly reduce the volume of the spilled oil, and it is also less labor and equipment intensive compared to other countermeasures (Mervin Fingas, 2016; Mullin & Champ, 2003; A. B. Nordvik, 1995). In recent years, ISB has gained considerable acceptance and has been widely used for managing several marine oil spill events (J. Fritt-Rasmussen et al., 2015; Potter & Buist, 2008; Schaum et al., 2010). For example, during the 2010 Deepwater Horizon (DWH) oil spill about 5% of the spilled oil was removed by using 410 burns (Schaum et al., 2010). These burns generated a large number of toxic residues and it is highly likely that most of these residues sank to the bottom of the ocean (S. A. Stout & Payne, 2016). It is important that we fully understand the environmental fate of the toxic chemicals trapped in these residues to estimate their long-term ecological impacts (Clement et al., 2017; Gustitus & Clement, 2017). To track the long-term degradation patterns of these toxic chemicals, one would need an internal conservative biomarker compound. In the published literature, C_{30}-αβ hopane (17α(H), 21β(H)-hopane) has been routinely used as an internal conservative biomarker to track the fate of oil spill residues (Z. D. Wang et al., 1999; Z. D. Wang, Stout, et al., 2006; F. Yin et al., 2015). Researchers have also used C_{30}-αβ hopane as an internal biomarker for quantifying the toxic compounds in burnt residues (R. M. Garrett et al., 2000; Jézéquel et al., 2014). For example, Stout and Payne (2016)

used C_{30}-αβ hopane as a conservative biomarker to assess the fate of various hydrocarbons in burnt DWH oil spill residues. Jezequel et al. (2014) compared the distributions of alkanes and polycyclic aromatic hydrocarbons (PAHs) in the crude oil before and after a bench scale ISB experiment by normalizing all the chemical data using C_{30}-αβ hopane concentration. Despite its widespread use, it is currently unclear whether such hopane normalization procedure is a valid methodology for characterizing burnt oil spill residues.

Literature data have shown that C_{30}-αβ hopane is resistant to several types of natural degradation processes (Z. D. Wang et al., 1999; Z. D. Wang, Stout, et al., 2006). However, more recently, John et al. (2018) conducted laboratory experiments to study the fate of C_{30}-αβ and other hopane compounds and demonstrated that several hopanes can degrade during ISB. In their study, they used two types of test samples—a model oil sample that containing 200 ng/mL of pure C_{30}-αβ hopane, and a field sample containing 40 mg/mL of sweet crude oil. Hexane was used as a burning aid in all the experiments. Their data show that after ISB, the amount of C_{30}-αβ hopane decreased by about 77% in the model oil and by 39% in the crude oil. However, the hopane diagnostic ratios remained relatively stable in all the burnt residues. Based on these results they recommended that one should exercise caution when using C_{30}-αβ hopane as the conservative biomarker to assess ISB residues.

John et al. (2018) was one of the first laboratory studies to show that hopane compounds can degrade during ISB. However, their laboratory-scale burning experiments were conducted under highly variable burning conditions with varying flame temperatures, which resulted in heterogeneous heating conditions. These experiments had very little control on the total amount of heat and the heating temperature. The study did not provide any data for thermal degradation kinetics. Furthermore, although John et al. (2018) observed that the ratios of various hopane

compounds remained constant in their laboratory-scale burning experiment, it is unclear whether these ratios will be preserved if the oil was exposed to very high temperatures for a long time. The primary objective of this study is to systematically vary the temperature and heating times to study heating efforts on hopane degradation process.

ISB of crude oil is influenced by a complex set of thermal combustion processes that include heating, flame burning and oxidation (Kök, Hughes, & Price, 1997; Kok, 2011). The contribution of each of these processes to the degradation of hopane biomarkers during ISB is currently unknown. During ISB, the temperature of the oil slick can go well over the ambient water temperature and the heat generated by the burning oil can significantly alter the oil composition (Mullin & Champ, 2003). During the burning process, the hydrocarbons evaporated from the surface of the oil slick will first ignite and the flame temperature can reach up to 900-1200 °C (Buist, 2003). Some of the heat generated from the burning process will be transferred back into the oil slick to vaporize different compounds in the liquid crude oil in the slick. The temperature at the surface of the oil slick can reach up to 350-500 °C when crude oil is burnt over open waters (Buist, 2003). It is necessary to keep the temperature of slick high enough to enhance volatilization and burning of compounds present in the slick. However, most of the heat generated during burning will be lost at the water-oil interface as the temperature of water at the interface will be close to the ambient ocean temperature (Buist, 2003; Jézéquel et al., 2014; Mullin & Champ, 2003). Therefore, buoys and fire-resistant booms are often used to confine the oil to form a thicker slick and this can increase the burning efficiency by keeping the burning oil away from the oil-water interface (Evans, Mulholland, Baum, Walton, & McGrattan, 2001). Other methods use conductive immersed objects to collect the heat from the burning flame and

transfer it to the deeper portions of the oil slick to enhance the burning efficiency (Arava, Walawalkar, Arsava, Sezer, & Rangwala, 2017; PI, 2015).

Heating facilitates most of the physio-chemical transformation occurring during ISB, however, during ISB the temperature and amount of heat to which the oil is exposed can vary considerably. The goal of this study is to investigate the thermal degradation patterns of hopanes when the oil is subject to direct heating for various amount of times at a set of fixed temperatures. Specifically, in this study we test the following three hypotheses: a) C_{30}-αβ and other hopanes present in crude oil will thermally degrade when oil is subject to heating; b) the rate of degradation will increase with the increase of heating temperature; and c) the ratios of various hopane compounds will not be altered by the heating process.

4.2 Experimental methods

4.2.1 Materials

All solvents used in this study were of analytical or higher grade. Solvents, silica gel and anhydrous sodium sulfate were purchased from VWR International, Suwanee, GA. MC252 crude oil was supplied by British Petroleum (BP). Hopane standards C_{30}-αβ hopane and C_{30}-ββ hopane were purchased from Chiron, Norway. The silica gel and anhydrous sodium sulfate were activated following a published protocol (Han, Nambi, & Clement, 2018; Z. D. Wang, Fingas, et al., 1994a).

4.2.2 Desgin of thermal degradation experiment

In this study, we analyzed two types of samples—a model oil which was a synthetic sample prepared using the hopane standard, and a crude oil sample recovered from the MC252 well during the Deepwater Horizon oil spill accident.

4.2.2.1 Design of model oil experiment

The model oil was prepared by dissolving C_{30}-αβ hopane standard in hexane (Gerald F John et al., 2018). The concentration of C_{30}-αβ hopane in the model oil was 200 ng/mL. 1 mL of the model oil was transferred into aluminum dishes and the solvent was allowed to evaporate in a fume hood to dryness and this resulted in yielding 200 ng of C_{30}-αβ hopane in the aluminum dishes.

4.2.2.2 Design of crude oil experiment

Crude oil solution was prepared by dissolving about 200 mg of MC252 source oil into 5 mL of dichloromethane yielding an oil concentration of 40 mg/mL. The concentration of C_{30}-αβ hopane in MC252 oil is about 50 mg/kg-oil (Schantz & Kucklick, 2011). 100 µL of the crude oil solution was added into aluminum dishes to prepare samples containing an estimated C_{30}-αβ hopane mass of 200 ng, which is similar to the amount of hopane in our model oil samples. The dichloromethane solvent was allowed to evaporate in the fume hood to dryness.

4.2.2.3 Model and crude oil samples heating procedure

To study the degradation of C_{30}-αβ hopane in the model oil, the aluminum dishes were transferred into an oven which was set at a constant temperature from 100 to 140 °C and were heated for 10 minutes. The heating time of samples in the oven was fixed to 10 minutes since small scale ISB events would typically last for about 10 minutes (Jézéquel et al., 2014). For degradation kinetics study, the model oil samples were heated at 100, 110 and 120 °C, respectively for 30 minutes. After heating, the residues in the aluminum dishes were dissolved in hexane and the final volume was adjusted to 1 mL. The samples (including unheated control samples) were spiked with 100 ng/mL of C_{30}-ββ hopane internal standard (IS) prior to GC/MS analysis. All the samples were prepared in duplicates and each sample was analyzed by GC/MS

in duplicates. Four measurements (duplicate samples and two injections per sample) were used to calculate the average and standard deviation.

To study the degradation of C_{30}-αβ and other hopane compounds in the crude oil sample, the aluminum dishes were transferred into an oven at a constant temperature from 140 to 240 °C and heated for 10 minutes. For degradation kinetics study, the crude oil samples were heated at 140, 180 and 200 °C, respectively for 60 minutes. After heating, the oil residues in the aluminum dishes were extracted 3 times with about 1 mL of dichloromethane for each time. The solution was then concentrated under a gentle stream of nitrogen to remove all the dichloromethane and redissolved into about 1 mL of hexane and was then purified using the cleanup procedure discussed in Section 2.3 below. A sample with 100 μL of unheated oil was also prepared using a similar procedure and was used as the control.

4.2.3 Samples cleanup procedure

The crude oil samples were cleaned using a previously published cleanup procedure (Han et al., 2018; G. F. John et al., 2016; Z. D. Wang, Fingas, et al., 1994a). A chromatographic column (250 mm × 10 mm) with a Teflon stopcock was serially rinsed with methanol, hexane and dichloromethane. The air-dried column was plugged with deactivated glass wool at the bottom and then packed with 3 g of silica gel and 1 g of anhydrous sodium sulfate. 20 mL of hexane was used to condition the column and the eluent was discarded. The control and heated crude oil samples in about 1 mL of hexane were transferred to the column. About 12 mL of hexane was charged to the column to elute aliphatic hydrocarbons. The eluent was concentrated under a gentle nitrogen stream and adjusted to a final volume of 1 mL. All the samples were spiked with 100 ng/mL of C_{30}-ββ hopane (IS) prior to GC/MS analysis. The control and heated

samples were prepared in duplicates and each sample was analyzed by GC/MS in duplicates. Four measurements were used to calculate the average and standard deviation.

4.2.4 GC/MS analysis

Hopane analysis was accomplished with an Agilent 7890 gas chromatograph fitted with Agilent 7000B triple quadrupole mass spectrometer. The hopanes were analyzed in the selected ion monitoring (SIM) mode at the target ion of m/z 191. The separation of various hopanes was achieved using an Agilent J&W DB-EUPAH column (20 m × 180 μm × 0.14 μm). The temperature of electron ionization (EI) source was set at 280°C and the carrier gas was helium at 1 mL/min. The GC oven temperature started at 35 °C (0.8 min hold) and was ramped to 120 °C at 7 °C/min; 240 °C at 5 °C/min; 320 °C at 3 °C/min, resulting in a total run time of 63.61 min. Hopane compounds were identified and analyzed by running hopane standards and comparing with published literature data (Gerald F John et al., 2018; Z. D. Wang et al., 1999). The hopane compounds analyzed in this study (from short to long retention time) include Ts, Tm, C_{29}-αβ norhopane, C_{30}-αβ hopane, C_{31}S-αβ homohopane, C_{31}R-αβ homohopane, C_{32}S-αβ bishomohopane, C_{32}R-αβ bishomohopane, C_{33}S-αβ trishomohopane, C_{33}R-αβ trishomohopane, C_{34}S-αβ tetrakishomohopane and C_{34}R-αβ tetrakishomohopane. The diagnostic ratios (DRs) of hopanes were calculated by computing different hopane concentration from various peak areas (Han & Clement, 2018).

4.2.5 Quantification of hopane degradation

The amount of hopane biomarkers remaining in the heated oil samples were calculated using a previously published analytical protocol (Gerald F John et al., 2018). The peak abundance ($H_{control}$) of each hopane chromatogram in the control sample was normalized to C_{30}-ββ hopane ($IS_{control}$) peak abundance to compute $H_{control}/IS_{control}$ ratio. Similarly, for the heated samples, the

chromatography peak abundance (H_{heat}) of each hopane was normalized to C_{30}-ββ hopane (IS_{heat}) peak abundance to compute H_{heat}/IS_{heat} ratio. Then the percent hopane remaining in the heated sample was estimated using the following equation.

$$\%remaining = \left(\frac{H_{heat}/IS_{heat}}{H_{control}/IS_{control}}\right) \times 100$$

4.2.6 Analysis of kinetics data

The thermal degradation data of C_{30}-αβ hopane concentration changes (time vs. concentration data) observed for both model oil and crude oil at each temperature were fitted to the following classic first order kinetic expression:

$$C(t) = C_o e^{-kt}$$

In the above equation, t is time, C_o is the initial hopane concentration and k (min^{-1}) is the first order kinetic constant. The degradation rate constants estimated for different temperatures (k vs T data) were then fitted to evaluate two Arrhenius model parameters Ea and A shown in the following expression:

$$k(T) = Ae^{\frac{-Ea}{RT}}$$

In the above Arrhenius model equation, T is the temperature, *R* is the universal gas constant which is equal to 8.314 J/(mol*K), *Ea* (kJ/mol) is the activation energy, and *A* (min^{-1}) is a model constant. The equation allows us to estimate the first order rate constant of C_{30}-αβ hopane degradation at other unknown heating temperature.

4.3 Results and discussion

4.3.1 Thermal degradation of C_{30}-αβ hopane in the model oil

Figure 4.1 shows the amount of C_{30}-αβ hopane remaining in the aluminum dishes compared to the control oil after heating the model oil samples for 10 minutes at 100, 105, 110,

115, 120 and 140 °C. As shown in Figure 4.1, the amount of C_{30}-αβ hopane decreases with the increase in heating temperature. After 10 mins of heating, C_{30}-αβ hopane levels in samples heated at 100 °C degraded by about 33% while the degradation level reached to 99% at 140 °C. The data show that thermal degradation is a major pathway for C_{30}-αβ hopane degradation and therefore these results validate our first hypothesis.

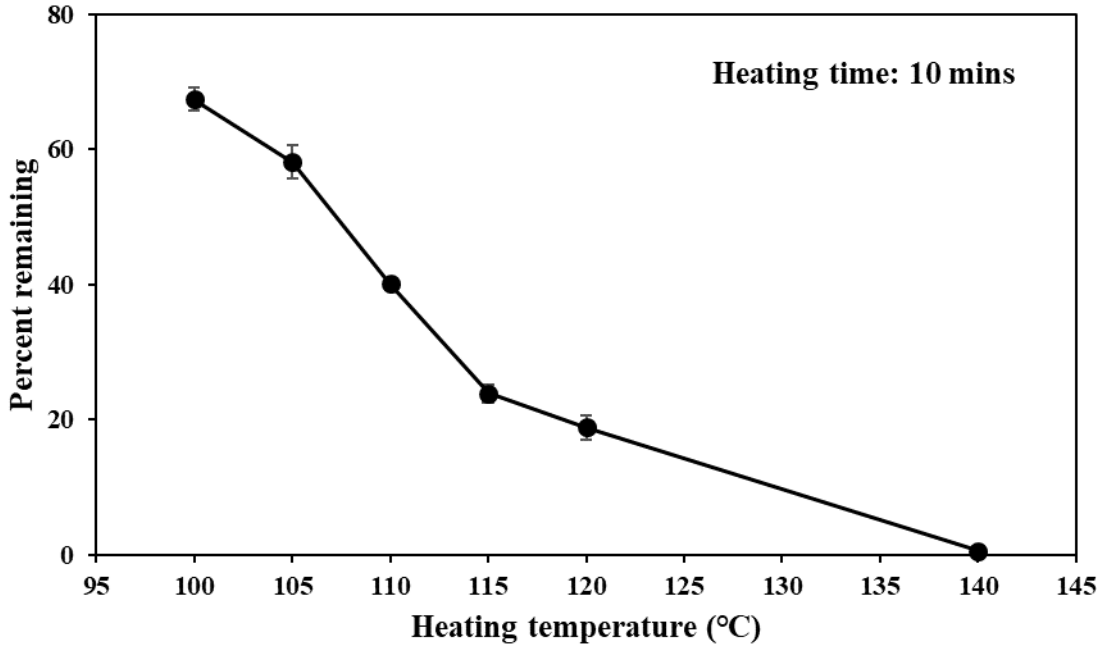

Figure 4.1 Thermal degradation levels of C_{30}-αβ hopane in the model oil at different temperatures after 10 minutes of heating.

To further investigate the kinetics of the thermal degradation process, the model oil was heated at three fixed temperatures (100, 110 and 120° C) for 30 minutes. The kinetic data in Figure 4.2 show that the rate of degradation of C_{30}-αβ hopane increased with the increase in heating temperature, which validates our second hypothesis. After 30 minutes of heating, about 54%, 79% and 97% of C_{30}-αβ hopane degraded at 100, 110 and 120 °C, respectively. Thermal degradation of C_{30}-αβ hopane followed a classic first order kinetics, and the fitted kinetic curves are shown in Figure 4.2. The rate constants for the three datasets were estimated to be: 0.032,

0.066 and 0.135 min^{-1} at 100, 110 and 120 °C, respectively. Based on the three rate constant values estimated at 100, 110 and 120 °C, the Arrhenius model constants *Ea* and *A* were estimated to be 87.7 kJ/mol and 6.11×10^{10} min^{-1}, respectively.

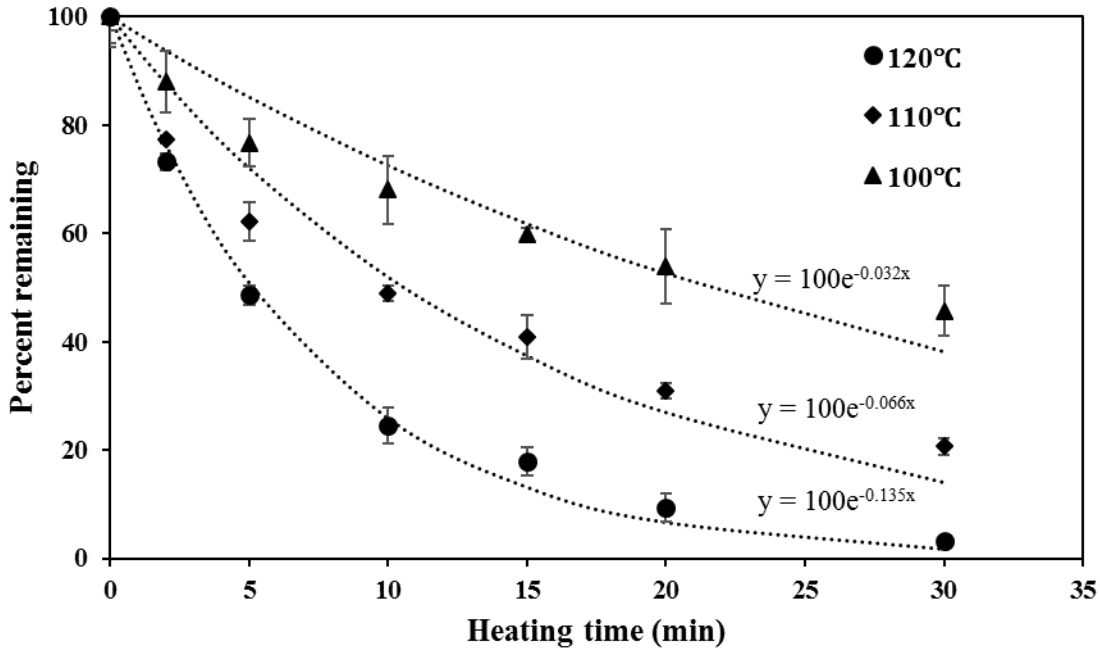

Figure 4.2 C_{30}-αβ hopane thermal degradation kinetic data for the model oil collected at different temperatures. The dotted lines are fitted first-order kinetic model results.

4.3.2 Thermal degradation of C_{30}-αβ hopane in MC252 crude oil

Figure 4.3 shows the amount of C_{30}-αβ hopane remaining in the crude oil when it was heated at 140, 160, 180, 200, 220 and 240 °C for 10 minutes. The results (see Figure 4.3) show that the degradation of C_{30}-αβ hopane in crude oil increased with increase in temperature. The data also show that between 200-220 °C the degradation of C_{30}-αβ hopane increased dramatically from 48% to 96%. Overall, these data also indicate that hopanes present in natural crude oil samples would require much higher temperature to degrade than the pure hopane present in the model samples.

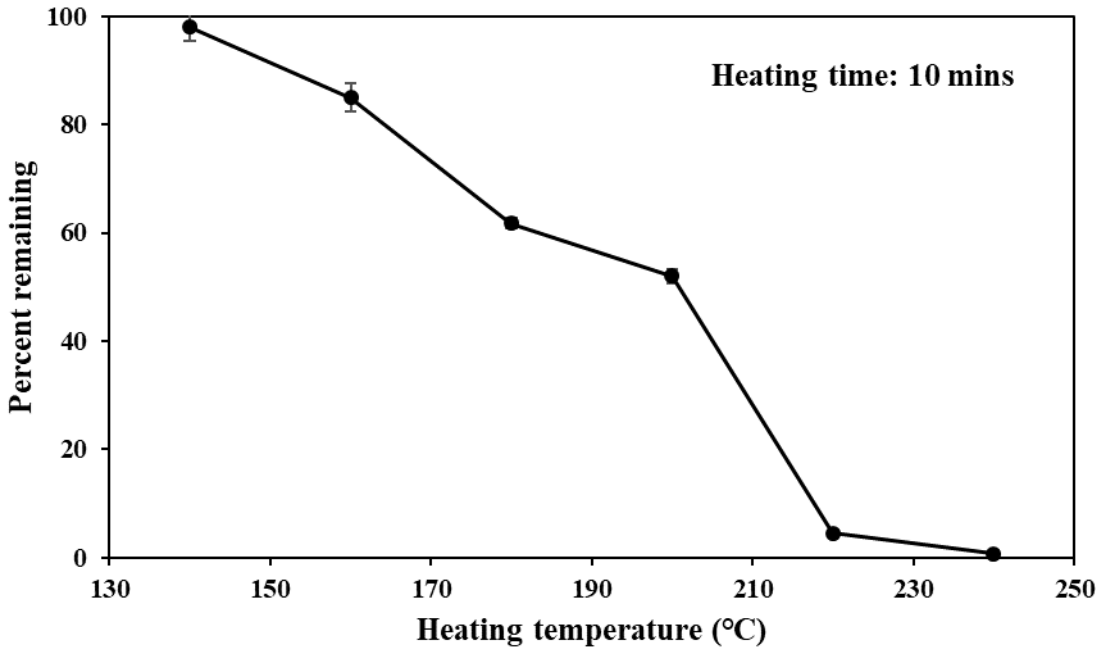

Figure 4.3 Thermal degradation levels of C_{30}-αβ hopane in MC252 source crude oil at different temperatures after 10 minutes of heating.

To evaluate the kinetics of the thermal degradation process, the crude oil was heated at 140, 180 and 200 °C for longer times and the amount of C_{30}-αβ hopane remaining in the crude oil was quantified. These results are presented in Figure 4.4. The data show that after 60 minutes of heating, only 21% of C_{30}-αβ hopane degraded at 140 °C, while more than 99% degraded at 200 °C. Similar to the model oil data, the thermal degradation kinetics of C_{30}-αβ hopane in crude oil also followed a first-order degradation pattern. The model profiles fitted using the EXCEL solver are also shown in Figure 4.4. The rate constant values were estimated to be: 0.004, 0.039 and 0.067 min^{-1} at 140, 180 and 200° C, respectively. The Arrhenius model constants, *Ea* and *A*, for these data were estimated to be 78.4 kJ/mol and 3.52×10^7 min^{-1}, respectively.

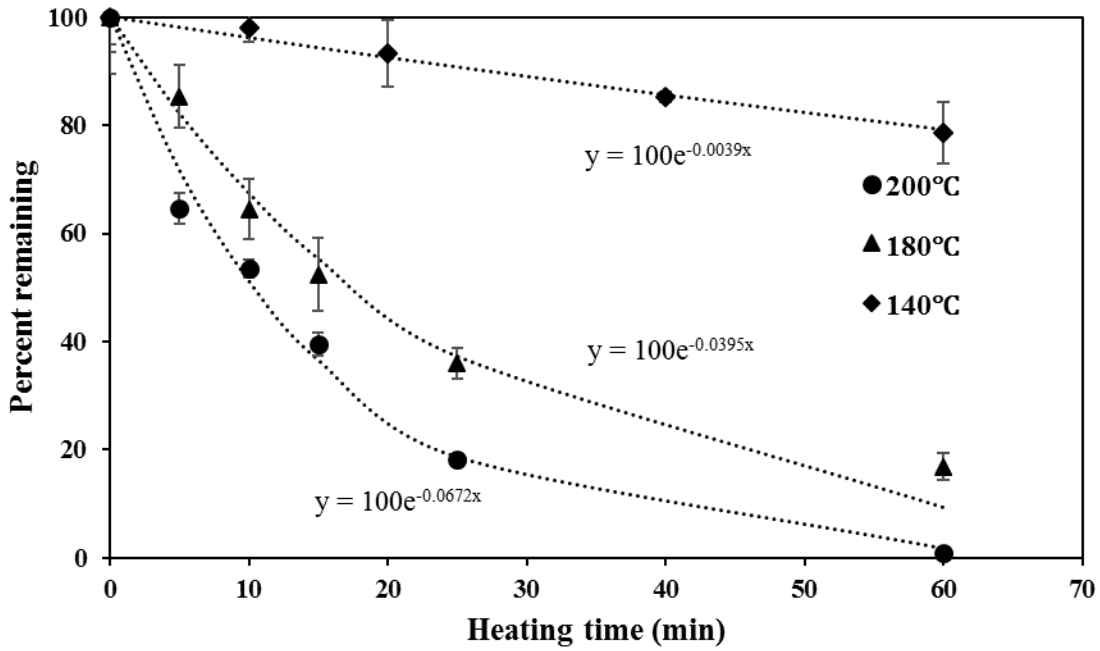

Figure 4.4 C_{30}-αβ hopane thermal degradation kinetics data for MC252 source crude oil collected at different temperatures. The dotted lines are fitted first-order kinetic model results.

4.3.3 Thermal degradation patterns of other hopanes present in MC252 crude oil

Oil spill studies typically use several types of hopanes for comparing the fingerprints of residues with the source oil (Mulabagal et al., 2013; Z. D. Wang et al., 1999). Figure 4.5 shows the distribution of various types of hopane biomarker compounds present in MC252 oil after heating it for 10 minutes at 160, 180, 200, 220 and 240 °C. Similar to C_{30}-αβ hopane (see Figure 4.3), the amount of different types of hopanes degraded over 10 minutes increased with increase in the heating temperature. Table 4.1 provides a detailed summary of the amount of hopanes that remained in the samples that were subject to 10 minutes of heating at various temperatures. The data show that at a fixed temperature, the degradation level decreased with increase in carbon number (or molecular weight). For example, when the sample was heated at 160 °C, about 72%

of T_s (C_{27}) and 75% of T_m (C_{27}) remained in the samples. Whereas, about 96% of higher molecular weight hopanes $C_{34}S$ and $C_{34}R$ remained undegraded in the heated samples.

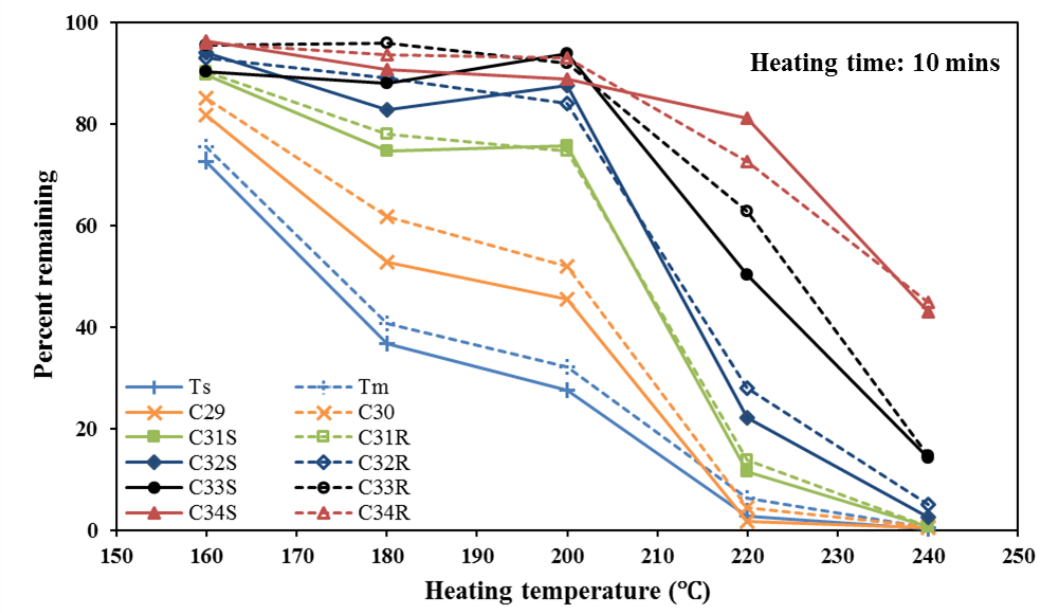

Figure 4.5 Thermal degradation patterns of different types of hopanes present in MC252 crude oil. The samples were heated at different fixed temperatures for 10 minutes.

Table 4.1 The percentage of different types of hopanes remaining in MC252 oil after heating it at different temperatures for 10 minutes (%). (-- indicates less than 1%).

T(°C)	Ts	Tm	C_{29}	C_{30}	$C_{31}S$	$C_{31}R$	$C_{32}S$	$C_{32}R$	$C_{33}S$	$C_{33}R$	$C_{34}S$	$C_{34}R$
160	72	75	82	85	90	90	94	93	90	95	96	96
180	37	41	52	62	75	78	83	89	88	96	91	94
200	27	32	45	52	76	75	87	84	94	92	89	93
220	3	6	2	4	11	14	22	28	50	63	81	72
240	--	--	--	1	1	1	3	5	14	15	43	45

The degradation kinetics of other hopanes were also studied by heating the crude oil at 200 °C for 5, 10, 15, 25 and 60 minutes. Figure 4.6 provides the kinetic data that show the degradation rate of various hopanes decreased with increase in carbon number. The percentage amount of hopanes remaining in all the samples are summarized in Table 4.2. These data show that low molecular weight compounds T_s and T_m depleted rather rapidly, and the percent

remaining is lower than 10% after heating the oil for 25 minutes at 200 °C. Whereas, more than 70% of $C_{34}S$ and $C_{34}R$ remained in the residues even after continuously heating the oil for 60 minutes. These results are consistent with the literature data that have shown that weathering of various petroleum hydrocarbons is correlated with the chain length and molecular weight (Z. Wang et al., 1998). Also, Stout and Payne (2016) analyzed various hydrocarbons in burnt residues and reported that both high boiling n-alkanes and hopanes underwent depletion during ISB and the depletion of hopanes decreased with increase in carbon numbers.

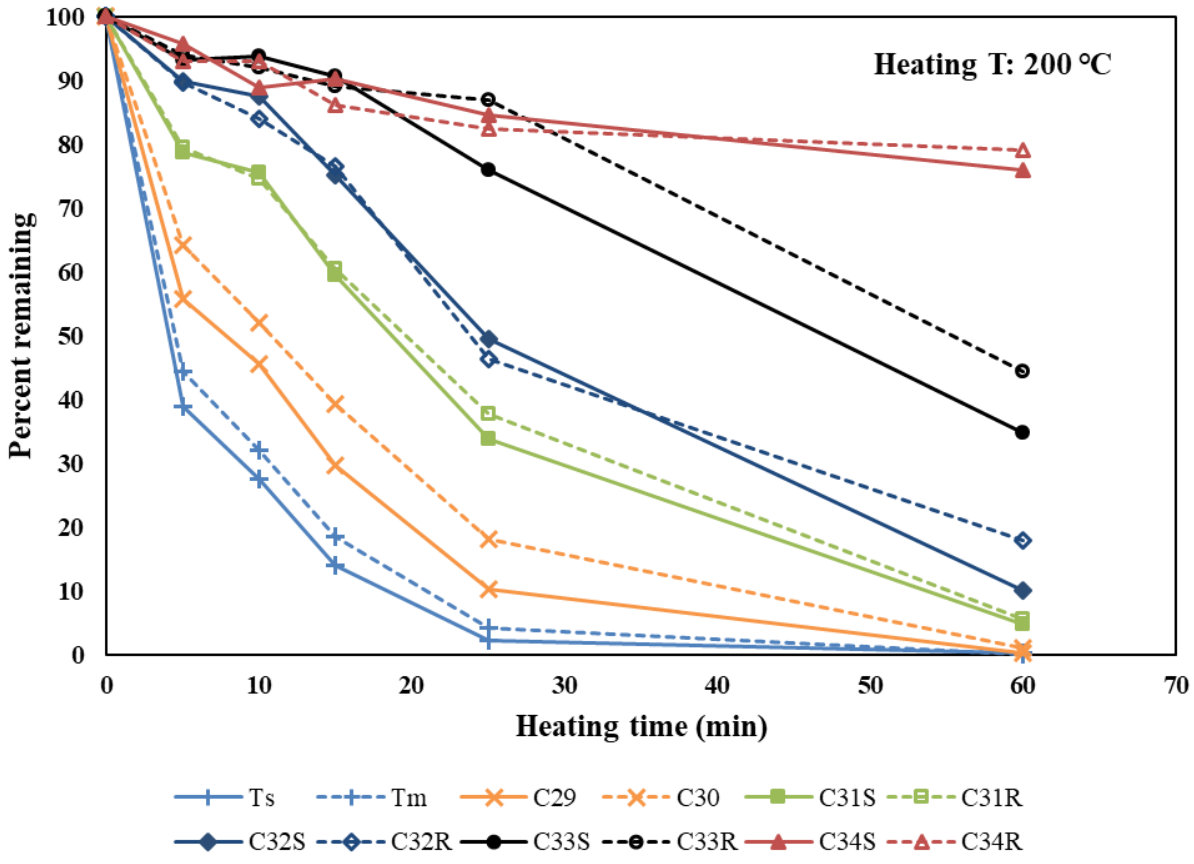

Figure 4.6 Thermal degradation kinetics of different types of hopanes in MC252 crude oil. The samples were heated for various amount of time at a fixed temperature of 200 °C.

Table 4.2 The percentage of different types of hopanes remaining in MC252 oil after heating it for various amount of time at a fixed temperature of 200 °C (%). (-- indicates less than 1%).

Time (mins)	Ts	Tm	C_{29}	C_{30}	$C_{31}S$	$C_{31}R$	$C_{32}S$	$C_{32}R$	$C_{33}S$	$C_{33}R$	$C_{34}S$	$C_{34}R$
5	39	44	56	64	79	79	90	90	93	94	96	93
10	27	32	45	52	76	75	87	84	94	92	90	93
15	14	18	30	39	59	60	75	77	91	89	90	86
25	2	4	10	18	34	38	50	46	76	87	84	82
60	--	--	--	1	5	5	10	18	35	44	76	79

4.3.4 Stability of hopane diagnostic ratios

The hopane diagnostic ratios are important information that are routinely used for source identification (Z. D. Wang et al., 1999; Fang Yin et al., 2015). We calculated seven widely used hopane diagnostic ratios and the results are summarized using classic radar plots (G. F. John et al., 2016; Mulabagal et al., 2013). Figure 4.7 shows the hopane diagnostic ratios in the oil residues after heating it at different temperatures for 10 minutes. When we compared diagnostic ratios of the unheated control sample with the data for the oil residues that were heated at 160, 180 and 200 °C, the data indicated that the ratios remained stable, although the individual hopanes degraded during the heating process. Since all the hopane ratios, except $C_{29}/C_{30,}$ are calculated based on the concentrations of respective isomers, the degradation levels are expected to be similar (especially at lower temperatures where the total degradation levels are low) and hence one would expect their ratios to conserve. Also the degradation levels of C_{29} and C_{30} can be expected to be quite similar since their carbon numbers are very close. Stout and Payne (2016) found that the ratios of hopanes present in their burnt residues were comparable to their control sample ratios, although the individual hopane compounds degraded differently during ISB.

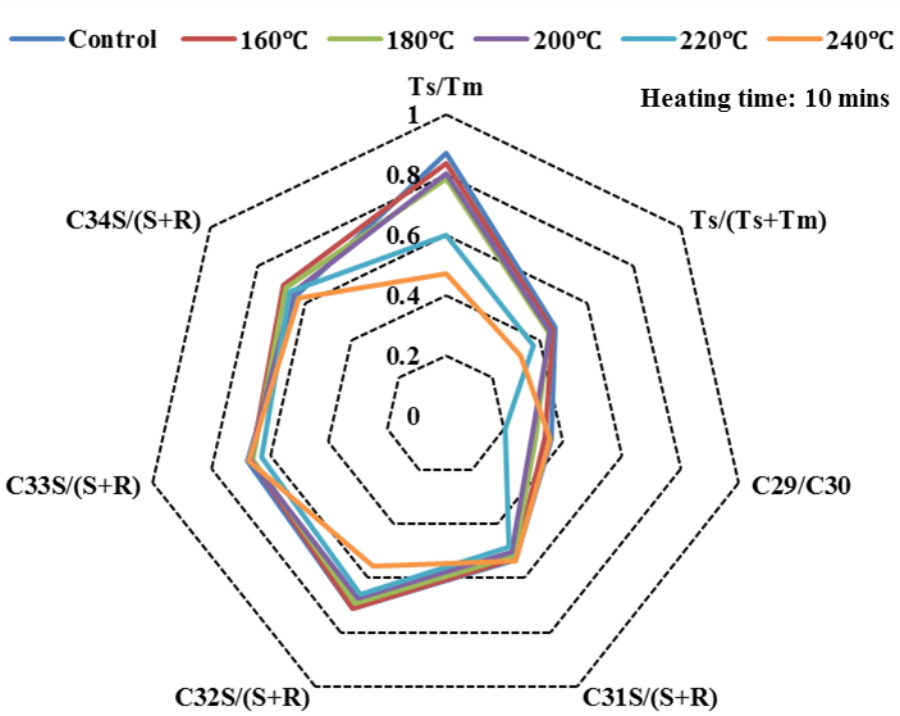

Figure 4.7 Comparison of characteristic hopane diagnostic ratios in MC252 crude oil residues after heating the oil at different temperatures for 10 minutes.

However, in this study, when we heated the sample at very high temperatures of 220 and 240 °C, the ratios did not conserve and therefore the shape of the radar plots changed considerably. It can be seen from the figure that the shape of T_s/T_m, $T_s/(T_s+T_m)$ and C_{29}/C_{30}, which are hopanes with relatively low carbon numbers, changed significantly. As shown in Table 4.1, these compounds were depleted by more than 90% at 220 and 240 °C, and their ratios also changed considerably when the samples were heated at these high temperatures.

Radar plots of hopane diagnostic ratios in the oil residues after heating it at 200 °C for different lengths of time are shown in Figure 4.8. Similar to previous results, T_s/T_m, $T_s/(T_s+T_m)$ and C_{29}/C_{30} are the most vulnerable ratios that were impacted by thermal degradation. For example, the diagnostic ratio of T_s/T_m changed gradually when the heating time was increased. When the heating time was increased to 25 and 60 minutes, more than 90% of T_s, T_m and C_{29}

were removed and the shapes of the diagnostic ratio radar plots were considerably different from control sample plots. Therefore, heating time is an important factor that can affect individual hopane depletion levels as well as the diagnostic ratios. In summary, the hopane diagnostic ratios are conserved when the heating temperature was relatively low and when the heating time was relatively short. However, when the heating temperature was high or when the heating time was long the hopane ratios were not conserved. These results falsify our third hypothesis and therefore we conclude that fingerprinting hopane diagnostic ratios might not be a valid approach for source identification of certain severely burnt ISB residues. From a practical point of view, field-scale ISB activities are highly complex operations that are impacted by several environmental factors including water temperature and other uncontrollable field conditions. Our findings are based on simplified laboratory-scale experiments and therefore further studies are necessary to better understand the fate of hopane biomarkers under complex field conditions.

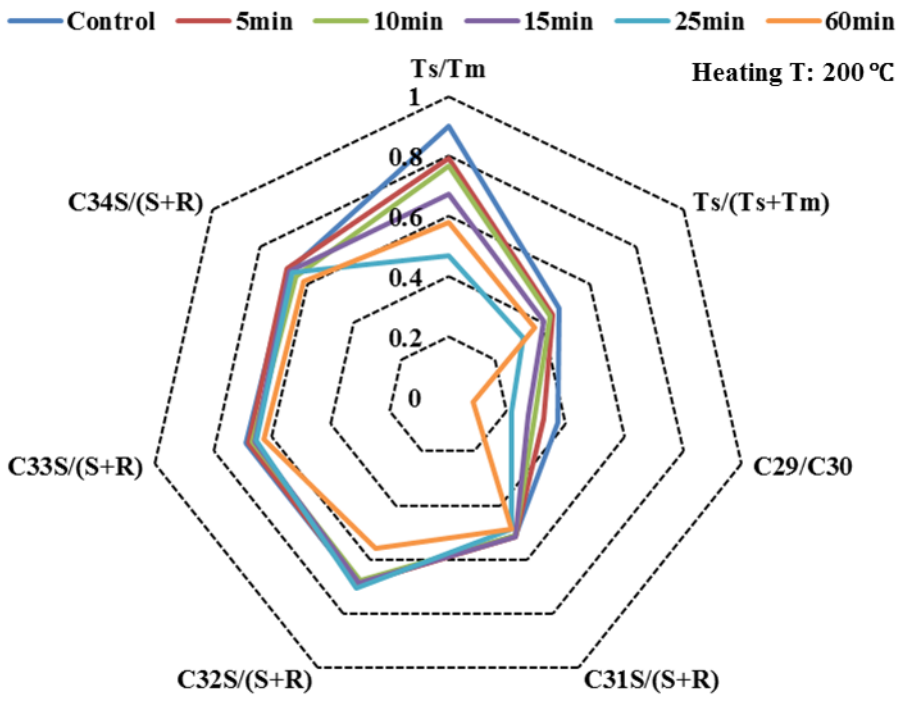

Figure 4.8 Comparison of characteristic hopane diagnostic ratios in MC252 crude oil residues after heating the oil for various amount of time at a fixed temperature of 200 °C.

4.4 Conclusion

The hopane biomarkers present in crude oil are vulnerable for degradation during ISB where temperature and heat delivered can vary considerably. In this study, a model oil sample containing C_{30}-αβ hopane, and a field crude oil sample were heated at various fixed temperatures for different amount of time. The results show that direct heating can degrade different types of hopane biomarkers present in crude oil.

The following conclusions can be made based on the results of this experimental study that explored the fate of hopane compounds present in crude oil when the oil is subject to direct heating. The data show that a) C_{30}-αβ and other hopane compounds will degrade when crude oil is heated at high temperature for long times; b) the degradation patterns follow first order kinetics and the rate constant increases with increase in temperature; and c) when the heating temperature is sufficiently high the diagnostic ratios of various hopane compounds will be altered by the heating process. We conclude that hopane compounds can be thermally degraded when the crude oil is heated at high temperatures. Therefore hopane levels might not be conserved during ISB process and caution should be exercised when using hopanes as conservative biomarker compounds for characterizing ISB residues.

Chapter 5

Environmental impacts of the Chennai oil spill accident – A case study

5.1 Introduction

Around 4:00 AM on January 28th 2017, two cargo ships, BW Maple, a liquid petroleum gas carrier, and MT Dawn Kanchipuram, a lubricant oil carrier, collided about two miles away from the Ennore Kamarajar shipping terminal, which is located about 10 miles north of Chennai city in South India (13°13'41.4"N 80°21'48.0"E). MT Dawn Kanchipuramwas carrying about 32,000 tons of heavy bunker fuel oil, and the accident released about 75 metric tons of the oil directly into the Bay of Bengal. Within 48 h, the oil spill contaminated about 25 miles of the coastline extending from Chennai's northern suburban town Ennore all the way to the southern suburban town Thiruvanmiyur (see Figure 5.1). During this oil spill event, several amenity beaches, including the iconic Marina Beach in Chennai city, were severely contaminated by petroleum residues. The spill occurred during the northeastern monsoon season when strong shoreline currents are directed in a predominantly southern direction (R. Kankara, Mohan, & Venkatachalapathy, 2011). Therefore, within a week, the shoreline currents transported the oil toward several southern amenity beaches all the way to the historic town of Mahabalipuram, a famous tourist destination located about 50 miles south of the spill location.

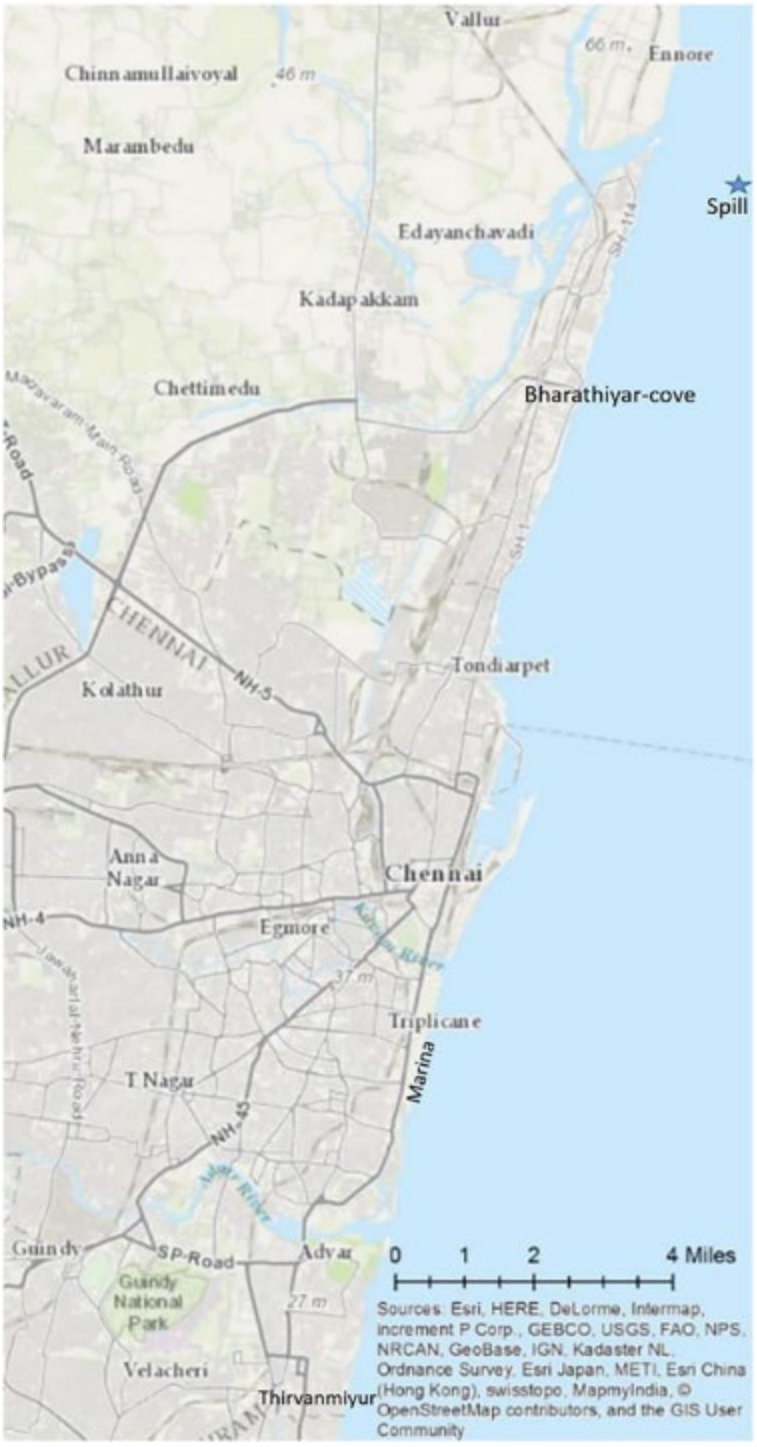

Figure 5.1 2017 Chennai oil spill location.

Oil spill residues washing onto amenity beaches is a common worldwide problem (Michel et al., 2013; Neff, Owens, Stoker, & McCormick, 1995; Suneel, Ciappa, & Vethamony, 2016;

Fang Yin et al., 2015). One of the goals of this study is to compare and contrast the Chennai oil spill data with the datasets collected for two recent oil spills that severely contaminated various amenity beaches located along the Gulf of Mexico (GOM) in North America; these two spills are: the 2010 Deepwater Horizon (DWH) oil spill (Nixon et al., 2016) and 2014 Galveston Bay (GB) oil spill (Bacosa, Thyng, Plunkett, Erdner, & Liu, 2016). The DWH oil spill, which started on April 20th 2010, when an oil drilling rig exploded, resulted in an unprecedented contamination event that released over 210,000,000 gal of sweet crude oil into the GOM. The spill contaminated over 1600miles of shoreline spanning from the Panhandle region of Florida to Eastern Texas (Michel et al., 2013). The residues from this spill continue to impact the GOM beaches along the Alabama shoreline until now (Clement et al., 2017; F. Yin et al., 2015). The GB oil spill occurred on March 22nd, 2014 when a bulk carrier, M/V Summer Wind, punctured the tank of the oil barge Kirby near Houston, Texas. This accident released about 168,000 gal of marine fuel oil into the bay. Within a week the spilled oil was transported by shoreline currents, and oil residues were deposited along various wildlife preserves located about 150 miles southwest of Galveston. Our research team has extensively investigated both these oil spills and have collected several important field and laboratory datasets (Clement et al., 2017; J. S. Hayworth et al., 2011; Fang Yin et al., 2015).

The overall objective of this case study is to present a comprehensive summary of the 2017 Chennai oil spill. We provide the details of the field observations made by our team while monitoring the effectiveness of initial cleanup activities completed at various sites in Chennai. We also completed a detailed chemical characterization study to quantify the weathering patterns of Chennai oil spill samples. We compare these data with DWH and GB oil spill datasets with a goal to understand the similarities and difference between these three spills. The Chennai oil

spill data is also used to assess the potential long term impacts of the spill on the Bay of Bengal shoreline ecosystem.

5.2 Field observations and sampling methods

Chennai is the capital of the southern Indian state of Tamil Nadu, which is located off the coast of Bay of Bengal. The coastal currents in this region naturally erode and transport sediments along the shoreline (Veerasingam, Venkatachalapathy, & Ramkumar, 2014). In order to prevent these coastal erosion problems, the city has installed a seawall made up of large granite boulders. In addition, in the northern area, the city has also installed groins, which are approximately 10-m wide structures constructed using granite boulders that extend into the sea for about 150 to 300m (Kannan, Anand, Sundar, Sannasiraj, & Rangarao, 2014). The seawalls and groins look similar, since both structures are made of similar type of rocks and boulders. However, the seawalls are always installed parallel to the shoreline, whereas the groins are installed perpendicular to the shoreline. Figure 5.2a shows an aerial view of some of the groins installed along North Chennai beaches, and Figure 5.2b shows a close-up picture of one of the groins extending into the ocean. In Northern beaches, the groins are installed every 1000 to 1500 ft; and between these groins, large amounts of sediment can be trapped to form sandy shoreline (see Figure 5.2b).

Figure 5.2 (a) The groins installed along North Chennai beaches; (b) a close-up view of a groin.

During the oil spill, the zones in the vicinity of the seawall-groin intersection region trapped significant amounts of oil. Figure 5.2a shows a seawall-groin intersection zone near Bharathiyar Beach, which is located about two miles southwest of the spill location. This groin is located very close to the spill location, and this region trapped a significant amount of floating oil sludge. A portion of the oil that accumulated near the shoreline was also directly deposited on the rocks used to construct the seawalls and groins. The Bharathiyar Beach was one of the heavily impacted field sites. Figure 5.3a shows the initial oiling period when the emulsified oil was actively washing toward the groin and directly depositing oil over the rocks. Initial cleanup efforts employed workers who walked into waist deep waters and manually scoped the floating oil with plastic buckets and passed them along a human chain (see Figure 5.3b). Figure 5.3c shows the buckets of emulsified oil recovered from this site, and Figure 5.3d shows volunteers collecting the recovered oil and storing them into large containers, which were later disposed away from the site. This collection method was used at multiple sites for several weeks to manually remove the floating oil sludge and beached oil-sand mixture. Although this method recovered large volumes of sludge and oil-sand mixture (the total amount is estimated to be

about 150 to 200 tons), the cleanup efforts also spread the contamination onto clean boulders located well above the water line. Therefore, after removing most of the floating oil, the cleanup efforts continued for several weeks to remove the residual oil sticking to the rocks. This was a highly labor intensive clean-up effort where the workers removed the oil from the rocks by either manually scrubbing each rock, or by washing each rock using high pressure water jets. Figure 5.4 inset shows a typical oil-tainted rock sample collected from the Bharathiyar Beach on March 23rd 2017, about two months after the spill. Figure 5.4 shows a cleanup worker sitting and manually scrubbing oil-tainted rocks, and also another worker using a hand held high-pressure washer to clean the rocks. The high pressure water jet dislodged a portion of the oil sticking to the rock back into the ocean, and a boom was used to contain this oil closer to the shoreline. Whenever possible, the floating oil was scooped out manually and the remaining unrecoverable oil fragments were allowed to disperse into the shoreline environment.

Figure 5.3 (a) Oil remain trapped near a groin-seawall boundary close to Bharathiyar beach a week after the spill; the figure also shows a human chain of workers manually removing the oil; (b) cleanup workers

scoping the floating oil; (c) recovered oil temporarily stored in buckets; (d) workers transporting the oil and transferring it into plastic containers.

Figure 5.4 Contaminated rocks in Bharathiyar beach cleaned manually by scrubbing rocks and also by using a high pressure washer. The inset shows a close-up view of an oil tainted rock sample (pictures taken on March 23rd 2017).

Our field sampling team surveyed several Chennai beaches for over two months. Our field observations indicated that the emulsified oil sludge was either deposited on the boulders (used to construct the seawall and groins) or was deposited on the sandy beaches. Sunken tar balls containing oil-sand mixture, which has been observed at many locations after the DWH oil spill event (Clement et al., 2017; J. S. Hayworth et al., 2011), has not been observed in any of the Chennai beaches. We also worked with a team of oceanographers and jointly completed an offshore survey on 23rd March 2017, searching for sunken oil spill residues. This 8-h long boat survey covered the entire 20-mile long Chennai coastline (from Ennore to Adyar). During this survey, we collected multiple grab samples at various sampling points located about 1 to 2 km

away from the shoreline (with water depths ranging from at 5 to 25m) and we did not find any evidence for the presence of sunken oil spill residues.

Our field observations also indicated that cleanup activities continued at heavily contaminated sites, such as the Bharathiyar Beach site, for over two months. During our field visits, we collected several oil spill samples and archived them for future use. In this study, we analyzed three of these archived field samples. The first sample is the reference oil, which was collected directly from the ship and was provided by the Indian Coast Guard; this sample is referred to here as "Source Oil". The second sample is a sample of the oil sludge or mousse that washed along the Northern Chennai shoreline six days after the spill; this sample is referred to as "Day-6 Oil". The third sample was scrapped from a contaminated rock located near Bharathiyar Beach on April 1st 2017, 62 days after spill; this sample is referred to as "Day-62 Oil". The source oil and Day-6 and Day-62 samples were the primary samples used in our chemical characterization efforts. In addition, samples of oil recovered from North Chennai beaches after about one day and after ten days were used to quantify the changes in the physical characteristics of the spilled oil.

5.3 Materials and methods

5.3.1 Laboratory materials

All solvents used in this study are analytical grade or higher, and they were used without any further purification. The organic solvents, silica gel (60–200 μm), and anhydrous sodium sulfate were purchased from VWR International, Suwanee, GA. Standard PAH mixture consisting of 27 PAHs (naphthalene, 1-methylnaphthalene, 2-methylnaphthalene, 2,6-dimethylnaphthalene, 2,3,5-trimethylnaphthalene, biphenyl, acenaphthylene, acenaphthene, fluorene, phenanthrene, 1-methylphenanthrene, anthracene, dibenzothiophene, fluoranthene,

pyrene, benzo(a)anthracene, chrysene, benzo(b)fluoranthene, benzo(j)fluoranthene, benzo(k)fluoranthene, benzo(e)pyrene, benzo(a)pyrene, perylene, dibenz(a,c)anthracene, dibenz(a,h)anthracene, indeno(1,2,3,-cd)pyrene and benzo(ghi)perylene) was purchased from Agilent Technologies,Wilmington, DE. Alkanes (*n*-C_8-C_{40}) calibration standard, which was used for quantifying total petroleum hydrocarbons (TPH) using a GC-FID method and also for quantifying various types of alkanes using a GC-MS method, was purchased from Supelco, Bellefonte, PA. The TPH internal standard 5-α androstane was purchased from Sigma Aldrich. The reference solution of four surrogate standards (SS), including naphthalene-d_8, acenaphthene-d_{10}, phenanthrene-d_{10} and benzo(a) pyrene-d_{12}, were purchased from Ultra Scientific Analytical Solutions, North Kingstown, RI. PAHs internal standard (IS) *p*-terphenyl-d_{14} (purity 98.5%) was purchased from AccuStandard, New Haven, CT, USA. The hopane internal standard, C_{30}ββ-hopane, was purchased from Chiron, Norway.

5.3.2 Samples preparation and cleanup methods

Activated silica gel was prepared using a well-established protocol (Z. D. Wang, Fingas, et al., 1994a). Specifically, 200 g silica gel was placed in a chromatographic column packed with glass wool at the bottom. The gel was sequentially rinsed three time with 250 mL of acetone, hexane and dichloromethane, respectively, and the rinsed sample was left in a fume hood for approximately 24 h. Later, the silica gel was dried at 45 °C for 8 h in an oven, after which it was activated by heating it at 180 °C for 20 h. The cleanup procedure also used anhydrous sodium sulfate which was heated at 400 °C for 4 h to remove any impurities. Activated silica gel and purified anhydrous sodium sulfate were stored in tightly sealed glass containers.

The silica gel cleanup column was set up based on a previously published method (Z. D. Wang, Fingas, et al., 1994a). A glass column (250mm long × 10 mm wide) with a teflon

stopcock was plugged at the bottom using glass wool, and it was sequentially rinsed with methanol, hexane and dichloromethane. The dried column was packed with 3 g of activated silica gel and 1 g of anhydrous sodium sulfate on the top. The column was first conditioned with 20 mL of hexane and the eluent was discarded. A known amount of sample (~30 mg) was dissolved in hexane, spiked with four surrogate standards, and was then transferred into the column. First, 12 mL of hexane was used to elute the aliphatic hydrocarbon fractions (designated as F1 fraction). Second, 15 mL of 50% dichloromethane in hexane (v/v) was used to elute aromatic hydrocarbons (designated as F2 fraction). Both F1 and F2 fractions were concentrated under a gentle stream of nitrogen and adjusted to 10mL. Then, 1 mL of F1 fraction was spiked with $C_{30}\beta\beta$-hopane and was used to analyze *n*-alkanes, hopanes and steranes, and 1 mL of F2 fraction was spiked with *p*-terphenyl-d_{14} and was used to analyze PAHs and their alkylated homologs. Additionally, 1 mL of F1 and 1 mL of F2 were combined to prepare new fraction F3. The F1, F2, and F3 samples were spiked with 5-α androstane (internal standard) and analyzed for TSH (total saturated hydrocarbons), TAH (total aromatic hydrocarbons) and TPH, respectively, using a GC-FID method (Z. D. Wang et al., 1999).

5.3.3 Details of GC-FID and GC/MS methods

The F1 and F2 fractions were analyzed using an Agilent Gas Chromatograph (7890) coupled to Triple Quadrupole Mass Spectrometer (7000B). All the samples were prepared in duplicate and analyzed in triplicate. The F1 fraction was analyzed for *n*-alkanes (m/z 85), hopanes (m/z 191) and steranes (m/z 217) in the selected ion monitoring (SIM) mode (Mulabagal et al., 2013; OSAT-2, 2011). Five groups of alkylated PAHs and seventeen other PAHs in the F2 fraction were analyzed using previously published analytical procedures (G. F. John et al., 2016; Fang Yin et al., 2015). The alkylated group of PAHs quantified and the standards used are

as follows: for Group 1, C_0-naphthalene was quantified using naphthalene; C_1-naphthalenes using 2-methylnaphthalene; C_2-naphthalenes using 2,6-dimethylnaphthalene; and C_3- and C_4-naphthalenes using 2,3,5-trimethylnaphthalene. For Group 2, C_0-phenanthrene was quantified using phenanthrene; and C_1- to C_4-phenanthrenes using 1- methylphenanthrene. For Group 3, C_0- to C_3-dibenzothiophenes were quantified using dibenzothiophene. For Group 4, C_0- to C_3-fluorenes were quantified using fluorene. For Group 5, C_0- to C_4-chrysenes were quantified using chrysene. Seventeen other PAHs thatwere quantified include: biphenyl, acenaphthylene, acenaphthene, anthracene, fluoranthene, pyrene, benzo(a)anthracene, benzo(b)fluoranthene, benzo(j)fluoranthene, benzo(k)fluoranthene, benzo(e)pyrene, benzo(a)pyrene, perylene, dibenz(a,c)anthracene, dibenz(a,h)anthracene, indeno(1,2,3,-cd)pyrene and benzo(ghi)perylene. The internal standard *p*-terphenyl-d_{14} was used to normalize the areas of all PAH chromatographic peaks observed in the F2 fraction. The recovery levels were monitored using four deuterated surrogate standards and were estimated to be: 73.6±10% for naphthalene-d_8, 82.9±7.1% for acenaphthene-d_{10}, 81.3±6.1% for phenanthrene-d_{10} and 148.8±6.3% for benzo(a)pyrene-d_{12}, respectively.

The changes in the relative distribution of petroleum hydrocarbons were analyzed using Agilent 7890 gas chromatograph fitted with a flame-ionization detector (FID). The capillary column used was 30 m × 0.32 mm × 0.25 μm HP-5, which was purchased from Agilent. For each sample, 5 μL of F3 fraction was injected in a splitless mode. The injector and detector temperature were set at 290 °C and 300 °C, respectively. The initial oven temperature was set at 50 °C for 2 min and then ramped at 6 °C/min to 300 °C for 16 min, which resulted in a total run time of 60 min.

5.4 Results and discussion

5.4.1 Physical characteristics of Chennai oil spill residues

The average density of the source oil was measured using the gravimetric method and was estimated to be 0.9 g/mL. The viscosity measurements were made using an Anton Paar Rheometer. Three samples were analyzed: the source crude, Day-1 mousse sample and Day-10 mousse. In order to avoid variations introduced by shear thinning effects of thick emulsions, all the viscosities measurements were made at a lower shear rate. The average viscosity values estimated for the source oil, Day-1, and Day-10 samples are 0.156, 118, and 850 Pa-s, respectively. Literature data showthat emulsification can rapidly increase oil viscosity by several orders of magnitude. For example, Fingas (2014a) found that emulsification processes can transform spilled oil into heavy, semisolid emulsions and the viscosity values can increase by a factor of 500 to 1000. Our measurements are consistent with these literature data.

5.4.2 Biomarker data for Chennai oil spill

Two types of biomarkers, hopanes and steranes, and the diagnostic ratios (DRs) of various types of hopanes have been widely used for fingerprinting and identifying oil spill residues (Mulabagal et al., 2013; Z. D. Wang, Stout, et al., 2006; Fang Yin et al., 2015). The hopane fingerprints for the source oil and for Day-6 and Day-62 samples are shown in Figure 5.5. The location of various hopane peaks was identified by comparing their relative retention times and elution patterns with literature data (Peters et al., 2005; Z. Wang & Fingas, 1997). The results show that all three hopane chromatograms (which are all normalized to the internal standard $C_{30}\beta\beta$-hopane) have a similar pattern. Also the relative responses of different types of hopanes in Day-6 and Day-62 samples are identical to the responses observed in the source crude indicating that the field samples must have originated from the original spill. These figures also

show that C_{27} to C_{35} pentacyclic hopanes are the major species with C_{30} and C_{29} forming the first set of dominant peaks and Ts and Tm forming the second set of dominant peaks (see Figure 5.5). The responses of C_{31} to C_{35} hopanes in these samples are relatively low compared to C_{30} hopane response.

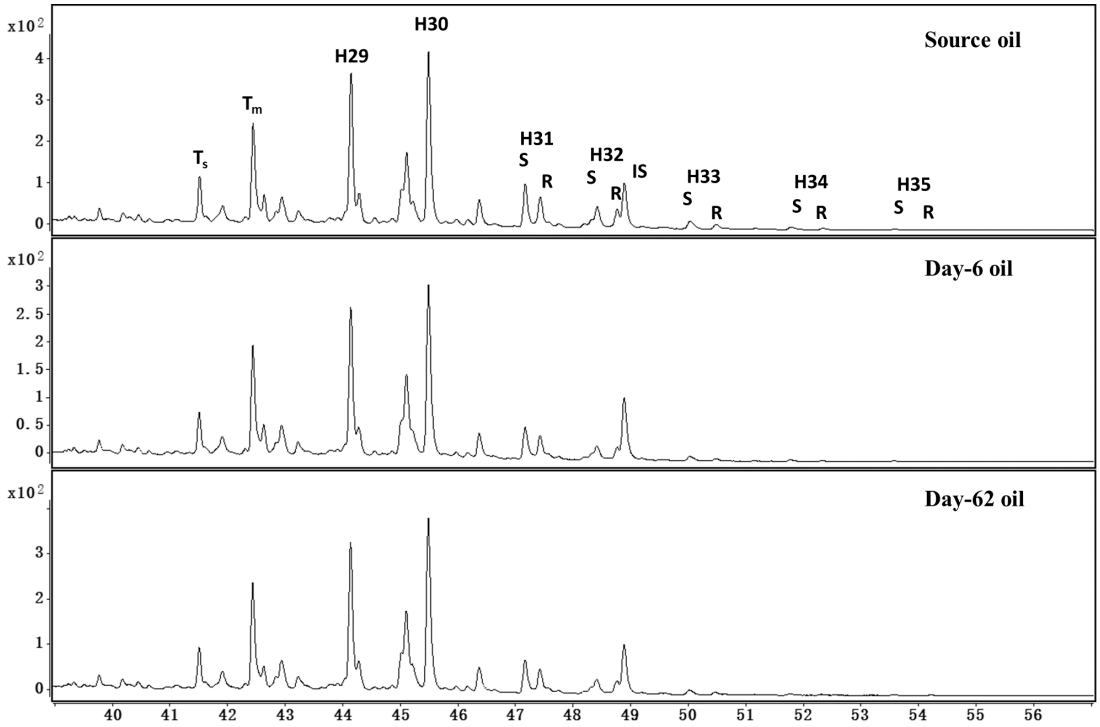

Figure 5.5 Extracted ion chromatogram of hopanes (m/z of 191) present in Chennai oil spill samples (data normalized to internal standard response).

Oil spill studies use several types of hopane diagnostic ratios to develop confirmative data for source identification. For example, the hopane ratios Ts/Tm, C_{29}/C_{30}, $C_{31}(S)/C_{31}(S + R)$, $C_{32}(S)/C_{32}(S + R)$, $C_{33}(S)/C_{33}(S+R)$, $C_{34}(S)/C_{34}(S+R)$ and $C_{35}(S)/C_{35}(S+R)$ have been used recently to identify the DWH and GB oil spill residues (Mulabagal et al., 2013; F. Yin et al., 2015). We computed these ratios for Chennai oil spill residues and compared them against the values estimated for GB and DWH oil spill samples, and the results are summarized in Table 5.1. These data show that the source oil has characteristic Ts/Tm and C_{29}/C_{30} values which can be used as unique indicators for identifying 2017-Chennai oil spill residues. In Figure 5.6 we

present all the diagnostic ratios in the form of radar plots and use them to compare the source oil data against Day-6 and Day-62 sample data. These radar plots show that the Day-6 and Day-62 samples are identical to the source oil sample, confirming that these field samples must have originated from the Chennai source oil.

Table 5.1 The comparison of hopane diagnostic ratios of oil samples from three different oil spills.

	Chennai Oil Spill	**Galveston Bay Oil Spill**	**DWH Oil Spill**
Ts/Tm	0.34	0.41	0.92
C_{29}/C_{30}	0.77	0.67	0.37
$C_{31}(S)/C_{31}(S+R)$	0.57	0.63	0.63
$C_{32}(S)/C_{32}(S+R)$	0.57	0.61	0.65
$C_{33}(S)/C_{33}(S+R)$	0.66	0.59	0.61
$C_{34}(S)/C_{34}(S+R)$	0.68	0.65	0.63
$C_{35}(S)/C_{35}(S+R)$	0.62	0.65	0.65

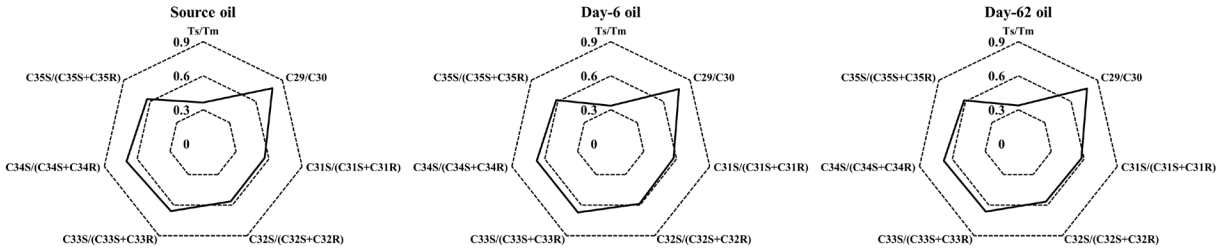

Figure 5.6 Radar plot of hopane diagnostic ratios of 3 Chennai oil samples.

Figure 5.7 shows the GC/MS chromatograms of steranes (at m/z 217) for all three samples. Similar to hopane data, the sterane chromatographic fingerprint profiles of Day-6 and Day-62 samples are similar to the source oil sample. Furthermore, these data show that steranes in Chennai oil spill residues are dominated by several high molecular weight compounds with C27-steranes yielding a major peak. These sterane data provide another set of fingerprints which can

be used to differentiate the 2017-Chennai oil spill residues from other past or future oil spill residues.

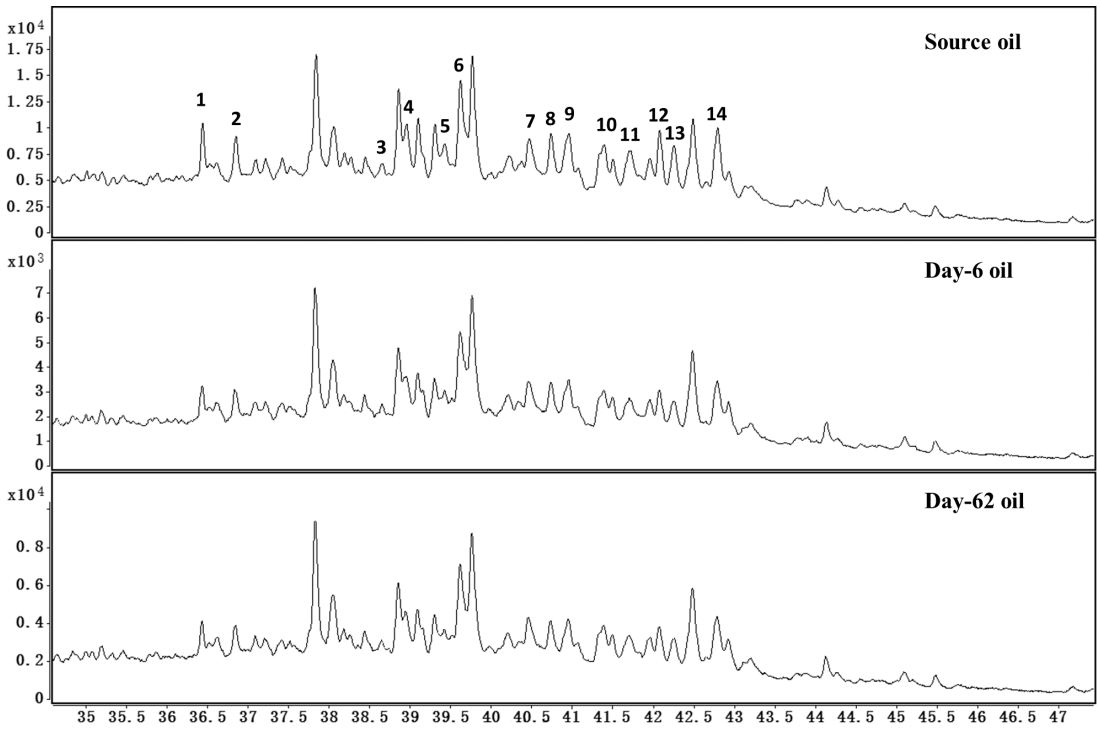

Figure 5.7 Extracted ion chromatograms of steranes (m/z of 217) for 3 Chennai oil samples. [Peak 1: DiaC_{27}βα(S); Peak 2: DiaC_{27}βα(R); Peak 3: C_{27}ααα(S); Peak 4: C_{27}αββ(R); Peak 5: C_{27}αββ(S); Peak 6: C_{27}ααα(R); Peak 7: C_{28}ααα(S); Peak 8: C_{28}αββ(R); Peak 9: C_{28}αββ(S); Peak 10: C_{28}ααα(R); Peak 11: C_{29}ααα(S); Peak 12: C_{29}αββ(R); Peak 13: C_{29}αββ(S); Peak 14: C_{29}ααα(R)].

The City of Chennai has one of the largest seaports and it routinely docks large tankers that transport various types of petroleum products from different countries. The city also dumps large amount of urban wastewater directly into the Bay of Bengal via a highly contaminated urban stream (known as the Cooum River) that discharges close to the spill location. Therefore, the Chennai shoreline is highly vulnerable to contamination from accidental tanker spills, and other illegal petroleum releases discharged into the Cooum River. The oil-fingerprinting dataset presented in this study is an important reference information that documents some of the unique

characteristics of this oil spill event, and it can be helpful to differentiate the 2017-Chennai oil spill residues from other petroleum residues originating from the past or future oil spills.

5.4.3 Understanding the volatilization patterns of Chennai oil spill

When crude or fuel oil is spilled into the coastal environment it can be impacted by various weathering processes including spreading, advection, volatilization, dissolution, photo-degradation, emulsification, sedimentation and microbial degradation (M. Board et al., 2003; Robert M Garrett et al., 1998; Guo & Wang, 2009; G. F. John et al., 2016; Roger C. Prince et al., 2003). Among these processes, volatilization is the most important weathering process that can rapidly remove large amount of oil during initial hours (M. F. Fingas, 1997). Other processes such as dissolution can transfer several soluble oil components directly into the water column. However, only a small amount of oil (usually much less than about 1% of total discharge) can actually partition into the water column; therefore, dissolution cannot measurably affect the overall oil mass balance (Mervin Fingas, 2016). The rate of volatilization is severely impacted by the ambient temperature and wind conditions. Chennai city is located within the thermal equator (13° North latitude) and the average temperature in this region during January and February is expected to be fairly high; therefore, volatilization should have played a significant role at this field site. Weather data indicated that the Chennai oil spill occurred on a hot day. The maximum temperature in Chennai on January 28th 2017 was recorded as 87 °F and the minimum was 75 °F. In order to understand volatilization rates, about 0.7 g of source oil was transferred to an aluminum dish and the oil was allowed to volatilize and/or photodegrade under both indoor and outdoor conditions. We monitored the weight loss to estimate the effective weathering levels due to volatilization. Our outdoor experiments were conducted in Alabama, USA, on June 19th 2017, when the average temperature was about 85 °F. The indoor

experiments were conducted in a dark laboratory fume hood maintained at 72 °F. These experimental conditions are approximately close the temperature levels experienced by the Chennai oil spill. The weathering level due to volatilization was computed using the following equation:

$$\%weathering = \left(1 - \frac{m_{weathered}}{m_0}\right) \text{X } 100,$$

where m_0 is the initial oil mass and $m_{weathered}$ is the weathered oil mass after certain amount of time. Figure 5.8 shows the weathering patterns of the source oil under both indoor and outdoor conditions. As expected, the rate of volatilization under indoor conditions was lower than the rate observed under outdoor conditions. Within 6 h, the indoor sample weathered by about 24% and the outdoor sample weathered by 32%. We also continued the indoor experiment for a longer period and found that the indoor sample weathered by 29% after 24 h. These data indicate that volatilization should have removed around 30% of the oil mass within the first two days. The Indian Coast Guard did not have appropriate contingency plans to respond to large oil spill events; therefore, remediation chemicals, such as liquid dispersants, were not deployed at this site during the initial period. Our laboratory data indicate that various natural processes (primarily volatilization) should have most likely removed considerable amount of oil mass during initial hours. Our chemical characterization data show that harmful contaminants, such as low molecular weight PAHs, volatilized rather rapidly during both indoor and outdoor weathering experiments (see Table 5.2). The concentration levels of naphthalene and biphenyl were low and several of these lightweight PAHs were undetectable after 6 h. Overall, the total amount of parent PAHs decreased by 38% in the indoor weathered sample and by 41% in the outdoor weathered sample. Any contingency plans to use liquid or solid dispersants to rapidly diffuse or sink future spills should be carefully evaluated. This is because, certain remediation

methods (e.g., the use of dispersants) have the potential to hinder volatilization, and this could result in transferring considerable amount harmful petroleum chemicals into the water column.

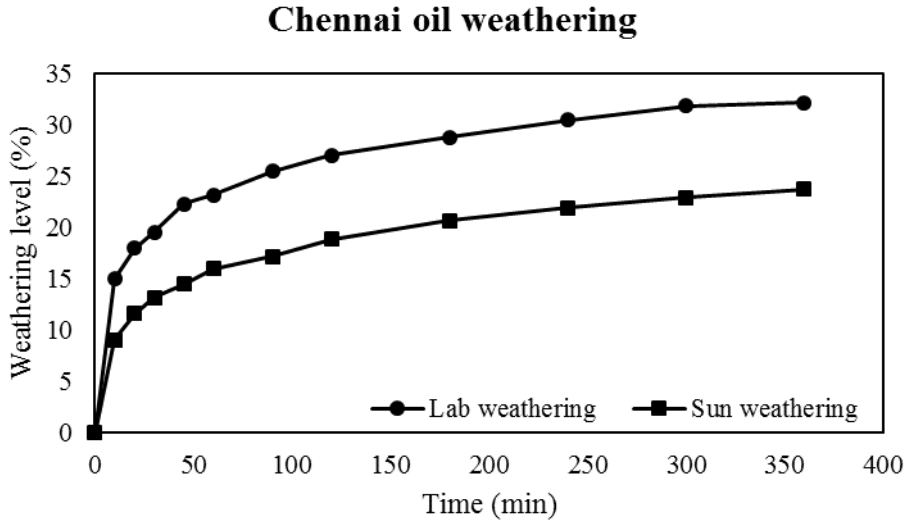

Figure 5.8 volatilization patterns of Chennai source oil under indoor and outdoor conditions.

Table 5.2 Parent PAHs concentration measured in source oil and indoor and outdoor-weathered oil (mg/kg of oil). Concentrations are normalized to initial oil weight.

Compound	Source oil	Indoor weathered oil	Outdoor weathered oil
Naphthalene	468 ± 17	DL	DL
Phenanthrene	183 ± 7	142 ± 1	131 ± 1
Dibenzothiophene	63 ± 2	51 ± 1	46 ± 1
Fluorine	58 ± 1	46 ± 1	37 ± 1
Chrysene	103 ± 2	98 ± 2	96 ± 1
Biphenyl	97 ± 2	7.7 ± 0.3	1.7 ± 0.2
Acenaphthylene	0.26 ± 0.18	0.17 ± 0.02	DL
Acenaphthene	39 ± 1	18 ± 1	13 ± 1
Anthracene	28 ± 1	27 ± 1	23 ± 1
Fluoranthene	23 ± 1	24 ± 1	23 ± 1
Pyrene	79 ± 1	76 ± 1	73 ± 1
Benzo(a)anthracene	92 ± 2	92 ± 1	90 ± 1
Benzo(b)fluoranthene	47 ± 5	46 ± 2	47 ± 1
Benzo(k)fluoranthene	29 ± 1	30 ± 1	29 ± 1
Benzo(j)fluoranthene	18 ± 1	16 ± 1	16 ± 1
Benzo(e)pyrene	72 ± 2	69 ± 2	69 ± 2
Benzo(a)pyrene	69 ± 2	61 ± 1	61 ± 1
Perylene	50 ± 1	47 ± 2	45 ± 1
Dibenz(a,c)anthracene	92 ± 11	75 ± 1	74 ± 1

Dibenz(a,h)anthracene	38 ± 1	26 ± 1	26 ± 1
Indeno(1,2,3,-cd)pyrene	33 ± 1	34 ± 2	35 ± 1
Benzo(ghi)perylene	108 ± 4	110 ± 6	118 ± 4
Total PAHs	1789	1096	1054

5.4.4 Characterization of total petroleum compounds and n-alkanes in Chennai oil spill samples

The GC-FID chromatograms for the Chennai oil spill samples are shown in Figure 5.9. These data show that all three samples have a similar type of carbon skeleton. Various types of carbon compounds present in the two field samples have weathered at different levels. The overall shape of the carbon skeleton in the field samples is similar to the source oil shape; this is another method to confirm the oil source (Z. D. Wang et al., 1999). The distribution pattern of various types of carbon compounds in a GC-FID chromatograph can also be helpful to rapidly differentiate oil spill samples (Merv Fingas, 2014a). For example, Wang et al. (1999) utilized GC-FID chromatograms to differentiate six types of petroleum products. Our data show that the overall abundance of various hydrocarbons in the Chennai source oil decrease with an increase in the carbon number; also, the source oil had substantial amount of C_{11}-C_{15} compounds. Since the low molecular weight hydrocarbons are susceptible to evaporation, due to their high vapor pressure (Lemmon & Goodwin, 2000), as expected, the field weathered samples show decreased amounts of lighter compounds. Comparison of Day-6 and Day-62 samples show that the lighter compounds continued to weather while the heavier compounds remained at high levels. The peak response levels of heavy hydrocarbons (greater than C_{18}) in the Day-62 sample are almost identical to levels observed in the Day-6 sample, indicating that the heavy compounds are resistant to weathering.

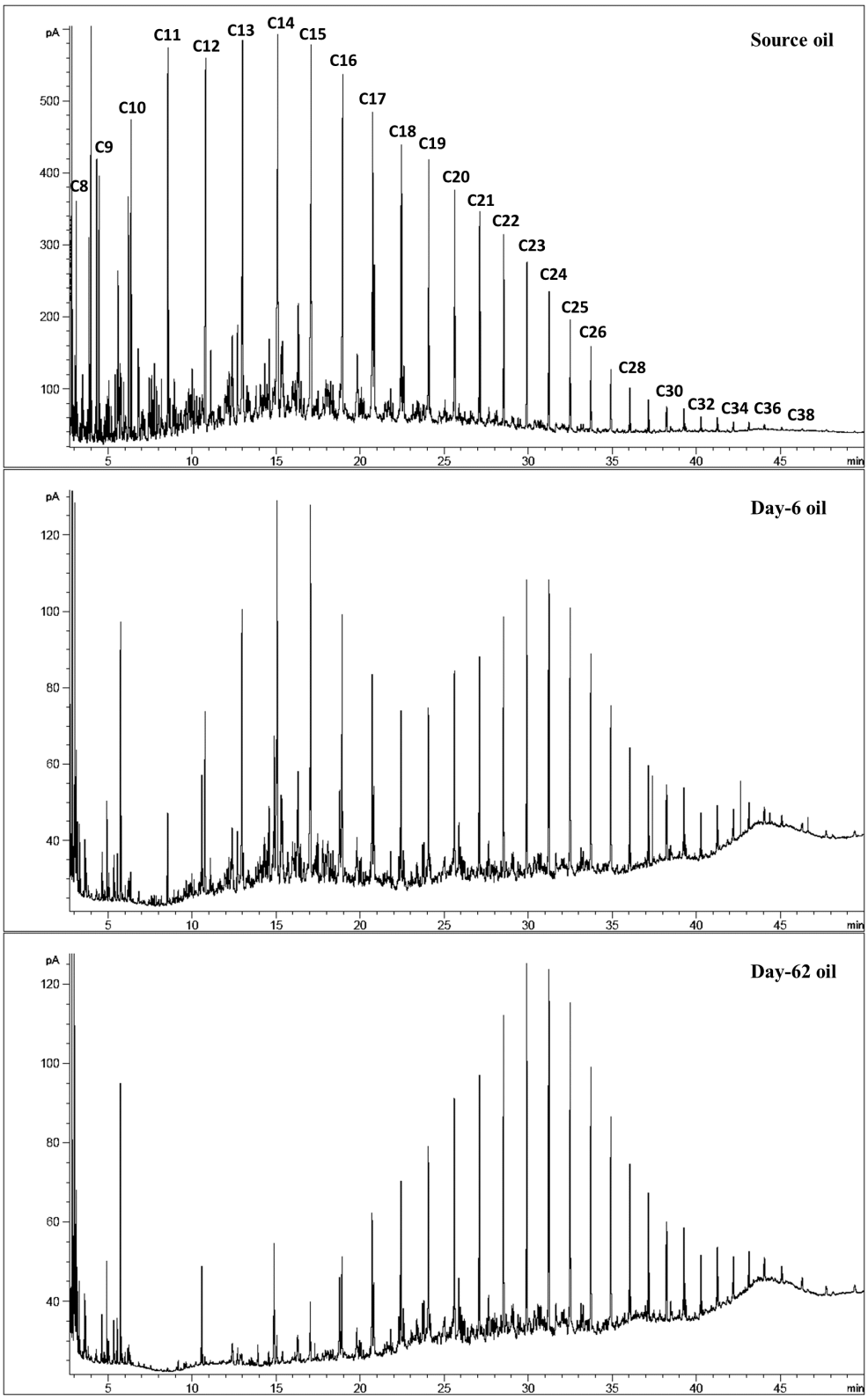

Figure 5.9 GC-FID chromatograms of petroleum hydrocarbons present in Chennai oil spill samples.

Table 5.3 summarizes the values of hydrocarbon groups measured in Chennai source oil and in Day-6 and Day-62 samples. The TPH value in the source oil was estimated to be 503mg/g with TSH (total saturated hydrocarbon) and TAH (total aromatic hydrocarbon) accounting for 77% and 23%, respectively. The ocean-scale weathering processes reduced the TPH values to 71 and 28 mg/g in Day-6 and Day-62 samples, respectively. However, the ratios of TSH/TPH and TAH/TPH did not change much, indicating both saturates and aromatics weathered at similar rates. The GC-UCM (unresolved complex mixture) present was about 38% in the Chennai source oil. However, after weathering over the ocean surface, the GC-UCM/TPH ratio almost doubled from 38% in the source oil to 61% and 66%, respectively in Day-6 and Day-62 samples, indicating that the resolvable compounds weathered at a faster rate than UCM compounds.

Table 5.3 Distribution of various types of GC-FID detectable petroleum hydrocarbons in Chennai oil spill samples.

	Source oil	**Day-6 oil**	**Day-62 oil**
TPH (mg/kg)	503	71	28
TSH/TPH	77%	81%	78%
TAH/TPH	23%	19%	22%
GC-UCM/TPH	38%	61%	66%

The saturated alkanes are another important class of petroleum compounds present in oil spill samples (Z. Wang & Fingas, 1997). The distribution of n-alkanes in all three Chennai oil spill samples was analyzed using the GC/MS SIM method (at m/z 85), and the GC–MS chromatogram is presented in Figure 5.10. The *n*-alkanes chromatogram shown in this figure provides higher resolution of the saturated hydrocarbon distribution (compared to Figure 5.9 GC-FID chromatograms); specifically, the interference due to the unresolved complex mixture is considerably reduced in the GC–MS data. The concentration of various types of n-alkanes

measured in all three Chennai oil spill samples are summarized in Table 5.4. As shown in the table, the total amount of n-alkanes are 126, 18.1, and 12.3 mg/g in source-oil, Day-6, and Day-62 samples, respectively.

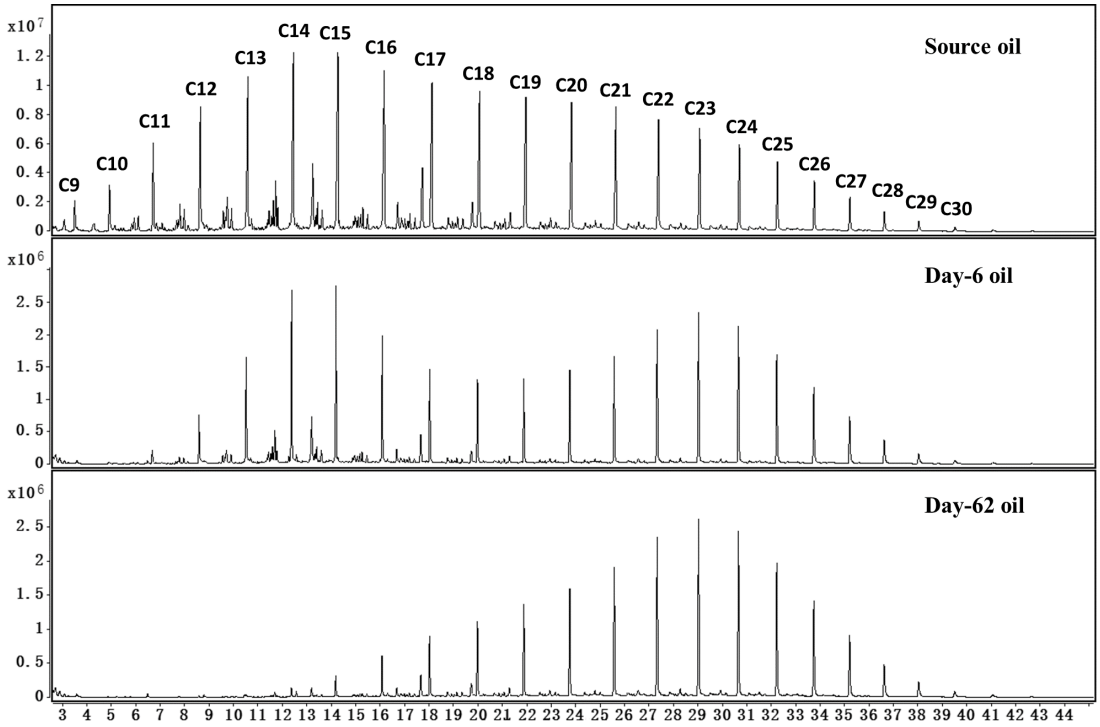

Figure 5.10 Extracted ion chromatograms of n-alkanes (m/z of 85) present in Chennai oil spill samples.

Table 5.4 Concentration of *n*-alkanes in Chennai oil spill samples (mg/kg-oil).

***n*-Alkanes**	**Source oil**	**Day-6 oil**	**Day-62 oil**
***n*-C_9**	12 ± 1	DL	DL
***n*-C_{10}**	3.9 ± 0.1	DL	DL
***n*-C_{11}**	6.3 ± 0.3	0.26 ± 0.02	DL
***n*-C_{12}**	8.2 ± 0.1	0.69 ± 0.03	DL
***n*-C_{13}**	9.1 ± 0.2	1.1 ± 0.1	0.03 ±0.01
***n*-C_{14}**	9.4 ± 0.3	1.5 ± 0.1	0.11 ± 0.02
***n*-C_{15}**	8.9 ± 0.2	1.4 ± 0.1	0.20 ± 0.03
***n*-C_{16}**	7.4 ± 0.1	1.0 ± 0.1	0.31 ± 0.04
Pristane	4.0 ± 0.1	0.43 ± 0.04	0.29 ± 0.02
***n*-C_{17}**	6.4 ± 0.2	0.73 ± 0.05	0.40 ± 0.03
Phytane	1.8 ± 0.1	0.21 ± 0.02	0.18 ± 0.02
***n*-C_{18}**	5.6 ± 0.1	0.63 ± 0.06	0.48 ± 0.05
***n*-C_{19}**	5.6 ± 0.2	0.67 ± 0.03	0.63 ± 0.05
***n*-C_{20}**	5.1 ± 0.1	0.74 ± 0.06	0.71 ± 0.05

***n*-C_{21}**	4.7 ± 0.1	0.87 ± 0.08	0.86 ± 0.06
***n*-C_{22}**	4.3 ± 0.3	1.1 ± 0.1	1.1 ± 0.1
***n*-C_{23}**	3.8 ± 0.1	1.2 ± 0.2	1.2 ± 0.1
***n*-C_{24}**	3.3 ± 0.1	1.2 ± 0.2	1.2 ± 0.1
***n*-C_{25}**	2.8 ± 0.2	1.0 ± 0.1	1.1 ± 0.1
***n*-C_{26}**	2.6 ± 0.1	0.88 ± 0.12	0.91 ± 0.09
***n*-C_{27}**	2.5 ± 0.1	0.74 ± 0.11	0.79 ± 0.07
***n*-C_{28}**	2.6 ± 0.2	0.59 ± 0.08	0.64 ± 0.05
***n*-C_{29}**	2.7 ± 0.1	0.54 ± 0.07	0.60 ± 0.04
***n*-C_{30}**	2.9 ± 0.1	0.50 ± 0.04	0.56 ± 0.02
Total *n*-alkanes	126	18.1	12.3

The alkane data can be used to estimate a weathering index (WI), which is a ratio of light to heavy alkanes (n-C_8 +n-C_{10}+n-C_{12} + n-C_{14})/(n-C_{22} + n-C_{24} + n-C_{26} + n-C_{28}). This index can be used to compare relative weathering levels at early stages (Z. D. Wang et al., 1999). The WI for Chennai source oil and Day-6 oil is 1.7 and 0.6, respectively, indicating that a large portion of lighter compounds have weathered in the Day-6 sample. The WI for Day-62 sample is 0.03 (close to zero), indicating that all lighter alkanes (less than C_{14}) have fully weathered.

Another two important ratios that can be used to assess weathering levels are: C_{17}/Pristane and C_{18}/Phytane. During early stages of weathering, C_{17}/Pristane and C_{18}/Phytane ratios are almost unaltered since they have similar early weathering rates. However, at later times the n-alkanes are more susceptible to biodegradation than isoprenoids (Z. Wang & Fingas, 1997). Therefore, C_{17}/Pristane and C_{18}/Phytane are widely used for source identification of mildly weathered oil spill products and are also used as an indicator to detect biodegradation effects (Z. Wang et al., 1998; Z. D. Wang et al., 1999). For the Chennai oil spill samples, the ratios of C_{17}/Pristane and C_{18}/Phytane are estimated to be 1.6 and 3.1 for source oil, 1.7 and 3.0 for Day-6 oil, and 1.4 and 2.7 for Day-62 oil. The slight reduction in this ratio for the Day-62 sample indicates that this sample could have undergone some degree of biodegradation. However, these

results should be considered as preliminary data, and more studies are needed to fully characterize the complex biodegradation processes occurring along the Chennai coastline, which is routinely impacted by various types of anthropogenic contaminants (R. S. Kankara, Arockiaraj, & Prabhu, 2016).

5.4.5 Chemical characterization of PAHs in Chennai oil spill samples

Table 5.5 shows the concentration levels of PAHs and their alkylated homologs present in all three samples. As expected, the source oil data is dominated by volatile light PAHs, mostly naphthalene, phenanthrene and their alkylated homologs. The naphthalene group and phenanthrene group of PAHs accounted for about 57% and 22% of the total PAHs (17,586mg/kg), respectively. Typically, during initial days, these lighter PAHs would rapidly volatilize or dissolve into the water column (Reddy et al., 2012). This effect can be observed by comparing source-oil with Day-6 sample data. Rapid initial weathering of lighter PAHs has led to sharp decrease in the total PAH value, which appears to have reduced from17,586 kg/day to 4854 mg/kg in about six days. Compound specific data show that the naphthalenes and phenanthrenes in Day-6 oil decreased by 82% and 58%, respectively, from their initial source oil levels. However, the PAH weathering rates have dropped considerably with time since the PAHs in the weathered oil are primarily dominated by heavy PAHs, which are difficult to weather. These results indicate that the rate of PAH weathering was high during initial days and the rate, however, has decreased substantially with time. Comparison of Day-6 and Day-62 samples further indicates that most of the heavy PAHs continue to resist weathering. The total amount of PAHs measured in the Day-62 sample (4016 mg/kg) is almost close to the value measured in Day-6 sample once again indicating that very little weathering has occurred at later times. The relative concentration levels of various types of PAHs in Day-6 and Day-62 samples

are different. For example, concentrations of naphthalene group of compounds in the Day-62 sample are low and they only account for 7% of the total PAHs. Whereas, the concentration of some of the high molecular weight PAHs, parent chrysene for example, has actually increased in the Day-62 sample (when compared to Day-6 sample) indicating that these recalcitrant chemicals are concentrating with time. The percentage of the heavy PAHs (4-6 rings) in the Day-62 sample is about 31% of the total PAHs. Several of these heavy PAHs are known to be highly toxic compounds and have the potential to adversely impact the health of coastal ecosystems (Djomo et al., 2004; Meador, Buzitis, & Bravo, 2008).

Table 5.5 Concentration of parent PAHs and alkylated PAHs present in Chennai oil spill samples (mg/kg-oil).

Compound	Source oil	Day-6 oil	Day-62 oil
C_0-naphthalene	468 ± 17	3.9 ± 0.4	DL
C_1-naphthalenes	1610 ± 39	140 ± 14	DL
C_2-naphthalenes	2908 ± 61	513 ± 56	9.3 ± 1.0
C_3-naphthalenes	2538 ± 62	579 ± 60	77 ± 1
C_4-naphthalenes	2428 ± 50	538 ± 56	195 ± 6
C_0-phenanthrene	183 ± 7	60 ± 7	44 ± 3
C_1-phenanthrenes	839 ± 23	343 ± 39	367 ± 38
C_2-phenanthrenes	1246 ± 39	539 ± 57	677 ± 65
C_3-phenanthrenes	1078 ± 16	459 ± 43	601 ± 50
C_4-phenanthrenes	581 ± 18	242 ± 24	325 ± 34
C_0-dibenzothiophene	63 ± 2	23 ± 2	14 ± 1
C_1-dibenzothiophenes	95 ± 2	40 ± 4	41 ± 3
C_2-dibenzothiophenes	138 ± 4	61 ± 5	79 ± 5
C_3-dibenzothiophenes	114 ± 2	51 ± 5	70 ± 5
C_0-fluorene	58 ± 1	16 ± 2	3.4 ± 0.1
C_1-fluorenes	244 ± 5	63 ± 6	34 ± 2
C_2-fluorenes	336 ± 8	94 ± 8	84 ± 4
C_3-fluorenes	432 ± 14	127 ± 12	146 ± 12
C_0-chrysene	103 ± 2	65 ± 5	94 ± 7
C_1-chrysenes	333 ± 4	169 ± 9	235 ± 19
C_2-chrysenes	419 ± 9	194 ± 12	265 ± 31
C_3-chrysenes	304 ± 6	111 ± 10	147 ± 24
C_4-chrysenes	156 ± 9	51 ± 2	66 ± 8
Biphenyl	97 ± 2	6.6 ± 0.8	DL
Acenaphthylene	0.26 ± 0.18	DL	DL

Acenaphthene	39 ± 1	9.9 ± 1.1	0.73 ± 0.04
Anthracene	28 ± 1	11 ± 1	5.4 ± 0.4
Fluoranthene	23 ± 1	13 ± 1	17 ± 1
Pyrene	79 ± 1	39 ± 4	52 ± 4
Benzo(a)anthracene	92 ± 2	61 ± 6	75 ± 11
Benzo(b)fluoranthene	47 ± 5	21 ± 1	29 ± 1
Benzo(k)fluoranthene	29 ± 1	19 ± 1	21 ± 1
Benzo(j)fluoranthene	18 ± 1	12 ± 1	14 ± 1
Benzo(e)pyrene	72 ± 2	32 ± 2	44 ± 3
Benzo(a)pyrene	69 ± 2	34 ± 3	44 ± 4
Perylene	50 ± 1	26 ± 2	30 ± 3
Dibenz(a,c)anthracene	92 ± 11	26 ± 1	32 ± 3
Dibenz(a,h)anthracene	38 ± 1	17 ± 1	21 ± 1
Indeno(1,2,3,-cd)pyrene	33 ± 1	15 ± 1	18 ± 1
Benzo(ghi)perylene	108 ± 4	30 ± 2	39 ± 2
Total PAHs	17,586	4,854	4,016

5.5 Conclusion and discussion

The objective of this case study report is to present field-scale observational data and chemical characterization data for the 2017 Chennai oil spill, a large oil spill accident that impacted one of the most populated cities in the world (Chennai is the 36th largest city). This incident was the first major oil spill encountered by this large Indian city. Although some theoretical planning studies have been completed in the past (R. S. Kankara et al., 2016), the local government did not have a practical contingency plan to manage large oil spills. Initially, the government authorities employed ad hoc clean-up methods that used flood water pumps to extract the floating oil, and these operations were largely ineffective. They then decided to use hundreds of workers to manually scoop the floating oil using plastic buckets. These workers received little or no training, and several of them did not have access to any protective equipment. Our field observations indicated that large amount of beached oil was initially recovered using this manual cleanup method. Unfortunately, the Chennai city does not have a facility to handle large volumes of hazardous petroleum wastes; therefore, the recovered oil was

either stored in barrels in offsite storage areas or tilled into native soil at a disposal facility, after mixing them with some amendments to promote bioremediation. The efficiency of these bioremediation methods is unclear, and more studies are needed to document these remediation efforts. The Indian Coast Guard also attempted to spray a dispersant on the emulsified oil several days after the spill. It has been estimated that a total of about 2800 L of dispersant (chemical details of this dispersant are not known to the authors) was used; however, these efforts likely had very little impact on the emulsified oil.

Chennai coastline has a unique flow pattern due to the presence of groins and seawalls, which are used to control beach erosion. These large structures played a significant role in controlling the oil transport process. The stagnant regions near groin-seawall interfaces trapped a significant amount of oil, and this process severely contaminated several northern beaches that are located closer to the spill. However, these stagnant zones also aided in containing the spilled oil within a relatively smaller region where manual methods could be efficiently used to scoop the oil. During the DWH spill, buoys were installed along the shoreline (which played a role similar to a seawall) to prevent beach contamination; field observations made by our team along the Alabama shoreline indicated that these buoys were mostly ineffective. Perhaps future efforts should consider installing buoys in a parallel-vertical pattern (mimicking the seawall-groin structure) to form stagnant zones which could be used to more effectively accumulate and recover floating oil spill residues.

Although both the DWH and Chennai oil spills occurred over warm waters, they behaved differently in the nearshore environment. One of the major differences is that the DWH oil spill mousse interacted with sand and sediments and sank; this resulted in forming large volumes of sunken tar mats and tar balls (Clement et al., 2017; Gustitus & Clement, 2017; Han & Clement,

2018; OSAT-2, 2011; P. Wang & Roberts, 2013). Chennai oil spill mouse also washed onto several sediment rich, high-energy sandy beaches located along the Bay of Bengal coastline; however our field surveys indicate no evidence of sinking. This dissimilarity is perhaps due to the difference in the type of the oil, and due to the differences in their weathering history. Chennai oil spill occurred closer to the shoreline and the oil had very little time to weather before reaching the shoreline. On the other hand, the DWH oil spill occurred far away from the shoreline (over 100 miles from sandy GOM beaches) and the oil had several weeks to weather before it washed onto the beaches. Typically, when a spill occurs closer to the shoreline, the emulsified mousse does not seem to sink. For example, the field observations made by our team after the GB oil spill, where a heavy fuel oil was spilled about a mile away from Galveston Bay shoreline, indicated no evidence for sinking near Galveston beaches. Overall, the weathering history can play a significant role in controlling oil spill sinking processes near sandy shoreline environments (Gustitus & Clement, 2017; Gustitus, John, & Clement, 2017).

The source oil discharged into the ocean during DWH and Chennai oil spills were different. A sweet crude oil was discharged after the DWH oilrig accident, whereas, a heavy fuel oil was released after the Chennai shipping accident. Therefore, the volatilization patterns of Chennai oil spill must have been different from the DWH oil spill volatilization patterns. Our laboratory investigations show that the Chennai oil volatilized by about 30% within a day. A similar type of experiment completed in one of our previous investigations indicated that the DWH oil volatilized by about 40% within a day (F. Yin et al., 2015). The differences in volatilization rates would have influenced the initial weathering patterns of several light hydrocarbon compounds including PAHs. Interestingly, the total amount of PAHs in DWH source oil (16,115 mg/kg) was almost close the value estimated for the Chennai source oil

(17,586 mg/kg). However, the DWH oil contained relatively small fraction of heavy PAHs. The amount of heavy PAHs (4 to 6 ring PAHs) in DWH oil contributed to about 0.5% of total PAHs (F. Yin et al., 2015). On the other hand, the Chennai source oil contained about 12% as heavy PAHs that can be highly resistant to weathering. These heavy PAHs are also highly toxic compounds and their long-term impacts on coastal systems are largely unknown. Therefore, more detailed monitoring studies are needed to fully understand the long-term environmental impacts of the Chennai oil spill residues on the Bay of Bengal coastal ecosystem.

Chapter 6

Conclusions and recommendations

6.1 Conclusions

The 2010 Deepwater Horizon oil spill has heavily contaminated the shoreline environment of Florida, Alabama, Mississippi, Louisiana, and parts of Texas. The background oil levels in Alabama's beaches have increased considerably and the toxic compounds in these oil residue samples have been impacting the shoreline system for the past nine years.

The GOM shoreline beaches have been historically contaminated by different types of oil residues discharged from oil rigs and natural oil seeps. Chemical petroleum biomarkers analysis is the routine method to identify the source of the oil spill residues. In this study, a field testing protocol based on unique physical characteristics was developed for identification of DWH oil spill residues. In this protocol, six physical characterization tests are used to identify the oil spill residues found along the sandy beaches. This protocol was verified by advanced chemical characterization tests and was found as a reliable, simple and cost-effective approach for differentiating DWH oil residues from other types of oil residues found in GOM sandy beaches. The findings of this investigation were published in (Han & Clement, 2018).

During 2010 DWH oil spill, in situ burning was employed as one of the remediation methods. In order to quantify the hazardous chemicals trapped in the ISB residues, C_{30}-αβ hopane was routinely used as a conservative biomarker as it is expected to be resistant to biochemical degradation. However, the stability of C_{30}-αβ hopane during ISB is currently not known. In this study, laboratory-scale crude oil ISB experiments were conducted to understand the fate of biomarker hopanes present in crude oil. Our data show that C_{30}-αβ hopane level in crude oil decreased after consecutive burns, and the depletion level of different types of hopanes

are inversely proportional to their carbon number (or molecular weight). Therefore, C_{30}-αβ hopane is not an ideal conservative biomarker for chemical quantification in ISB residues. However, the characteristic hopane diagnostic ratios could be used for fingerprinting the ISB residues. The findings of this investigation were published in a journal paper (G. F. John et al., 2016).

High temperature heating is one of the key processes experienced by the crude oil during ISB, therefore, the degradation patterns of hopane biomarkers in crude oil were studied by direct heating. Experimental data show that C_{30}-αβ hopane would degrade when crude oil is subject to heating and the amount of C_{30}-αβ hopane remaining in crude oil decreased with the increase in heating temperature. Similar to the results in ISB study, the degradation level of hopane biomarkers decreased with the increase in carbon number (or molecular weight), indicating the low molecular weight hopanes are more vulnerable to heating. The hopane diagnostic ratios in the oil after heating were compared with control sample, which showed that the ratios developed from light molecular weight hopanes altered by the heating process. The findings of this investigation were submitted to a research journal.

Field observation results from our case study investigation of the 2017 Chennai oil spill indicated that the initial oiling pattern was significantly affected by the groin-seawall structures installed along shoreline. Our chemical characterization data show that Chennai oil samples have unique hopane and sterane fingerprints which can be used for tracking these residues. Volatilization appears to be the major weathering process that removed a large amount of oil during the early period. Our data also shows that some heavy PAHs could have enriched in the residues and hence the long-term toxicity of these residues is a concern. The findings of this investigation were published in a journal paper (Han et al., 2018).

6.2 Recommendations

This study investigated the unique characteristics of DWH oil spill residues found along GOM sandy beaches, and also investigated the fate of hopane biomarkers during ISB. There are still a number of scientific issues that require further investigation. Some possible future research directions are described below.

DWH oil spill accident occurred in April 2010, but the oil residues from this spill are continuously washing onto GOM shoreline till now based on our field observations. Some of the sandy beaches are still severely impacted by the oil spill residues trapped in the nearshore environment. It was pointed out that the contaminated shoreline environment has been recovering slowly over the past several years (Clement et al., 2017; Joel S Hayworth et al., 2015). However, the total amount of residues remaining along this shoreline is still largely unknown. Also, the background levels and the recovery rate of the spill must be investigated.

It is well established that DWH oil spill residues contain various toxic compounds, and PAHs are one of the most important groups of toxic environmental contaminants present in crude oil. Recent studies show that several of the high molecular weight PAHs in DWH oil spill residues are highly resistant to weathering (G. F. John et al., 2016; F. Yin et al., 2015). While studies focus on the ecological impacts of fresh crude oil, few have considered the DWH oil spill residues trapped in the sandy beaches. Therefore, field scale research on understanding the bioavailability of toxic compounds in the oil spill residues and their ecological impacts are needed.

Our study shows that C_{30}-αβ hopane in crude oil can be degraded during burning or during direct heating. However, the experimental setup used in our study was too ideal and small scale. Under uncontrolled field conditions, numerous environmental factors such as water temperature

and wind speed can affect the ISB activities. Therefore, the degradation level of hopane biomarkers can be variable during field-scale ISB. Further studies are necessary to test the findings and better understand the fate of hopane biomarkers under complex field conditions.

References

Aeppli, C., Carmichael, C. A., Nelson, R. K., Lemkau, K. L., Graham, W. M., Redmond, M. C., . . . Reddy, C. M. (2012). Oil weathering after the Deepwater Horizon disaster led to the formation of oxygenated residues. *Environmental Science & Technology, 46*(16), 8799-8807.

Aeppli, C., Nelson, R. K., Radovic, J. R., Carmichael, C. A., Valentine, D. L., & Reddy, C. M. (2014). Recalcitrance and Degradation of Petroleum Biomarkers upon Abiotic and Biotic Natural Weathering of Deepwater Horizon Oil. *Environmental Science & Technology, 48*(12), 6726-6734. doi:10.1021/es500825q

Allen, A. A., & Ferek, R. J. (1993). *Advantages and disadvantages of burning spilled oil.* Paper presented at the International Oil Spill Conference.

Arava, S., Walawalkar, A. J., Arsava, K. S., Sezer, H., & Rangwala, A. S. (2017). A Novel In-situ Combustion Concept for Hazardous Waste Clean Up.

Atlas, R. M., & Hazen, T. C. (2011). Oil biodegradation and bioremediation: a tale of the two worst spills in US history. *Environmental Science & Technology, 45*(16), 6709–6715.

Bacosa, H. P., Thyng, K. M., Plunkett, S., Erdner, D. L., & Liu, Z. (2016). The tarballs on Texas beaches following the 2014 Texas City "Y" Spill: modeling, chemical, and microbiological studies. *Marine Pollution Bulletin, 109*(1), 236-244.

Balkas, T., Salihoğlu, I., Gaines, A., Sunay, M., & Matthews, J. (1982). Characterization of floating and sinking tar balls in the marine environment. *Marine Pollution Bulletin, 13*(6), 202-205.

Barakat, A. O., Mostafa, A., ElGayar, M. S., & Rullkotter, J. (1997). Source-dependent biomarker properties of five crude oils from the Gulf of Suez, Egypt. *Organic Geochemistry, 26*(7-8), 441-450. doi:Doi 10.1016/S0146-6380(97)00028-4

Board, M., Board, O. S., & Council, N. R. (2003). *Oil in the sea III: inputs, fates, and effects*: national academies Press.

Board, O. S., & Council, N. R. (2005). *Oil spill dispersants: efficacy and effects*: National Academies Press.

Boehm, P. D., Douglas, G. S., Burns, W. A., Mankiewicz, P. J., Page, D. S., & Bence, A. E. (1997). Application of petroleum hydrocarbon chemical fingerprinting and allocation techniques after the Exxon Valdez oil spill. *Marine Pollution Bulletin, 34*(8), 599-613. doi:Doi 10.1016/S0025-326x(97)00051-9

Brocks, J. J., Logan, G. A., Buick, R., & Summons, R. E. (1999). Archean molecular fossils and the early rise of eukaryotes. *science, 285*(5430), 1033-1036.

Buist, I. (2003). Window-of-opportunity for in situ burning. *Spill Science & Technology Bulletin, 8*(4), 341-346.

Clement, T., John, G., & Yin, F. (2017). Chapter 16—Assessing the Increase in Background Oil–Contamination Levels Along Alabama's Beaches Resulting From the Deepwater Horizon Oil Spill. *Oil Spill Science and Technology (Second Edition). Boston: Elsevier Inc*, 851-888.

Dave, D., & Ghaly, A. E. (2011). Remediation technologies for marine oil spills: A critical review and comparative analysis. *American Journal of Environmental Sciences, 7*(5), 423.

Djomo, J. E., Dauta, A., Ferrier, V., Narbonne, J. F., Monkiedje, A., Njine, T., & Garrigues, P. (2004). Toxic effects of some major polyaromatic hydrocarbons found in crude oil and aquatic sediments on Scenedesmus subspicatus. *Water Research, 38*(7), 1817-1821.

Douglas, G. S., Bence, A. E., Prince, R. C., McMillen, S. J., & Butler, E. L. (1996). Environmental stability of selected petroleum hydrocarbon source and weathering ratios. *Environmental Science & Technology, 30*(7), 2332-2339. doi:DOI 10.1021/es950751e

Evans, D. D., Mulholland, G. W., Baum, H. R., Walton, W. D., & McGrattan, K. B. (2001). In situ burning of oil spills. *Journal of research of the National Institute of Standards and Technology, 106*(1), 231.

Fingas, M. (2014a). *Handbook of oil spill science and technology*: John Wiley & Sons.

Fingas, M. (2014b). *Review of Emissions from Oil Fires.* Paper presented at the International Oil Spill Conference Proceedings.

Fingas, M. (2016). *Oil spill science and technology*. Cambridge, MA 02139: Gulf professional publishing.

Fingas, M., & Fieldhouse, B. (2004). Formation of water-in-oil emulsions and application to oil spill modelling. *Journal of Hazardous Materials, 107*(1), 37-50. doi:https://doi.org/10.1016/j.jhazmat.2003.11.008

Fingas, M. F. (1997). Studies on the evaporation of crude oil and petroleum products: I. the relationship between evaporation rate and time. *Journal of Hazardous Materials, 56*(3), 227-236.

Fingas, M. F. (2013). Modeling oil and petroleum evaporation. *Journal of Petroleum Science Research, 2*(3), 104-115.

Fingas, M. F., Lambert, P., Li, K., Wang, Z., Ackerman, F., Nelson, R., . . . Nadeau, R. (1999). *Studies of emissions from oil fires.* Paper presented at the International Oil Spill Conference.

Fritt-Rasmussen, J., Ascanius, B. E., Brandvik, P. J., Villumsen, A., & Stenby, E. H. (2013). Composition of in situ burn residue as a function of weathering conditions. *Marine Pollution Bulletin, 67*(1-2), 75-81.

Fritt-Rasmussen, J., Wegeberg, S., & Gustavson, K. (2015). Review on Burn Residues from In Situ Burning of Oil Spills in Relation to Arctic Waters. *Water Air and Soil Pollution, 226*(10), 329. doi:ARTN 329

10.1007/s11270-015-2593-1

Garrett, R. M., Guenette, C. C., Haith, C. E., & Prince, R. C. (2000). Pyrogenic polycyclic aromatic hydrocarbons in oil burn residues. *Environmental Science & Technology, 34*(10), 1934-1937. doi:DOI 10.1021/es991255j

Garrett, R. M., Pickering, I. J., Haith, C. E., & Prince, R. C. (1998). Photooxidation of crude oils. *Environmental Science & Technology, 32*(23), 3719-3723.

Goodman, R. (2003). Tar balls: the end state. *Spill Science & Technology Bulletin, 8*(2), 117-121.

Gullett, B. K., Aurell, J., Holder, A., Mitchell, W., Greenwell, D., Hays, M., . . . George, I. (2017). Characterization of emissions and residues from simulations of the Deepwater Horizon surface oil burns. *Marine Pollution Bulletin, 117*(1), 392-405.

Guo, W. J., & Wang, Y. X. (2009). A numerical oil spill model based on a hybrid method. *Marine Pollution Bulletin, 58*(5), 726-734. doi:https://doi.org/10.1016/j.marpolbul.2008.12.015

Gustitus, S. A., & Clement, T. P. (2017). Formation, Fate, and Impacts of Microscopic and Macroscopic Oil‐Sediment Residues in Nearshore Marine Environments: A Critical Review. *Reviews of Geophysics, 55*(4), 1130-1157.

Gustitus, S. A., John, G. F., & Clement, T. P. (2017). Effects of weathering on the dispersion of crude oil through oil-mineral aggregation. *Science of The Total Environment, 587*, 36-46.

Han, Y., & Clement, T. P. (2018). Development of a field testing protocol for identifying Deepwater Horizon oil spill residues trapped near Gulf of Mexico beaches. *PloS one, 13*(1), e0190508.

Han, Y., Nambi, I. M., & Clement, T. P. (2018). Environmental impacts of the Chennai oil spill accident–A case study. *Science of The Total Environment, 626*, 795-806.

Hayworth, J. S., Clement, T. P., John, G. F., & Yin, F. (2015). Fate of Deepwater Horizon oil in Alabama's beach system: Understanding physical evolution processes based on observational data. *Marine Pollution Bulletin, 90*(1-2), 95-105.

Hayworth, J. S., Clement, T. P., & Valentine, J. F. (2011). Deepwater Horizon oil spill impacts on Alabama beaches. *Hydrology and Earth System Sciences, 15*(12), 3639-3649. doi:10.5194/hess-15-3639-2011

Hostettler, F. D., Lorenson, T. D., & Bekins, B. A. (2013). Petroleum fingerprinting with organic markers. *Environmental Forensics, 14*(4), 262-277.

Jezaquel, R. (2014). *Assessment of Oil Burning Efficiency-Development of a Burning Bench.* Paper presented at the International Oil Spill Conference Proceedings.

Jézéquel, R., Simon, R., & Pirot, V. (2014). *Development of a burning bench dedicated to in situ burning study: assessment of oil nature and weathering effect.* Paper presented at the Proceedings of the 37th AMOP Technical Seminar on Environmental Contamination and Response, Environment Canada, Ottawa, ON.

John, G. F., Han, Y., & Clement, T. P. (2018). Fate of hopane biomarkers during in-situ burning of crude oil—A laboratory-scale study. *Marine Pollution Bulletin, 133*, 756-761.

John, G. F., Han, Y. L., & Clement, T. P. (2016). Weathering patterns of polycyclic aromatic hydrocarbons contained in submerged Deepwater Horizon oil spill residues when re-exposed to sunlight. *Science of The Total Environment, 573*, 189-202. doi:10.1016/j.scitotenv.2016.08.059

Kankara, R., Mohan, R., & Venkatachalapathy, R. (2011). Hydrodynamic modelling of Chennai coast from a coastal zone management perspective. *Journal of Coastal Research, 29*(2), 347-357.

Kankara, R. S., Arockiaraj, S., & Prabhu, K. (2016). Environmental sensitivity mapping and risk assessment for oil spill along the Chennai Coast in India. *Marine Pollution Bulletin, 106*(1-2), 95-103.

Kannan, R., Anand, K., Sundar, V., Sannasiraj, S., & Rangarao, V. (2014). Shoreline changes along the Northern coast of Chennai port, from field measurements. *ISH Journal of Hydraulic Engineering, 20*(1), 24-31.

Kennicutt, M. C. (2017). Oil and Gas Seeps in the Gulf of Mexico. In *Habitats and Biota of the Gulf of Mexico: Before the Deepwater Horizon Oil Spill* (pp. 275-358). New York, NY: Springer.

Kirman, Z. D., Sericano, J. L., Wade, T. L., Bianchi, T. S., Marcantonio, F., & Kolker, A. S. (2016). Composition and depth distribution of hydrocarbons in Barataria Bay marsh sediments after the Deepwater Horizon oil spill. *Environmental Pollution, 214*, 101-113. doi:10.1016/j.envpol.2016.03.071

Kök, M., Hughes, R., & Price, D. (1997). Combustion characteristics of crude oil-limestone mixtures: High pressure thermogravimetric analysis and their relevance to in-situ combustion. *Journal of Thermal Analysis and Calorimetry, 49*(2), 609-615.

Kok, M. V. (2011). Characterization of medium and heavy crude oils using thermal analysis techniques. *Fuel processing technology, 92*(5), 1026-1031.

Kujawinski, E. B., Kido Soule, M. C., Valentine, D. L., Boysen, A. K., Longnecker, K., & Redmond, M. C. (2011). Fate of dispersants associated with the Deepwater Horizon oil spill. *Environmental Science & Technology, 45*(4), 1298-1306.

Lemmon, E. W., & Goodwin, A. R. H. (2000). Critical properties and vapor pressure equation for alkanes CnH2n+2: Normal alkanes with n <= 36 and isomers for n=4 through n=9. *Journal of physical and chemical reference data, 29*(1), 1-39.

Lessard, R. R., & DeMarco, G. (2000). The significance of oil spill dispersants. *Spill Science & Technology Bulletin, 6*(1), 59-68.

Lin, Q., Mendelssohn, I. A., Carney, K., Miles, S. M., Bryner, N. P., & Walton, W. D. (2005). In-situ burning of oil in coastal marshes. 2. Oil spill cleanup efficiency as a function of oil type, marsh type, and water depth. *Environmental Science & Technology, 39*(6), 1855-1860.

Liu, Z., Liu, J., Zhu, Q., & Wu, W. (2012). The weathering of oil after the Deepwater Horizon oil spill: insights from the chemical composition of the oil from the sea surface, salt marshes and sediments. *Environmental Research Letters, 7*(3), 035302.

Lubchenco, J., McNutt, M. K., Lehr, B., Sogge, M., Miller, M., Hammond, S. R., & Conner, W. G. (2010). BP Deepwater Horizon oil budget what happened to the oil.

MacDonald, I. R., Garcia‐Pineda, O., Beet, A., Asl, S. D., Feng, L., Graettinger, G., . . . Huffer, F. (2015). Natural and unnatural oil slicks in the Gulf of Mexico. *Journal of Geophysical Research: Oceans, 120*(12), 8364-8380.

McNutt, M. K., Camilli, R., Crone, T. J., Guthrie, G. D., Hsieh, P. A., Ryerson, T. B., . . . Shaffer, F. (2012). Review of flow rate estimates of the Deepwater Horizon oil spill. *Proceedings of the National Academy of Sciences of the United States of America, 109*(50), 20260-20267. doi:10.1073/pnas.1112139108

Meador, J. P., Buzitis, J., & Bravo, C. F. (2008). Using fluorescent aromatic compounds in bile from juvenile salmonids to predict exposure to polycyclic aromatic hydrocarbons. *Environmental Toxicology and Chemistry, 27*(4), 845-853.

Michel, J., Owens, E. H., Zengel, S., Graham, A., Nixon, Z., Allard, T., . . . White, M. (2013). Extent and degree of shoreline oiling: Deepwater Horizon oil spill, Gulf of Mexico, USA. *PloS one, 8*(6), e65087.

Mulabagal, V., Yin, F., John, G. F., Hayworth, J. S., & Clement, T. P. (2013). Chemical fingerprinting of petroleum biomarkers in Deepwater Horizon oil spill samples collected from Alabama shoreline. *Marine Pollution Bulletin, 70*(1-2), 147-154. doi:10.1016/j.marpo1bul.2013.02.026

Mullin, J. V., & Champ, M. A. (2003). Introduction/overview to in situ burning of oil spills. *Spill Science & Technology Bulletin, 8*(4), 323-330.

Neff, J. M., Owens, E. H., Stoker, S. W., & McCormick, D. M. (1995). Shoreline oiling conditions in Prince William Sound following the Exxon Valdez oil spill. In *Exxon Valdez oil spill: Fate and effects in Alaskan waters*: ASTM International.

Nixon, Z., Zengel, S., Baker, M., Steinhoff, M., Fricano, G., Rouhani, S., & Michel, J. (2016). Shoreline oiling from the Deepwater Horizon oil spill. *Marine Pollution Bulletin, 107*(1), 170-178. doi:https://doi.org/10.1016/j.marpolbul.2016.04.003

Nordvik, A. B. (1995). The Technology Windows-of-Opportunity for Marine Oil-Spill Response as Related to Oil Weathering and Operations. *Spill Science & Technology Bulletin, 2*(1), 17-46. doi:Doi 10.1016/1353-2561(95)00013-T

Nordvik, A. B. (1995). The technology windows-of-opportunity for marine oil spill response as related to oil weathering and operations. *Spill Science & Technology Bulletin, 2*(1), 17-46.

OSAT-2. (2011). Summary Report for Fate and Effects of Remnant Oil in the Beach Environment.

Pelz, O., Brown, J., Huddleston, M., Rand, G., Gardinali, P., Stubblefield, W., . . . Exponent, M. (2014). Selection of a surrogate MC252 oil as a reference material for future aquatic toxicity tests and other studies. *survival, 20*, 25,000,000.

Perring, A., Schwarz, J., Spackman, J., Bahreini, R., De Gouw, J., Gao, R., . . . Peischl, J. (2011). Characteristics of black carbon aerosol from a surface oil burn during the Deepwater Horizon oil spill. *Geophysical Research Letters, 38*(17).

Peters, K. E., Walters, C. C., & Moldowan, J. M. (2005). *The biomarker guide* (Vol. 1): Cambridge University Press.

PI, A. S. R. (2015). *A Novel Experimental Approach to Enhance Burning Of Oil-Water Emulsions by Immersed Objects.* Worcester Polytechnic Institute,

Plant, N. G., Long, J. W., Dalyander, P. S., Thompson, D. M., & Raabe, E. A. (2013). *Application of a hydrodynamic and sediment transport model for guidance of response efforts related to the Deepwater Horizon oil spill in the Northern Gulf of Mexico along the coast of Alabama and Florida* (2331-1258). Retrieved from

Potter, S., & Buist, I. (2008). *In-Situ Burning for Oil Spills in Arctic Waters: State-of-the-Art and Future Research Needs.* Paper presented at the Oil Spill Response: A Global Perspective, Dordrecht.

Prahl, F. G., Dymond, J., & Sparrow, M. A. (2000). Annual biomarker record for export production in the central Arabian Sea. *Deep Sea Research Part II: Topical Studies in Oceanography, 47*(7), 1581-1604.

Prince, R. C., Elmendorf, D. L., Lute, J. R., Hsu, C. S., Haith, C. E., Senius, J. D., . . . Butler, E. L. (1994). 17. alpha.(H)-21. beta.(H)-hopane as a conserved internal marker for estimating the biodegradation of crude oil. *Environmental Science & Technology, 28*(1), 142-145.

Prince, R. C., Garrett, R. M., Bare, R. E., Grossman, M. J., Townsend, T., Suflita, J. M., . . . Lessard, R. R. (2003). The Roles of Photooxidation and Biodegradation in Long-term Weathering of Crude and Heavy Fuel Oils. *Spill Science & Technology Bulletin, 8*(2), 145-156. doi:https://doi.org/10.1016/S1353-2561(03)00017-3

Ramesh, S., Bhattacharya, D., Majrashi, M., Morgan, M., Clement, T. P., & Dhanasekaran, M. (2018). Evaluation of behavioral parameters, hematological markers, liver and kidney functions in rodents exposed to Deepwater Horizon crude oil and Corexit. *Life sciences, 199*, 34-40.

Ramseur, J. L. (2010). *Deepwater Horizon oil spill: the fate of the oil*.

Reddy, C. M., Arey, J. S., Seewald, J. S., Sylva, S. P., Lemkau, K. L., Nelson, R. K., . . . Camilli, R. (2012). Composition and fate of gas and oil released to the water column during the

Deepwater Horizon oil spill. *Proceedings of the National Academy of Sciences of the United States of America, 109*(50), 20229-20234.

Romero, I. C., Schwing, P. T., Brooks, G. R., Larson, R. A., Hastings, D. W., Ellis, G., . . . Hollander, D. J. (2015). Hydrocarbons in Deep-Sea Sediments following the 2010 Deepwater Horizon Blowout in the Northeast Gulf of Mexico. *PloS one, 10*(5), e0128371. doi:ARTN e0128371

10.1371/journal.pone.0128371

Schantz, M. M., & Kucklick, J. R. (2011). Interlaboratory Analytical Comparison Study to Support Deepwater Horizon Natural Resource Damage Assessment: Description and Results for Crude Oil QA10OIL01. *National Institute of Standards and Technology (NIST) Report, Gaithersburg, MD, 20899*.

Schaum, J., Cohen, M., Perry, S., Artz, R., Draxler, R., Frithsen, J. B., . . . Phillips, L. (2010). Screening Level Assessment of Risks Due to Dioxin Emissions from Burning Oil from the BP Deepwater Horizon Gulf of Mexico Spill. *Environmental Science & Technology, 44*(24), 9383-9389. doi:10.1021/es103559w

Shen, J. (1984). Minimization of interferences from weathering effects and use of biomarkers in identification of spilled crude oils by gas chromatography/mass spectrometry. *Analytical chemistry, 56*(2), 214-217.

Shigenaka, G., Overton, E., Meyer, B., Gao, H., & Miles, S. (2015). *Physical and chemical characteristics of in-situ burn residue and other environmental oil samples collected during the Deepwater Horizon spill response.* Paper presented at the Interspil Conference.

Short, J. W., Lindeberg, M. R., Harris, P. M., Maselko, J. M., Pella, J. J., & Rice, S. D. (2004). Estimate of oil persisting on the beaches of Prince William Sound 12 years after the Exxon Valdez oil spill. *Environmental Science & Technology, 38*(1), 19-25.

Stout, S. A. (2016). Oil spill fingerprinting method for oily matrices used in the Deepwater Horizon NRDA. *Environmental Forensics, 17*(3), 218-243.

Stout, S. A., & Douglas, G. S. (2004). Diamondoid hydrocarbons - Application in the chemical fingerprinting of natural gas condensate and gasoline. *Environmental Forensics, 5*(4), 225-235. doi:10.1080/15275920490886734

Stout, S. A., & Payne, J. R. (2016). Chemical composition of floating and sunken in-situ burn residues from the Deepwater Horizon oil spill. *Marine Pollution Bulletin, 108*(1-2), 186-202. doi:10.1016/j.marpolbul.2016.04.031

Stout, S. A., Uhler, A. D., & McCarthy, K. J. (2005). Middle distillate fuel fingerprinting using drimane-based bicyclic sesquiterpanes. *Environmental Forensics, 6*(3), 241-251. doi:10.1080/15275920500194407

Suneel, V., Ciappa, A., & Vethamony, P. (2016). Backtrack modeling to locate the origin of tar balls depositing along the west coast of India. *Science of The Total Environment, 569*, 31-39.

Suneel, V., Vethamony, P., Naik, B., Vinod Kumar, K., Sreenu, L., Samiksha, S., . . . Sudheesh, K. (2014). Source investigation of the tar balls deposited along the Gujarat coast, India, using chemical fingerprinting and transport modeling techniques. *Environmental Science & Technology, 48*(19), 11343-11351.

Suneel, V., Vethamony, P., Zakaria, M., Naik, B., & Prasad, K. (2013). Identification of sources of tar balls deposited along the Goa coast, India, using fingerprinting techniques. *Marine Pollution Bulletin, 70*(1-2), 81-89.

Urbano, M., Elango, V., & Pardue, J. H. (2013). Biogeochemical characterization of MC252 oil: sand aggregates on a coastal headland beach. *Marine Pollution Bulletin, 77*(1-2), 183-191.

USEPA. (1993). *Provisional guidance for quantitative risk assessment of polycyclic aromatic hydrocarbons*: Environmental Criteria and Assessment Office, Office of Health and Environmental Assessment, US Environmental Protection Agency.

van Gelderen, L., Malmquist, L. M., & Jomaas, G. (2017). Vaporization order and burning efficiency of crude oils during in-situ burning on water. *Fuel, 191*, 528-537.

Veerasingam, S., Venkatachalapathy, R., & Ramkumar, T. (2014). Distribution of clay minerals in marine sediments off Chennai, Bay of Bengal, India: Indicators of sediment sources and transport processes. *International Journal of Sediment Research, 29*(1), 11-23.

Ventikos, N. P., Vergetis, E., Psaraftis, H. N., & Triantafyllou, G. (2004). A high-level synthesis of oil spill response equipment and countermeasures. *Journal of Hazardous Materials, 107*(1), 51-58. doi:https://doi.org/10.1016/j.jhazmat.2003.11.009

Volkman, J. K., Barrett, S. M., Blackburn, S. I., Mansour, M. P., Sikes, E. L., & Gelin, F. (1998). Microalgal biomarkers: A review of recent research developments. *Organic Geochemistry, 29*(5-7), 1163-1179. doi:Doi 10.1016/S0146-6380(98)00062-X

Wang, P., & Roberts, T. M. (2013). Distribution of Surficial and Buried Oil Contaminants across Sandy Beaches along NW Florida and Alabama Coasts Following the Deepwater Horizon Oil Spill in 2010. *Journal of Coastal Research, 29*(6A), 144-155.

Wang, S. D., Shen, Y. M., & Zheng, Y. H. (2005). Two-dimensional numerical simulation for transport and fate of oil spills in seas. *Ocean Engineering, 32*(13), 1556-1571. doi:10.1016/j.oceaneng.2004.12.010

Wang, Z., & Fingas, M. (1997). Developments in the analysis of petroleum hydrocarbons in oils, petroleum products and oil-spill-related environmental samples by gas chromatography. *Journal of Chromatography A, 774*(1-2), 51-78.

Wang, Z., Fingas, M., Blenkinsopp, S., Sergy, G., Landriault, M., Sigouin, L., . . . Westlake, D. (1998). Comparison of oil composition changes due to biodegradation and physical weathering in different oils. *Journal of Chromatography A, 809*(1-2), 89-107.

Wang, Z., Fingas, M., & Sergy, G. (1995). Chemical characterization of crude oil residues from an arctic beach by GC/MS and GC/FID. *Environmental Science & Technology, 29*(10), 2622-2631.

Wang, Z., Fingas, M., Shu, Y., Sigouin, L., Landriault, M., Lambert, P., . . . Mullin, J. (1999). Quantitative characterization of PAHs in burn residue and soot samples and differentiation of pyrogenic PAHs from petrogenic PAHs− The 1994 mobile burn study. *Environmental Science & Technology, 33*(18), 3100-3109.

Wang, Z., Fingas, M., Yang, C., & Christensen, J. H. (1964). *Crude Oil and Refined Product Fingerprinting: Principles*: Academic Press.

Wang, Z., & Fingas, M. F. (2003). Development of oil hydrocarbon fingerprinting and identification techniques. *Marine Pollution Bulletin, 47*(9), 423-452. doi:https://doi.org/10.1016/S0025-326X(03)00215-7

Wang, Z., Hollebone, B., Fingas, M., Fieldhouse, B., Sigouin, L., Landriault, M., . . . Weaver, J. W. (2003). Characteristics of spilled oils, fuels, and petroleum products: 1. Composition and properties of selected oils. *United States Enviromental Protection Agency*.

Wang, Z., & Stout, S. (2010). *Oil spill environmental forensics: fingerprinting and source identification*: Elsevier.

Wang, Z. D., & Fingas, M. (2003). Fate and identification of spilled oils and petroleum products in the environment by GC-MS and GC-FID. *Energy Sources, 25*(6), 491-508. doi:10.1080/00908310390195570

Wang, Z. D., Fingas, M., & Li, K. (1994a). Fractionation of a Light Crude-Oil and Identification and Quantitation of Aliphatic, Aromatic, and Biomarker Compounds by Gc-Fid and Gc-Ms .1. *Journal of Chromatographic Science, 32*(9), 361-366.

Wang, Z. D., Fingas, M., & Li, K. (1994b). Fractionation of a Light Crude-Oil and Identification and Quantitation of Aliphatic, Aromatic, and Biomarker Compounds by Gc-Fid and Gc-Ms .2. *Journal of Chromatographic Science, 32*(9), 367-382.

Wang, Z. D., Fingas, M., & Page, D. S. (1999). Oil spill identification. *Journal of Chromatography A, 843*(1-2), 369-411. doi:Doi 10.1016/S0021-9673(99)00120-X

Wang, Z. D., Fingas, M., & Sergy, G. (1994). Study of 22-Year-Old Arrow Oil Samples Using Biomarker Compounds by Gc/Ms. *Environmental Science & Technology, 28*(9), 1733-1746. doi:DOI 10.1021/es00058a027

Wang, Z. D., Stout, S. A., & Fingas, M. (2006). Forensic fingerprinting of biomarkers for oil spill characterization and source identification. *Environmental Forensics, 7*(2), 105-146. doi:10.1080/15275920600667104

Wang, Z. D., Yang, C., Fingas, M., Hollebone, B., Peng, X. Z., Hansen, A. B., & Christensen, J. H. (2005). Characterization, weathering, and application of sesquiterpanes to source identification of spilled lighter petroleum products. *Environmental Science & Technology, 39*(22), 8700-8707. doi:DOI 10.1021/es051371o

Wang, Z. D., Yang, C., Hollebone, B., & Fingas, M. (2006). Forensic fingerprinting of diamondoids for correlation and differentiation of spilled oil and petroleum products. *Environmental Science & Technology, 40*(18), 5636-5646. doi:10.1021/es060675n

Yang, C., Wang, Z. D., Hollebone, B. P., Brown, C. E., & Landriault, M. (2009). Characteristics of bicyclic sesquiterpanes in crude oils and petroleum products. *Journal of Chromatography A, 1216*(20), 4475-4484. doi:10.1016/j.chroma.2009.03.024

Yim, U. H., Ha, S. Y., An, J. G., Won, J. H., Han, G. M., Hong, S. H., . . . Shim, W. J. (2011). Fingerprint and weathering characteristics of stranded oils after the Hebei Spirit oil spill. *Journal of Hazardous Materials, 197*, 60-69.

Yim, U. H., Ha, S. Y., An, J. G., Won, J. H., Han, G. M., Hong, S. H., . . . Shim, W. J. (2011). Fingerprint and weathering characteristics of stranded oils after the Hebei Spirit oil spill. *Journal of Hazardous Materials, 197*, 60-69. doi:10.1016/j.jhazmat.2011.09.055

Yin, F., Hayworth, J. S., & Clement, T. P. (2015). A tale of two recent spills—comparison of 2014 Galveston Bay and 2010 Deepwater Horizon oil spill residues. *PloS one, 10*(2), e0118098.

Yin, F., John, G. F., Hayworth, J. S., & Clement, T. P. (2015). Long-term monitoring data to describe the fate of polycyclic aromatic hydrocarbons in Deepwater Horizon oil submerged off Alabama's beaches. *Science of The Total Environment, 508*, 46-56. doi:10.1016/j.scitotenv.2014.10.105

Zakaria, M. P., Horinouchi, A., Tsutsumi, S., Takada, H., Tanabe, S., & Ismail, A. (2000). Oil pollution in the Straits of Malacca, Malaysia: Application of molecular markers for source identification. *Environmental Science & Technology, 34*(7), 1189-1196.